

COMPUTER SIMULATION OF MINING SUBSIDENCE
USING THE ZONE AREA METHOD

COMPUTER SIMULATION OF MINING SUBSIDENCE
USING THE ZONE AREA METHOD

M. Karmis and C. Haycocks

Department of Mining and Minerals Engineering
Virginia Polytechnic Institute and State University
Blacksburg, Virginia

FINAL REPORT

Prepared for the

Office of Mineral Institutes
Bureau of Mines
U.S. Department of Interior

Emile Allge

March 1983

UNITED STATES
DEPARTMENT OF THE INTERIOR
BUREAU OF MINES

APPROVAL AND DISTRIBUTION OF GRANT REPORTS

Title: Computer Simulation of Mining Subsidence Using the Zone Area Method by M. Karmis and C. Haycocks

Report Date: March 1983 Type of Report (Final/Interim): FINAL

Sponsoring Organization: Bureau of Mines/OSM

Value/Impact of results: Development of accurate methods for predicting subsidence

Users/Audience: Mine Operators

Grantee Name: Virginia Polytechnic Institute and State University (VPI)

Grant Number: G1115512, G1105051 Total Grant Funding: \$162,698.00

TPO: _____ Program Manager: _____

Has grantee filed a Patent Form DI 12177 Yes No If yes, attach Solicitor's approval to make public.

Press Release Recommendation: Yes No
Recommended for Open File: Yes No
Recommended for NTIS: Yes No

If no, explain:
Does not meet NTIS standards

WASHINGTON OFFICE ONLY	
Date Rec'd	_____
OFR #	<u>102-83</u>
NTIS #	<u>NA</u>
# of pages	_____
Price \$	_____

Distribution: (Check or fill in as appropriate)

DOI Library. OSM Library Office of Assistant Director --Mining Research (1 copy)

10 BOM Research Centers All These only: Pittsburgh, Denver, Spokane, Twin Cities (2 copies ea

4 Field Office Centers All These only: _____

DOE, Carbondale, IL DOE, Pittsburgh, PA MSHA, Arlington, VA National Mine H&S Academy, Beckley, WV

State Geologists in _____

Other: Grants Management Office (sent 1 copy on April 22, 1983)

If not recommended for distribution, state why: _____

CONCURRENCES {

Program Manager (Date) _____

R.A. Munn
Division Chief
Chief, Office of Mineral Institutes (Date) JUN 1 1983

Assistant Director (Date) _____

V.P. Munn (no press release) 6-3-83

COMPUTER SIMULATION OF MINING SUBSIDENCE
USING THE ZONE AREA METHOD

M. Karmis and C. Haycocks

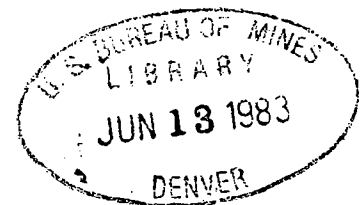
Department of Mining and Minerals Engineering
Virginia Polytechnic Institute and State University
Blacksburg, Virginia

FINAL REPORT

Prepared for the

Office of Mineral Institutes
Bureau of Mines
U.S. Department of Interior

March 1983



DISCLAIMER NOTICE

This report is based upon work supported by the Mining and Mineral Resources Research Institutes Program, U.S. Department of the Interior. Any opinions, findings and conclusions or recommendations expressed in this publication are those of the authors and do not necessarily reflect the views of the sponsor.

ACKNOWLEDGEMENTS

The investigators of this project were Dr. Michael Karmis and Dr. C. Haycocks. A number of graduate students were also responsible for completing this research effort: G. Goodman, B. Webb and T. Triplett.

The authors would like to express their appreciation to many coal companies and federal agencies for their cooperation and support in this project. Finally, acknowledgement is due to D. Hasenfus for the preparation of the manuscript.

TABLE OF CONTENTS

ACKNOWLEDGEMENTS 11

LIST OF FIGURES iv

LIST OF TABLES vi

I. INTRODUCTION 1

II. THE DEVELOPMENT OF THE ZONE AREA METHOD 3

III. COMPUTER MODELING OF THE ZONE AREA METHOD 23

IV. COLLECTION AND ANALYSIS OF SUBSIDENCE CASE STUDIES 29

V. DEVELOPMENT OF AN EMPIRICAL SUBSIDENCE PREDICTION MODEL 39

VI. APPLICATION OF THE ZONE AREA METHOD 47

VII. CONCLUSIONS 59

REFERENCES 61

APPENDIX A. PROGRAM FLOWCHARTS A

APPENDIX B. INPUT DATA B

APPENDIX C. PROGRAM OUTPUT C

APPENDIX D. PUBLICATIONS BASED ON THIS RESEARCH D

LIST OF FIGURES

	<u>PAGE</u>
Figure 1. Law of Superposition (After Brauner, 1973)	5
Figure 2. Kohne's Influence Function (After Sinclair, 1963)	6
Figure 3. Radius, R, vs Draw Angle (After Sinclair, 1963)	7
Figure 4. Bals' Influence Function (After Sinclair, 1963)	8
Figure 5. Meyers and Drent Influence Function (After Sinclair, 1963) .	11
Figure 6a. Half-Zone Extraction	13
Figure 6b. Zone Extraction for Half-Maximum Subsidence	13
Figure 7. The Zone Area Method	16
Figure 8. Coal Pillar Reduction Effects (After Marr, 1975)	18
Figure 9. Pillar Reduction Correction Curve (After Marr, 1975)	20
Figure 10. Positions of the Four Pillar Boundary Equations	24
Figure 11. Intersection Points and Extracted Sectors for a Pillar-Zone System (Two Cases)	26
Figure 12. Location of Longwall Coal Mines in the United States (O'Rourke & Turner, 1979)	30
Figure 13. Variation of Draw Angle with Width-to-Depth Ratio	32
Figure 14. Influence of Width-to-Depth Ratio on the Maximum Subsidence Factor	33
Figure 15. Effect of Width-to-Depth Ratio on the Position of the Inflection Point	34
Figure 16. Influence of Shale on s/S for all Case Studies	36
Figure 17. Influence of Sandstone and Limestone on s/S for Critical and Supercritical Panels	37
Figure 18. Influence of Shale on s/S for Critical and Supercritical Panels	38
Figure 19. Characteristic Subsidence Profile for Subcritical Extractions	40

cont.

LIST OF FIGURES (cont.)

	<u>PAGE</u>
Figure 20. Characteristic Subsidence Profile and Critical and Supercritical Extractions	41
Figure 21. Referencing System (Brauner, 1973)	42
Figure 22. Determination of the Hyperbolic Tangent Profile Function for Subcritical Extractions	43
Figure 23. Determination of the Hyperbolic Tangent Profile Function for Critical and Supercritical Extraction	44
Figure 24. Effect of Panel Lithology and Width-to-Depth Ratio on the Maximum Subsidence	46
Figure 25. Variations of Rib-Side Subsidence with Width-to-Depth Ratio	50
Figure 26. Variation of Zone Factors with Percent Hard Rock for Zones B, C, D	52
Figure 27. Variation of Zone Factor with Percent Hard Rock for Zone A, E, F	53
Figure 28. Field Profile vs Zone Area Predicted Profile	55
Figure 29. Field Profile vs Zone Area Predicted Profile	56
Figure 30. Field Profile vs Zone Area Predicted Profile	57
Figure 31. Field Profile vs Predicted Profiles Using Appalachian Model	58

LIST OF TABLES

	<u>PAGE</u>
Table 1. Maximum Subsidence as a Percent of Seam Thickness	48
Table 2. Subsidence as a Percent of Maximum Subsidence	49

I. INTRODUCTION

Surface subsidence is an inevitable consequence of many underground mining operations and has been recognized as such since the fifteenth century. Damage resulting from this phenomenon ranges from simple land settlement to severe structural damage to buildings and has been witnessed in rural (Illinois, Colorado, West Virginia, Virginia, Pennsylvania) as well as in urban areas (Pennsylvania, West Virginia, Illinois, Wyoming). In fact, it is estimated that over 2 million acres of land across the United States have been affected by mining subsidence, of which 140,000 acres are in urban areas (Singh, 1978; Johnson and Miller, 1979). Further, it is estimated that during the next twenty years an additional 1.5 to 2.4 million acres of land will also be affected by mining.

Subsidence prevention is not feasible, at least under the existing technologic and economic constraints of underground coal mining. Foreign experience has demonstrated, however, that subsidence can be successfully controlled if an accurate method of predicting ground movements is available. Such techniques have been developed in many coalfields, where it is currently accepted that subsidence can be predicted within ± 20 percent of the actual values. Furthermore, such movements can be translated into anticipated structural failures using established damage criteria, thus enabling appropriate precautionary measures to be implemented.

The art of subsidence prediction and hence its control, for both longwall and room-and-pillar mining systems, is far from approaching maturity in this country. It is important, therefore, to develop and implement subsidence prediction methods, which can provide mining operators in this country with flexible and rational estimations of mining subsidence.

The objective of this research effort was to develop a computer model of subsidence prediction based on the zone area method. This technique was chosen because of its potential to investigate a mining plan of any shape, thus facilitating subsidence prediction over longwall as well as room-and-pillar coal mining systems.

To investigate and develop regional subsidence trends, a comprehensive subsidence data bank was established, which included published as well as unpublished information on subsidence measurements. Based on these case studies, some fundamental characteristics of longwall subsidence were established and this information was utilized to develop an empirical prediction method. The established relationships were also used for the formulation and subsequent testing of the modeling procedures. From the results and comparisons of this study it was demonstrated that the zone area method has considerable potential for accurate, rational and flexible subsidence predictions.

II. THE DEVELOPMENT OF THE ZONE AREA METHOD

Subsidence has been recognized in Britain since the early fifteenth century, as revealed from court records of disputes and litigations related to property damage above mine workings (Shadbolt, 1978).

The first attempts to investigate and analyze the mechanisms associated with mining subsidence, however, date back to the 1800's and were pursued by Belgian engineers. This research effort was initiated as a result of the widespread movements and subsequent structural damage suffered by the city of Liege in the 1820's. The most notable achievement of the Belgian school of that era was the publication of Gonot's treatise "Loie de la Normal" in 1871 (Gonot, 1871).

Since that time, many theories have been advanced to explain the mechanism of ground movement as it develops from the excavation, through the superincumbent strata, to the surface. Such theories include the original concepts of beams, arches, domes and the contemporary mathematical modeling principles of strata movement assuming two extreme concepts, a continuous elastic and a stochastic medium, for the superincumbent strata. An excellent review of the development of these theories is given by Shadbolt (1978). In conjunction with the theories of mass strata movement in the vicinity of mine workings, the topic of surface subsidence predictions has also been the subject of extensive research. The development of reliable and rational techniques of subsidence prediction is imperative if this phenomenon is to be recognized and controlled within acceptable environmental levels. Empirical as well as mathematical methods have been proposed to fulfill this objective and a comprehensive analysis of these methods has been presented in the literature (Voight and Pariseau, 1970; Brauner, 1973; Shadbolt, 1978; Virginia Polytechnic Institute and State University, 1980).

The zone area method of subsidence prediction is based on the theory of influence functions, one of the most fundamental concepts in the study of mining subsidence. The theory of influence functions implies the acceptance of the law of superposition, which states that the total subsidence, due to an underground excavation, is the sum of the individual subsidences resulting from each of the infinitesimal extractions or influences comprising the excavation (Figure 1). According to this principle, therefore, strata movements radiate to the ground surface from point sources at the excavation level. Furthermore, an influence area can be attributed to every surface point. Complete extraction of the influence area will cause maximum subsidence, whereas partial extraction will produce incomplete subsidence of the point in question.

The original work on the influence functions is accredited to both German and Dutch engineers and dates back to the early 1920's, when Kohne, a Surveyor and Manager of the Emscher Water Board in Essen, Germany, developed the first influence function method for predicting mining subsidence in that coal region. Kohne suggested that the subsidence of any surface point, P, is influenced by the extraction of two zones, representing two concentric rings about the point in question, as shown in Figure 2.

The inner zone is subtended by twice the angle of break and accounts for two-thirds of the maximum subsidence of point P, whereas the outer zone is subtended by twice the angle of draw and is responsible for the remainder. Keinhorst (1928), a co-worker and Kohne's successor at the Emscher Board, developed further these principles and, in addition, attempted to analyze the resultant horizontal displacements.

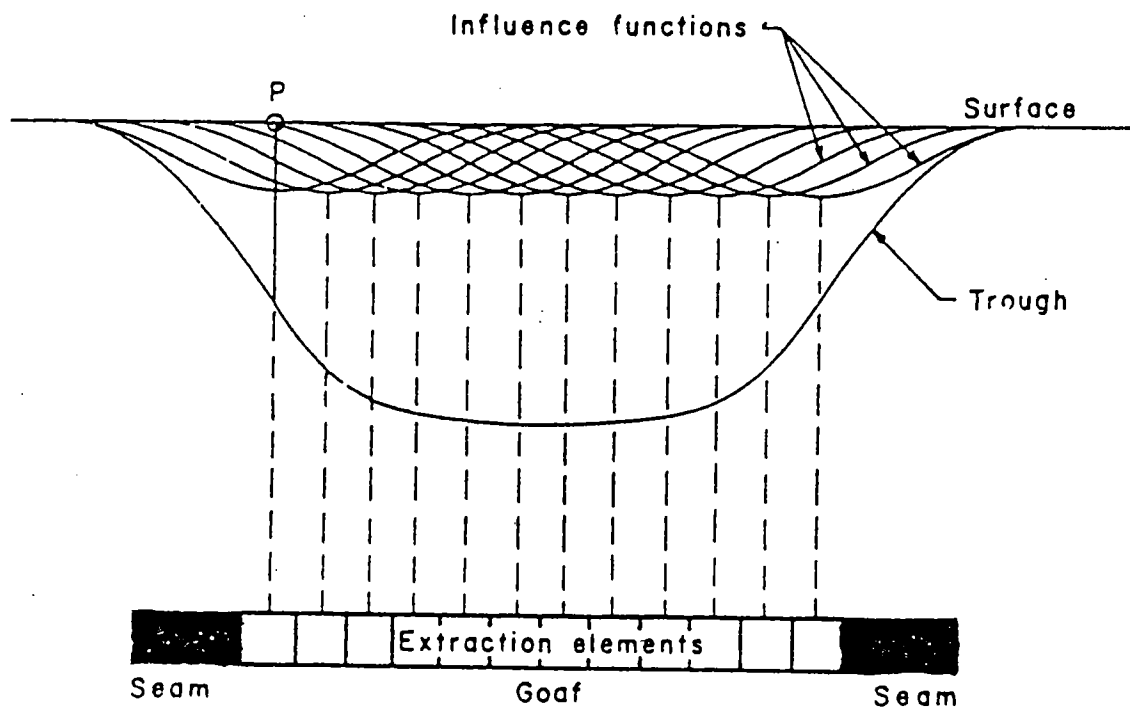


Figure 1: Law of Superposition
(after Brauner, 1973)

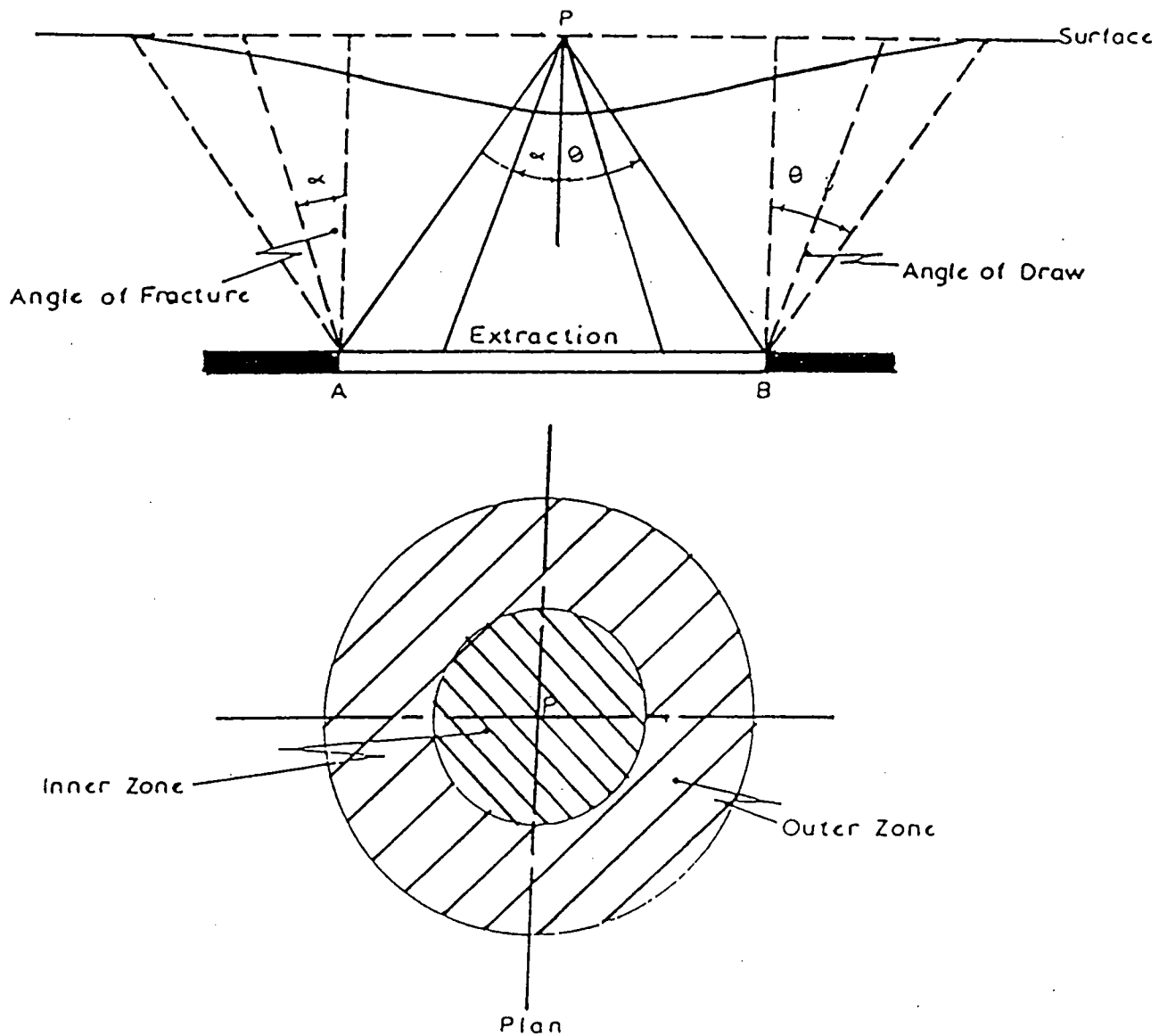


Figure 2: Kohne's Influence Function
(After Sinclair, 1963)

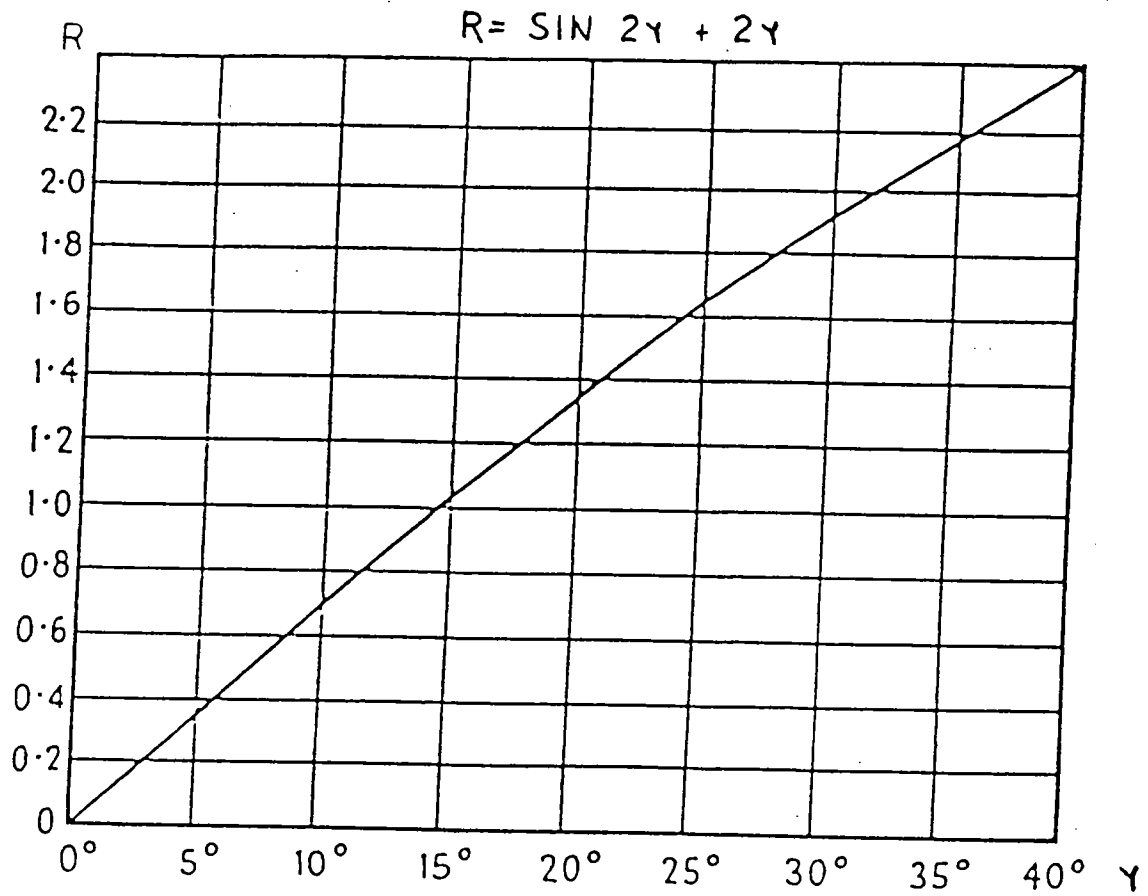


Figure 3: Radius, R, vs Draw Angle,
(After Sinclair, 1963)

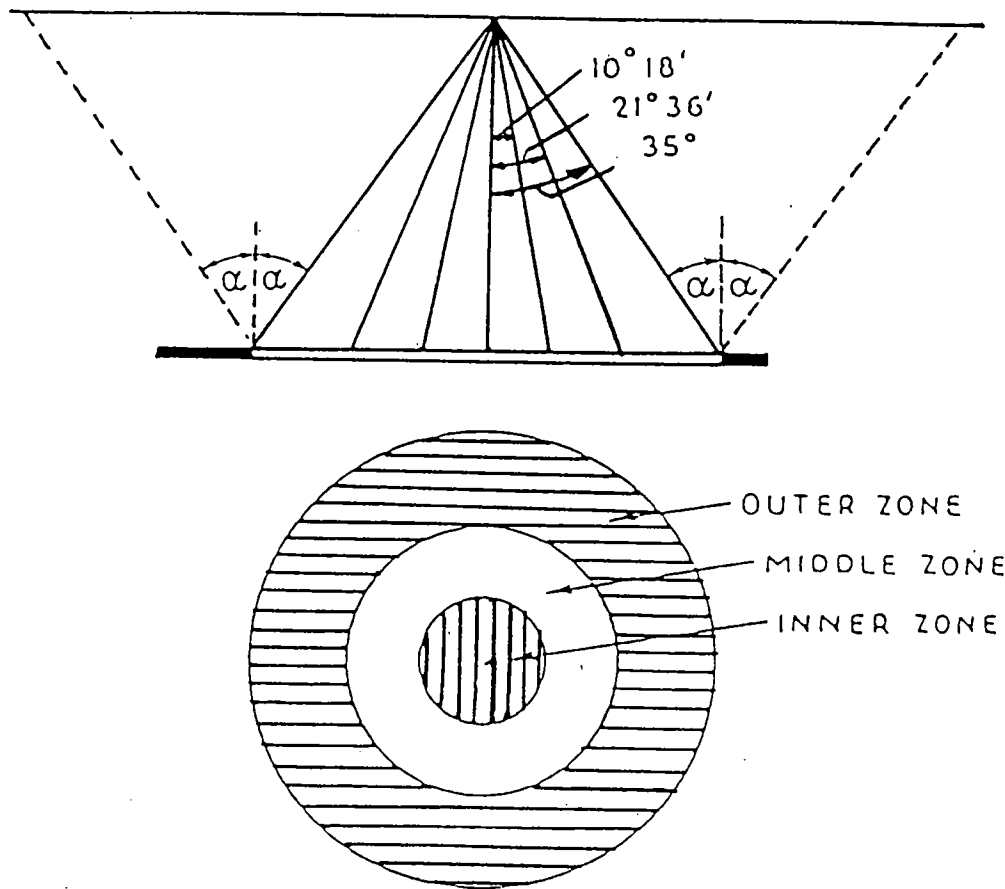


Figure 4: Bals' Influence Function
(After Sinclair, 1963)

However, it was Bals, a German mine surveyor, who first developed a mathematical formulation of mining subsidence using the principle of influence functions (Bals, 1932). In his analysis, Bals assumed that the extracted area consisted of an infinitely large number of small and equal masses, each exerting an attraction on the surface point inversely proportional to the square of the separating distance, in accordance with Newton's Law of gravitation. Consequently, the subsidence, s , of any point on the surface can be expressed as

$$s = S.a.t \quad . . . (1)$$

where

S = maximum subsidence of the point.

a = influence coefficient or factor.

t = time coefficient, equal to one for completed or static subsidence profiles.

Assuming total extraction, Bals developed an influence expression in the form of $\sin 2Y + 2Y$, where Y is the angle of draw and $2Y$ is the apex angle of the cone, determine by the complete extraction of the influence area, as shown in Figure 3.

In order to calculate the subsidence of a point above a partially extracted area, Bals divided the total area into a number of annular rings or zones of equal influence (Figure 4). The apex angle, $2Y_n$, subtending each ring of radius R_n , was calculated from the graphical expression of the influence equation. Using this procedure the partially extracted areas, for a particular size of excavation, can be computed and their sum, multiplied by the influence of the zones on the maximum subsidence, can be used to calculate

the influence coefficient, a , of equation (1). The application of this method has been well documented in the literature (Bals, 1932; Grond, 1953; Sinclair, 1963; Zenc, 1969; Brauner, 1973; Adamek and Jeran, 1981).

Later developments on the influence functions are attributed to Dutch engineers Meyers and Drent of the Dutch State Mines (Grond, 1953; Sinclair, 1969; Shadbolt, 1978). From their vast experience in observing mining subsidence over the South Limburg coalfield, Meyers and Drent suggested that the area of influence below a surface point, P , be divided into five concentric rings or zones of equal radius, as shown in Figure 5. The subsidence, s , of that point can be expressed, therefore, as

$$s = a_1x_1t + a_2x_2t + \dots + a_5x_5t \quad \dots(2)$$

where

$a_1, a_2 \dots a_5$ = influence factors for each zone

$x_1, x_2 \dots x_5$ = proportional extracted areas

(equal to one for complete extraction)

t = seam thickness

In using the above equation, the proportional extracted areas must be determined from the mine plans, in a manner similar to Bals method. The influence factors, however, must be calculated from measured subsidence profiles, by solving a series of five equations.

This method has been very popular with the Dutch State Mines and it has been suggested that such subsidence predictions were within five to fifteen percent of the observed values. It is interesting to note, however, that although these early influence functions methods became very popular in Central Europe, they were also criticized and considered non-applicable by

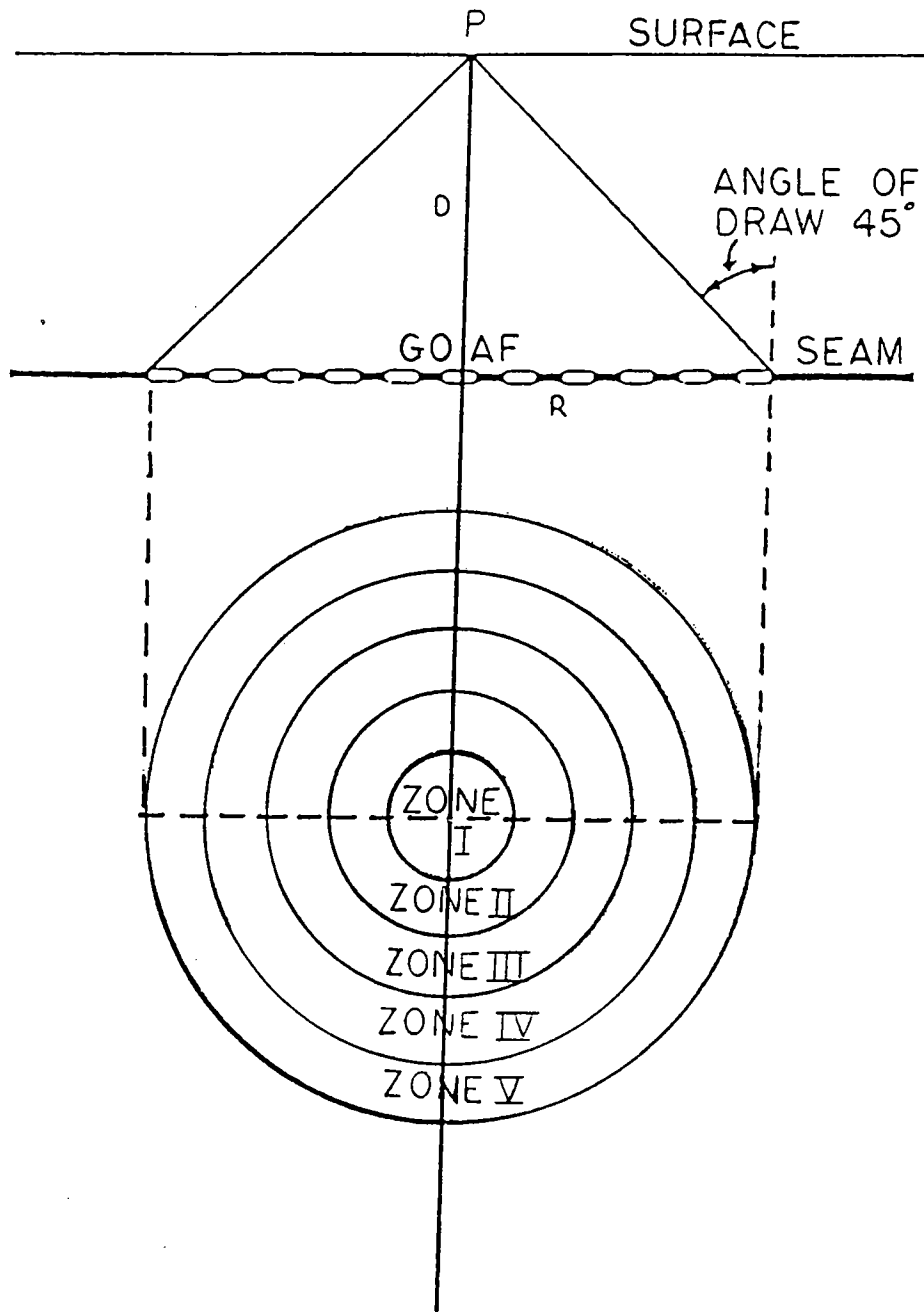


Figure 5: Meyers and Drent Influence Function
(After Sinclair, 1963)

investigators in other parts of the world. Perhaps the most quoted limitation of this approach is that of the ribside subsidence.

Assume a surface point located directly above the edge of a critical excavation. In this case only half of each zone has been extracted (Figure 6a), thus resulting in a subsidence equal to half the maximum value and causing inflection of the subsidence profile at this point. This deduction was contradicted by many field studies in Germany as well as in Britain. In the latter case, subsidence over ribside was found to be in the order of 20 percent of the maximum, or approximately 18 percent of the seam thickness (Marr, 1975). Furthermore, in most case studies, half maximum subsidence was located at a distance of $0.143h$ inside the ribside, where h is the depth of the workings, which in turn implied that the proportional areas extracted must be greater than half the total zones (Figure 6b).

Bals was aware of the ribside subsidence limitation of the influence area method and suggested that smaller subsidence factors may be used for the points above the ribside. Such an approach, however, was disputed by other investigators as being non-practical and unnecessarily complex (Niemczyk as quoted in Flaschentrager, 1957). A more efficient method of correcting ribside subsidences is to deduct from the extraction area the compensation zone. The latter, according to Flaschentrager (1957), is the zone of incomplete closure at the ribside of the excavation, which for the purpose of the calculations, can be treated as if it were unmined (Brauner, 1973). This procedure will result in lower ribside subsidences than the original value of half the maximum subsidence and thus will lead to more representative values.

Refinement of the influence functions was, therefore, necessary and it was accomplished by the development of the zone area method in Britain (Marr,

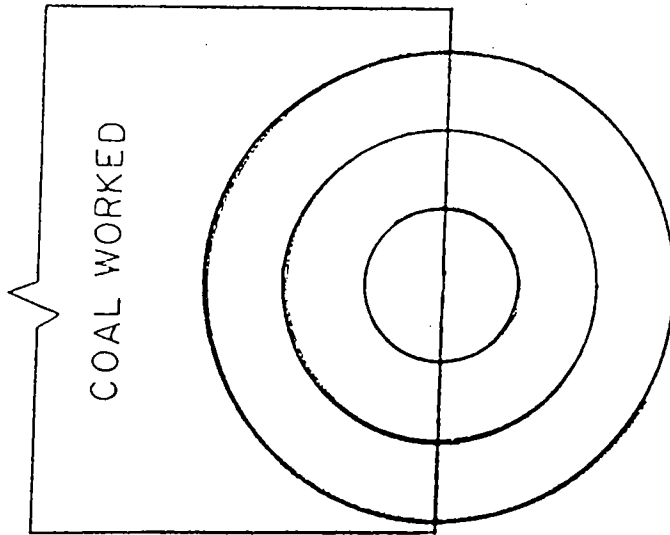


Figure 6a: Half-Zone Extraction

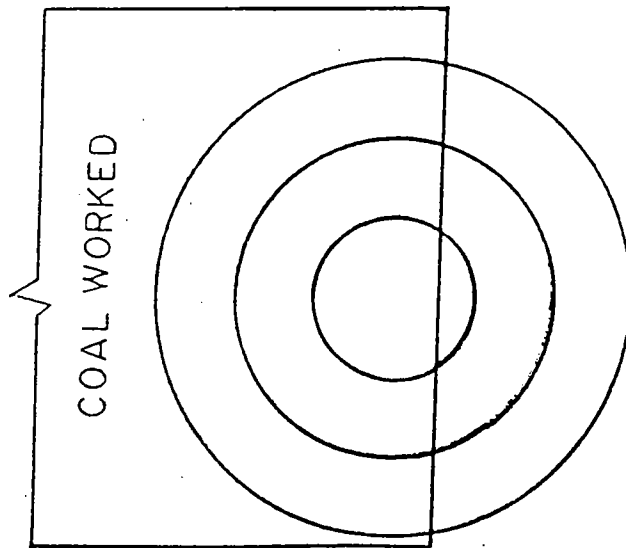


Figure 6b: Zone Extraction for Half-Maximum Subsidence

1975). This technique was originally designed to compliment the Subsidence Engineers' Handbook for predicting ground movements over non-uniform extractions (NCB, 1975).

Research suggested that the influence area of a surface point be divided into seven annular zones. The radius of the influence area, R, was defined as

$$R = h \tan y$$

where

$$h = \text{mining depth}$$

$$y = \text{draw angle}$$

Assuming a draw angle of 35 degrees for British mining conditions, the radius of the influence area is 0.7 of the mining depth, with each zone radius being 0.1 of the mining depth.

In applying this method, each zone was assigned a zone factor to weight its contribution to the final subsidence value, i.e.

$$s/m = ax_1 + bx_2 + cx_3 + dx_4 + ex_5 + fx_6 + gx_7 \dots (3)$$

where a, b, c, . . . = zone factors

x_1, x_2, x_3, \dots = proportional extracted areas

s = subsidence

m = seam thickness

Further research indicated that this expression did not satisfy the rib-side subsidence conditions mentioned earlier. To eliminate this discrepancy, the British investigated a non-linear relationship between subsidence, s, and proportional extracted area, x, in the form of

$$s = Ax^n$$

where

A = zone factor

n = influence constant, unity if the relationship is linear

By incorporating this concept to the seven term expression given earlier, the following equation can be obtained (Figure 7):

$$s/m = ax_1^n + bx_2^n + cx_3^n + dx_4^n + ex_5^n + fx_b^n + gx_7^n + \dots (4)$$

In applying the above equation, the zone factors and the influence constant must be determined from field measurements. For example, assuming complete extraction, the subsidence factor (in this case corresponding to critical or complete subsidence) is given by

$$s/m = a(1.00)^n + b(1.00)^n + c(1.00)^n + d(1.00)^n + e(1.00)^n + g(1.00)^n \dots (5)$$

In addition, above the ribside each zone is half extracted and the subsidence factor is given by

$$s/m = a(0.50)^n + b(0.50)^n + c(0.50)^n + d(0.50)^n + e(0.50)^n + f(0.50)^n + g(0.50)^n \dots (6)$$

By solving equations 5 and 6, the influence constant, n, can be determined for a critical extraction,

$$n = \frac{\log S/m - \log s/m}{\log 2} \dots (7)$$

where S/m and s/m are the subsidence factors at the panel center line and the ribside, respectively.

In cases of subcritical extractions, the above equation must be modified to the following format:

$$n = \frac{\log S/m - \log s/m}{\log 2 - \log A_e}$$

where

A_e is the proportional extracted area.

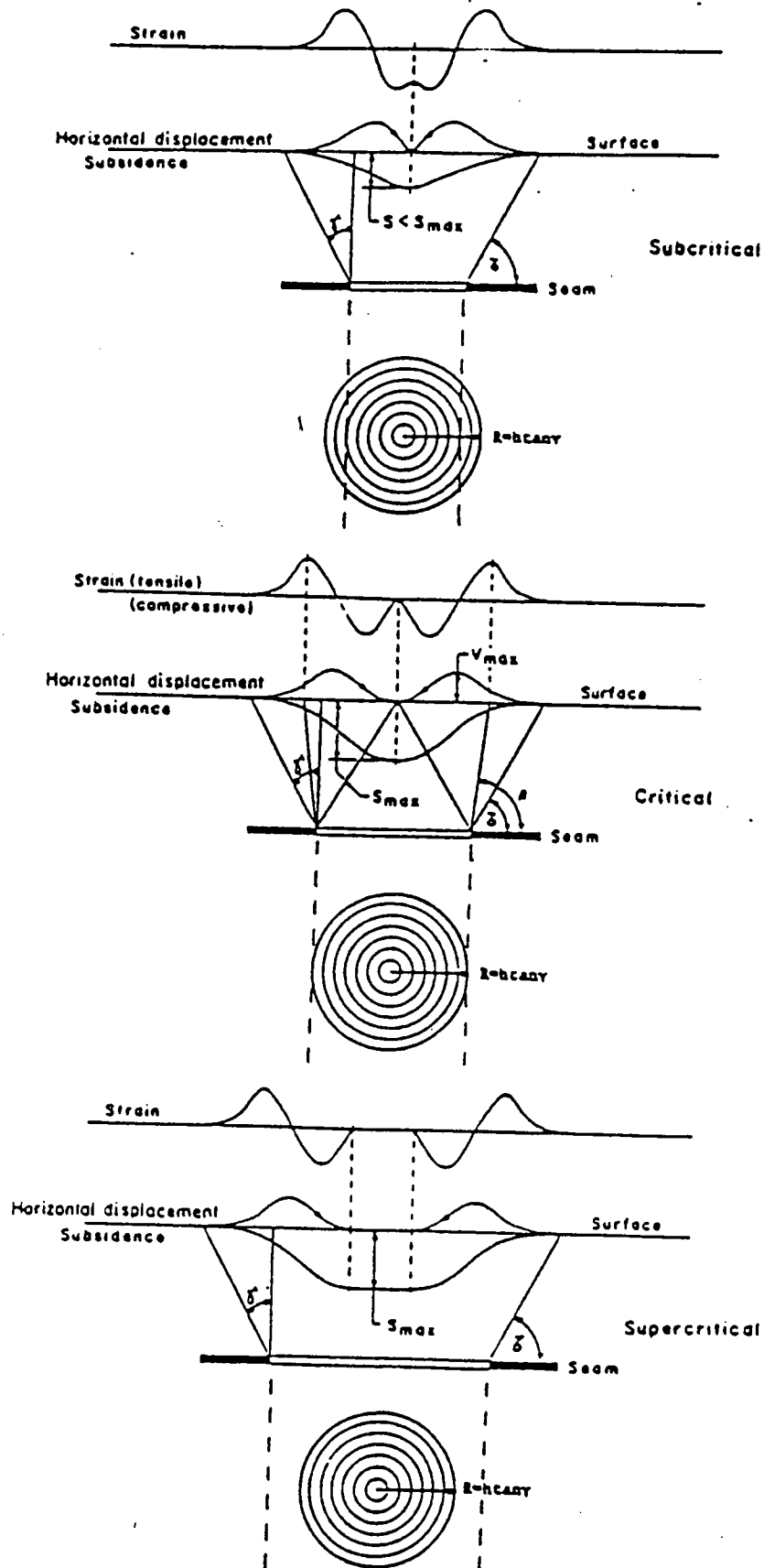


Figure 7: The Zone Area Method

Once the value of the influence constant is determined for a given situation, the zone factors can be calculated by solving the following seven-by-seven matrix:

$$\begin{bmatrix} s/m_1 \\ s/m_2 \\ s/m_3 \\ s/m_4 \\ s/m_5 \\ s/m_6 \\ s/m_7 \end{bmatrix} = 1.00^n \begin{bmatrix} x_{11} & x_{12} & x_{13} & x_{14} & x_{15} & x_{16} & x_{17} \\ x_{21} & x_{22} & x_{23} & x_{24} & x_{25} & x_{26} & x_{27} \\ x_{31} & x_{32} & x_{33} & x_{34} & x_{35} & x_{36} & x_{37} \\ x_{41} & x_{42} & x_{43} & x_{44} & x_{45} & x_{46} & x_{47} \\ x_{51} & x_{52} & x_{53} & x_{54} & x_{55} & x_{56} & x_{57} \\ x_{61} & x_{62} & x_{63} & x_{64} & x_{65} & x_{66} & x_{67} \\ x_{71} & x_{72} & x_{73} & x_{74} & x_{75} & x_{76} & x_{77} \end{bmatrix} \begin{bmatrix} a \\ b \\ c \\ d \\ e \\ f \\ g \end{bmatrix}$$

Analysis of British profiles for panels with various width-to-depth ratios yielded the following values for the zone factors and the influence constant:

$$\begin{array}{ll}
 n = 2.296 & d = 0.219 \\
 a = 0.056 \text{ (inner zone)} & e = 0.109 \\
 b = 0.199 & f = 0.045 \\
 c = 0.259 & g = 0.130 \text{ (outer zone)}
 \end{array}$$

The effect of coal pillars on the final subsidence profile cannot be neglected. Empirical studies revealed that the recorded subsidence over the center of a coal pillar was less than that expected by superposition if the pillar's width-to-depth ratio (W/h) was less than 0.5 (Figure 8).

It was decided that a zone area method could be used to determine the necessary subsidence reduction for a pillar with W/h less than or equal to

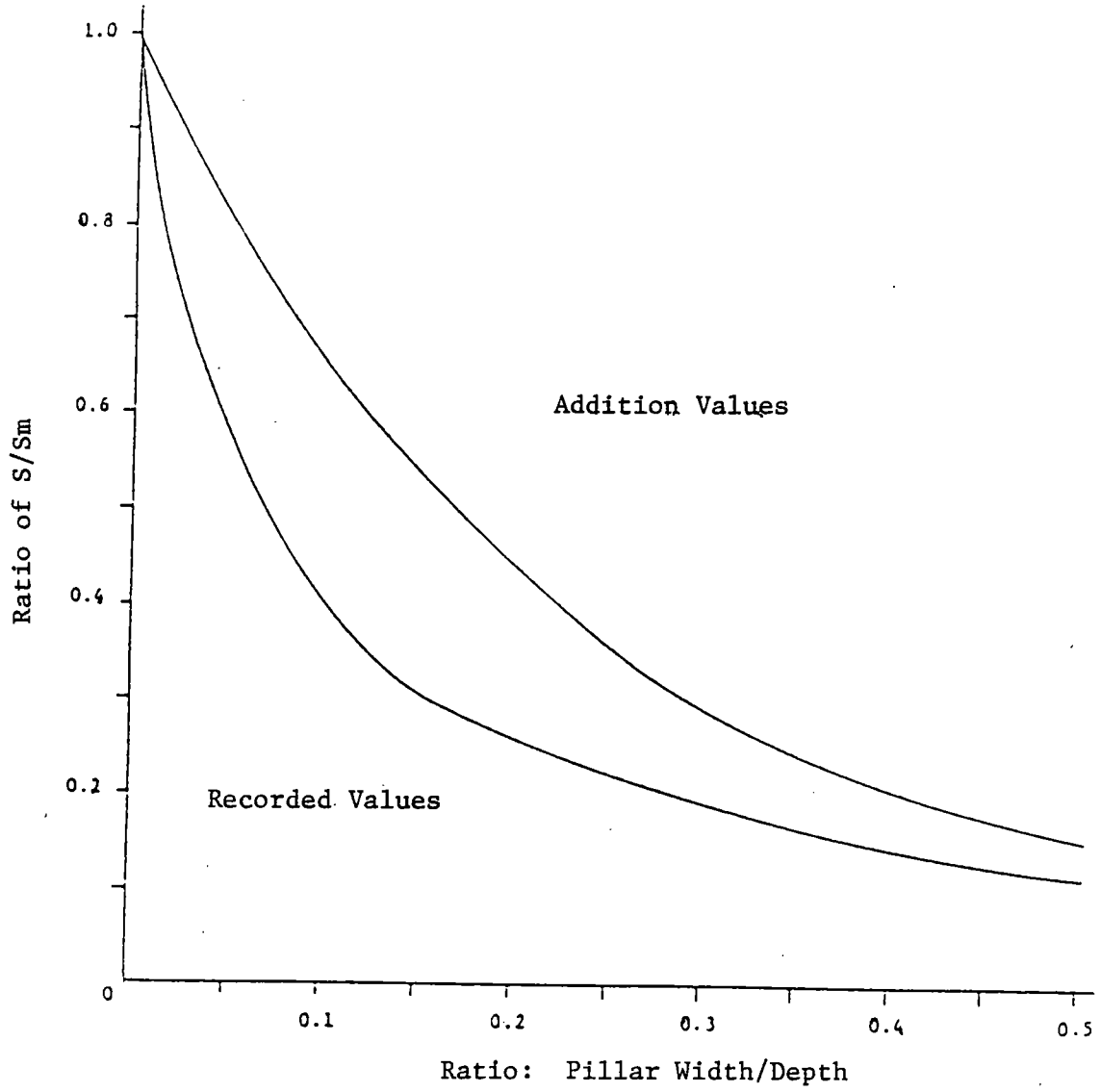


Figure 8: Coal Pillar Reduction Effects
(after Marr, 1975)

0.5. Experience indicated that pillars with W/h of 1.00 resulted in zero subsidence, i.e., a reduction of 90 percent of the extracted seam thickness. The application of this information yielded a maximum reduction radius of 0.5h. For convenience, 5 zones were used, each having a radius of 0.1 of the depth.

Empirical evidence indicates that over the edge of very wide pillars, the subsidence should be less than or equal to half the maximum reduction, or 0.45. The proportional extracted areas in the half-extracted zones must be raised to a power greater than or equal to unity. Empirical profiles show that reduction values at the rib-side exceed 0.45, thus indicating a linear relationship between reduction values and proportional extracted areas.

Analysis of reduction profiles yielded the following five zone system for subsidence reduction due to the presence of a pillar:

$$R = 0.215x_1 + 0.300x_2 + 0.270x_3 + 0.110x_4 + 0.005x_5$$

where x_1, x_2, x_3, \dots = proportional pillar areas (x_1 = inner zone)

To further correct the subsidence over pillars, the curve shown in Figure 9 was utilized to determine a corrected reduction value.

To evaluate the subsidence of a point situated over a pillar with W/h ratio less than 0.5, the subsidence is first predicted using a seven zone system for all working areas, including the area of the pillar. A five zone reduction system is then applied to the pillar in question to determine the reduction value. This value is further corrected by Figure 9. Subtraction of this result from the seven zone value represents the actual subsidence of the point over the pillar (Marr, 1975).

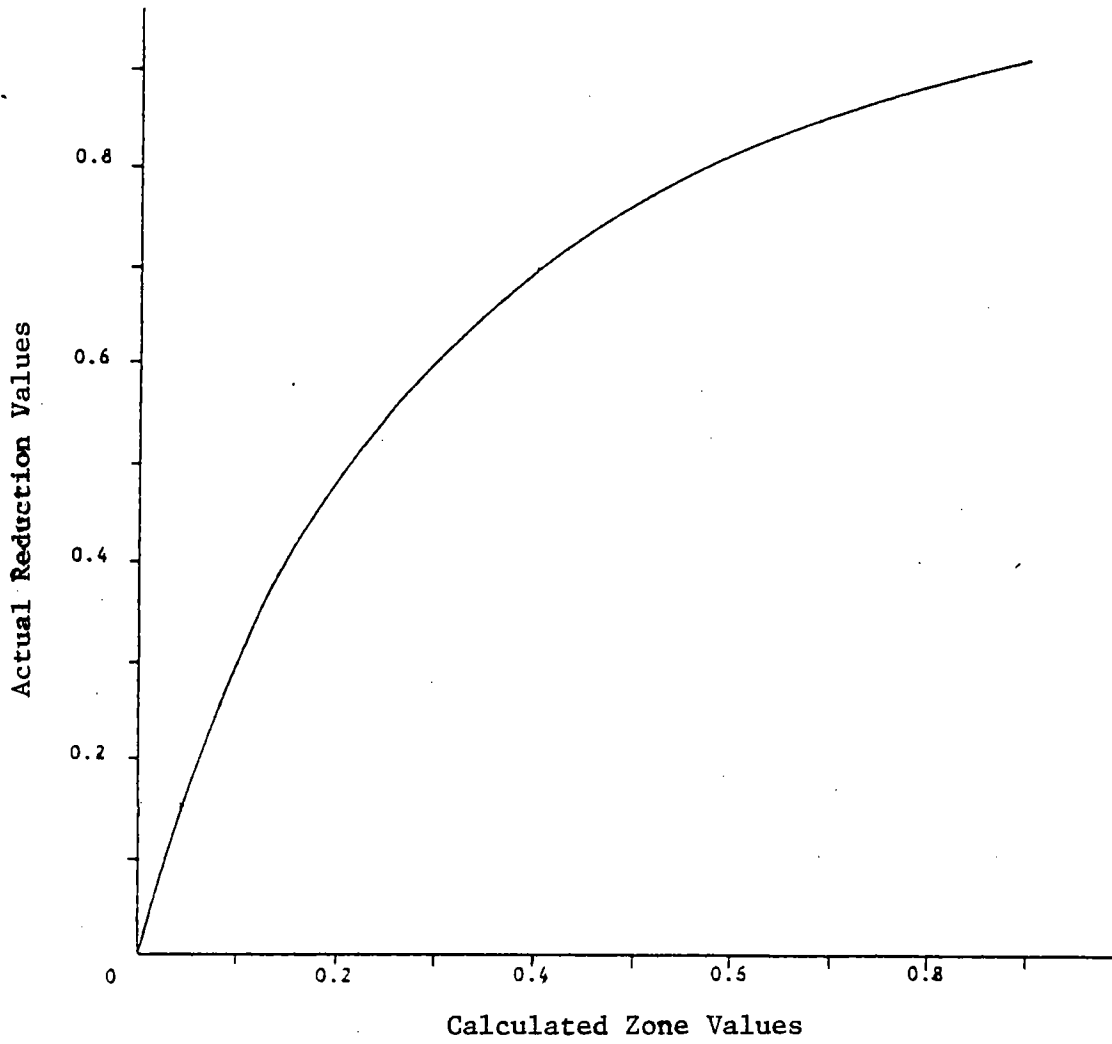


Figure 9: Pillar Reduction Correction Curve
(after Marr, 1975)

Subsidence prediction using the zone area method is accurate for seam gradients up to 20 degrees, as the area of influence remains circular up to this point. For steeper gradients, the application of this method is questionable.

III. COMPUTER MODELING OF THE ZONE AREA METHOD

A computer program was developed in this research to effectively utilize the zone area method of subsidence modeling and to facilitate repeated evaluations of the seven term zone system over a large area. The development of this program required a number of assumptions. The panels and pillars were assumed to be rectangular in shape, thus facilitating the development of an algorithm to compute the necessary proportional extracted areas for each zone. The requirement of rectangular panels and pillars is a reasonable assumption, approximating most mining layouts. Panels and pillars were also aligned with a generated north-south coordinate grid, allowing each to be easily defined and located. Finally, barrier pillars separating two extracted panels were assumed to have extensive wastes on both sides.

The determination of the proportional extracted area of each zone is critical to the calculation of subsidence by the zone area method. It was discovered that a subtractive method was most applicable, whereby all pillars were individually checked for an intersection with a particular zone. The intersected areas of each zone were summed and then subtracted from the area of that particular zone, thus yielding the extracted area.

The boundaries of each pillar were designated by a series of four linear equations. Two of these equations were identified as the north-south boundaries and were of the form $X=c$, where "c" was the easting coordinate of each boundary. Similarly, the two east-west boundaries were represented as $Y=b$, where "b" corresponded to their northing coordinates (Figure 10).

The equation of any zone, centered at a point (r, s) on the generated coordinate grid, is that of a circle, i.e.,

$$(X - r)^2 + (Y - s)^2 = R^2 \quad (8)$$

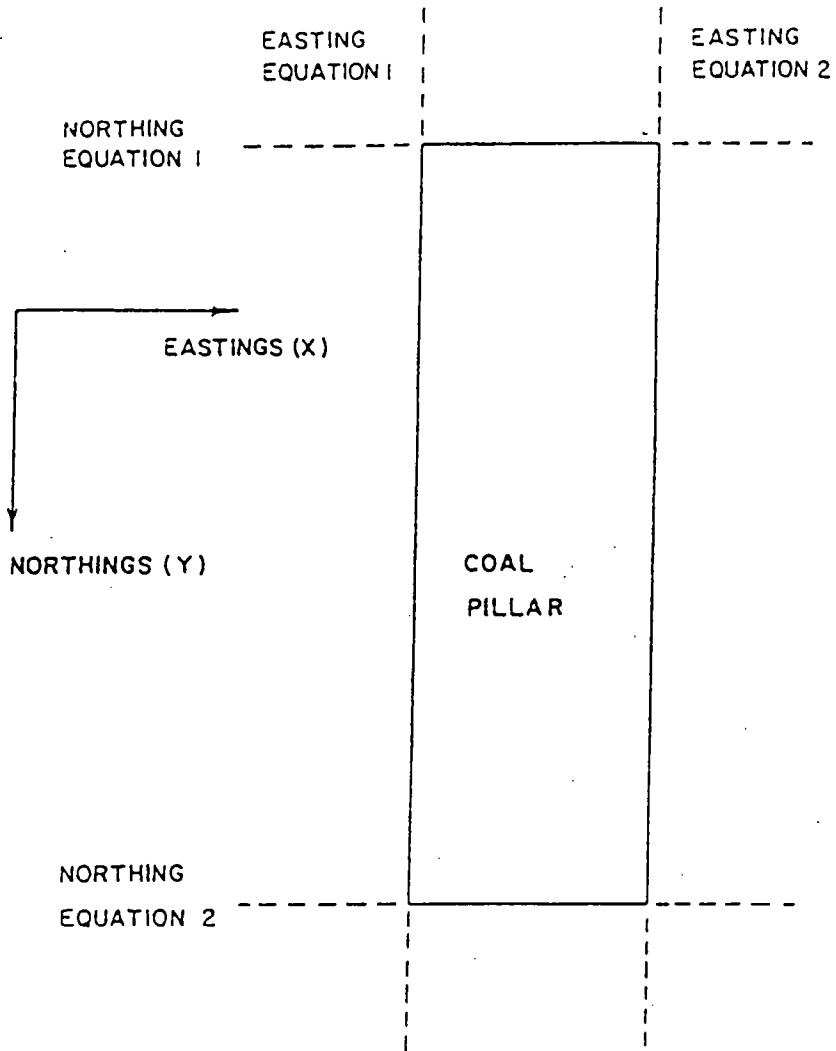


Figure 10: Positions of the Four Pillar Boundary Equations.

where "R" is the radius of that particular zone. To determine possible intersections between a zone and a certain pillar or panel, each of the four boundary equations was separately substituted into the above equation. By solving the resulting expression for either X or Y, possible intersections were located which enabled calculation of the coordinates. The intersection of a circular zone with a rectangular pillar or panel will yield, at most, three different extracted sectors as shown in Figure 11. This enabled an algorithm to be developed, which could determine the size and shape of each extracted sector, given the intersection coordinates.

The technique of double integration was selected to evaluate the area of each sector using the generated data. This method provided adequate versatility in evaluating sectors of varying shape. In applying this procedure, two distinct integration forms were possible. The first integrated in the easting or x-direction followed by an integration in the northing or y-direction. The other form simply reversed the integration order. By arranging each expression in general terms, the area of any extracted sector could be determined by, simply, substituting the required boundary values.

Considering the latter as an example and utilizing Sector 3 in Figure 11b, integration would proceed in the Y-direction first, followed by integration in the X-direction. This would yield the following expression:

$$\text{Area} = \int_{X_2}^F \int_{Y_1}^S + R^2 + (x - r)^2 \text{ dydx}$$

where X_2 and F are the easting limits of integration.

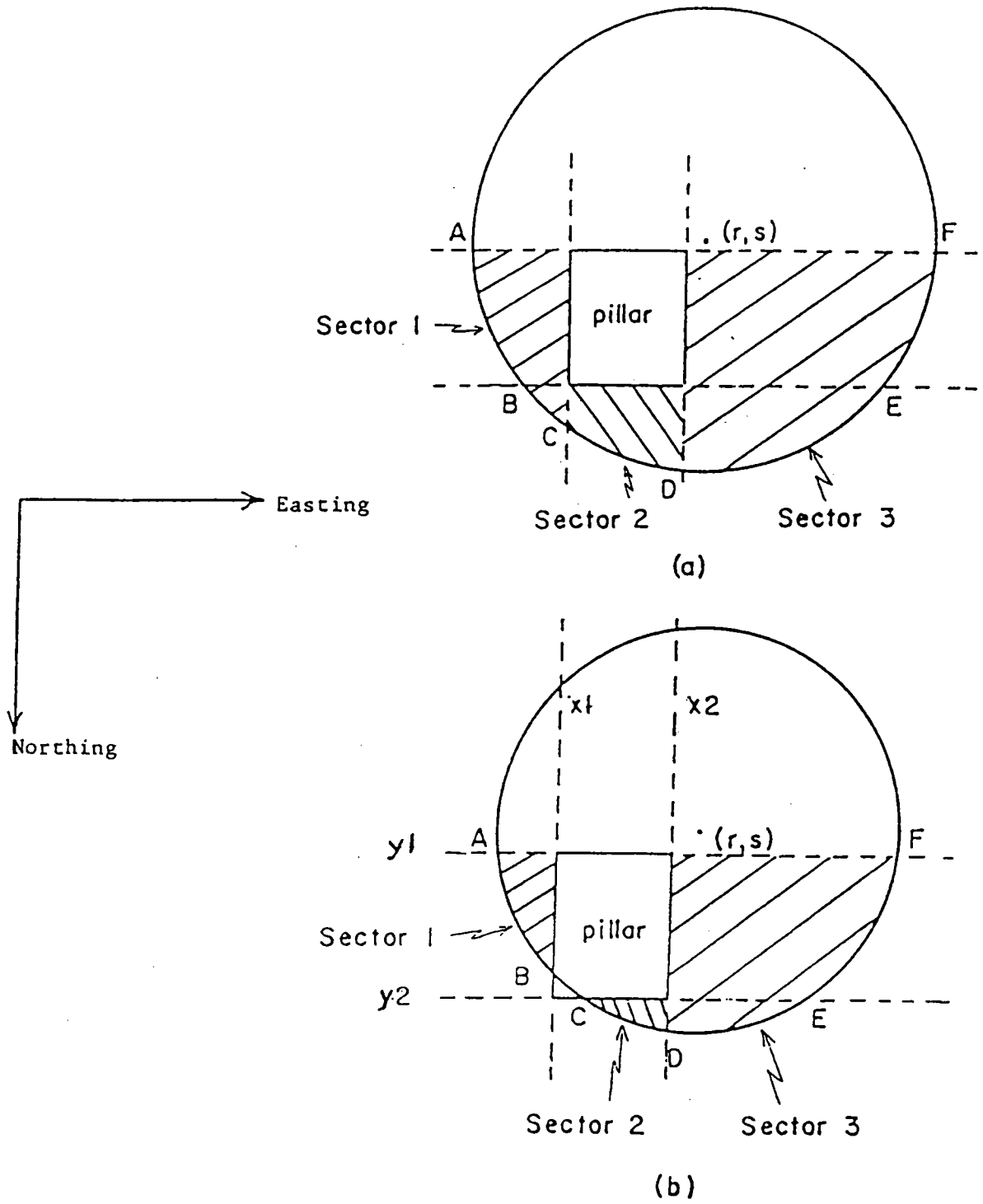


Figure 11: Intersection Points and Extracted Sectors For a Pillar-Zone System (Two Cases)

The inner integral provides integration limits in the northing direction. The upper limit is simply the circle or zone equation solved for Y. Evaluation of this integral yields the equation

$$\text{Area} = \int_{X_2}^F [R^2 - (X - r)^2 - (Y_1 - s)] dx$$

The first term of the equation has the form $(a^2 - b^2)$ and computation of the integral will determine an expression relating intersection coordinates and zone origin coordinates to the area of the sector: i.e.

$$\text{Area} = 0.5(X-r)(R^2 - (X-r)^2)^{0.5} + R^2 \sin^{-1} ((X-r)/|R|) - (y_1 - S) \Big|_{x_2}^F$$

A similar relation for initial integration in the X-direction can be obtained, as shown:

$$\text{Area} = 0.5(Y-r)(R^2 - (Y-r)^2)^{0.5} + R^2 \sin^{-1} ((Y-r)/|R|) - (x_1 - S) \Big|_{y_1}^F$$

Application of these equations allows computation of proportional extracted areas for zones centered over extracted panels. Modification of the algorithm was required to determine extracted areas when the zones are centered over a barrier pillar. In order to compute these values accurately, the coordinates of the extracted panel and of the barrier pillar are interchanged, so that the proceeding expressions can be used to determine proportional extracted areas.

The computer model consists of a MAIN program plus eight subroutines which conduct specialized functions necessary for the operation of the program. A detailed flowchart is given in Appendix A.

The MAIN program is responsible for the input of data, initialization of values and final output. After the data is entered into the program, a coordinate grid is established over the investigation area according to user specifications. Zone evaluation begins in the upper-left (north-west) corner of the grid and proceeds in the easterly or positive direction until the maximum easting coordinate is reached. The zone origin then moves back to the minimum easting boundary and increases its northing coordinate by one grid. The evaluation process proceeds as before until the maximum northing boundary is reached, at which time subsidence computation ends.

The implementation of the zone area computer model requires the following input information:

- coordinates of area of interest where subsidence is to be investigated
- panels and pillars defined by rectangular coordinates
- zone interval
- draw angle, zone factors and influence constant representative of the area being investigated
- seam and surface dips and gradients
- extraction height
- graphics input, if desired.

The output of the subsidence model consists of a listing of the user's input information, as well as the subsidence values predicted by the zone area model. The values are listed according to their northing coordinate with further division by their easting coordinate. Graphics output consists of cross-sectional graphs and contour maps printed on either the Versatec or Calcomp plotters.

Examples of input and output files are given in Appendices B and C.

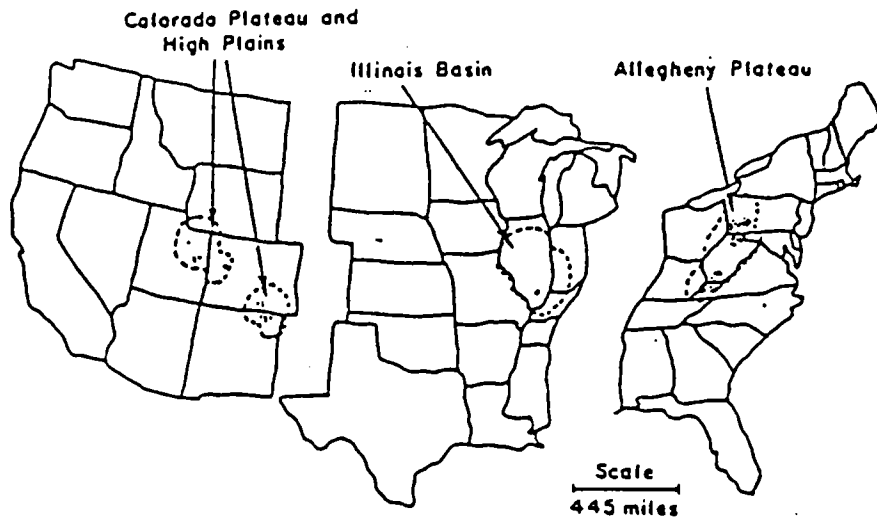
IV. COLLECTION AND ANALYSIS OF SUBSIDENCE CASE STUDIES

Subsidence information from foreign coalfields cannot be applied directly to mining conditions in this country. Subsidence depends on regional geology, strata properties and mining methods and, as a result, it exhibits regional characteristics. Substantial differences in subsidence trends can be expected, therefore, not only between British and domestic observations, but also, between those observed in the various coal regions in this country.

During this investigation, a major effort was undertaken to develop a comprehensive data bank on mining subsidence, which can be utilized to establish regional subsidence characteristics in the United States. Furthermore, such information can be used to validate the applicability of the various methods of subsidence prediction and control in this country.

In order to accomplish this objective, all relevant published information on mining subsidence was collected and, in addition, numerous coal companies were contacted to contribute any unpublished information that might be of interest to this study. Due to the lack of information pertaining to regional subsidence trends, the coal-producing areas were grouped into three main regions (Figure 12), based only on structural geology characteristics, namely the Allegheny Plateau, the Illinois Basin and the Colorado Plateau and High Plains (O'Rourke and Turner, 1979). All collected information, therefore, was assigned to one of these regions and for the zone area analysis, each region is treated individually.

The data collection phase has been very successful and a substantial number of case studies have been gathered, particularly with reference to longwall panels in the Appalachian coalfield. Preliminary analysis of these data has revealed some interesting subsidence characteristics in this region.



Legend:
• site of coal mine

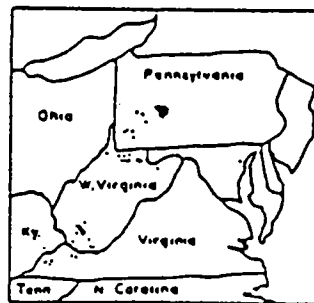


Figure 12: Location of Longwall Coal Mines in the United States. (O'Rourke & Turner, 1979)

The observed angles of draw ranged from 12 to 34 degrees. It is interesting to note, however, that for panel width-to-depth ratios in excess of 1.2 a constant angle of draw was reached, (Figure 13). This trend is considerably smaller than that suggested by the British case studies, which have indicated an average draw angle of 35 degrees (Marr, 1959).

The range of the maximum subsidence factors for the collected case studies is shown in Figure 14, together with the NCB limits for caving. The Appalachian data clearly show smaller subsidence factors than those forecasted by the Subsidence Engineer's Handbook. It should also be noted, that for panel width-to-depth ratios of more than 1.2 the maximum subsidence factor appears to approach asymptotic conditions.

From these results it is possible to conclude that the NCB's empirical prediction methods will overpredict both subsidence magnitude as well as the area of influence of the underground extraction, when applied to domestic conditions. Furthermore, such overestimations can be considerable. Therefore, although the methodologies and concepts suggested by the Subsidence Engineer's Handbook are of immense value, quantitative deductions using this method must be treated with caution when referring to the Appalachian conditions.

The results also suggest that critical conditions are reached for W/h ratios of about 1.2 as opposed to 1.4 for British conditions. This conclusion is also confirmed from the relationship of Figure 15 where the position of the inflection point is shown as a function of panel width-to-depth ratio. This relationship also suggests that, for critical extractions, the inflection point is located about $0.20h$ inside the ribside, whereas similar measurements in the U.K. have indicated a distance of about $0.14h$. Such trends are

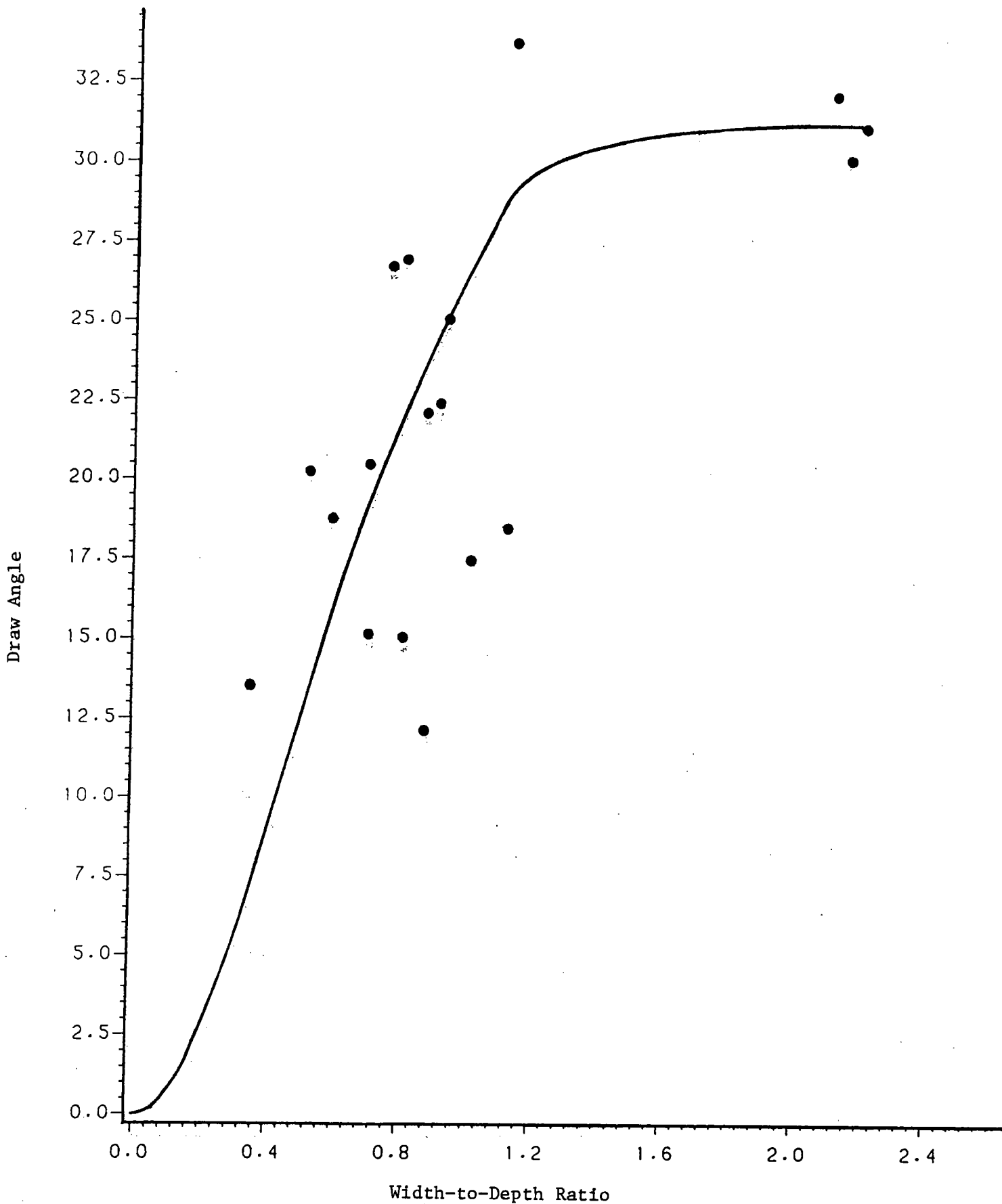


Figure 13: Variation of Draw Angle with Width-to-Depth Ratio

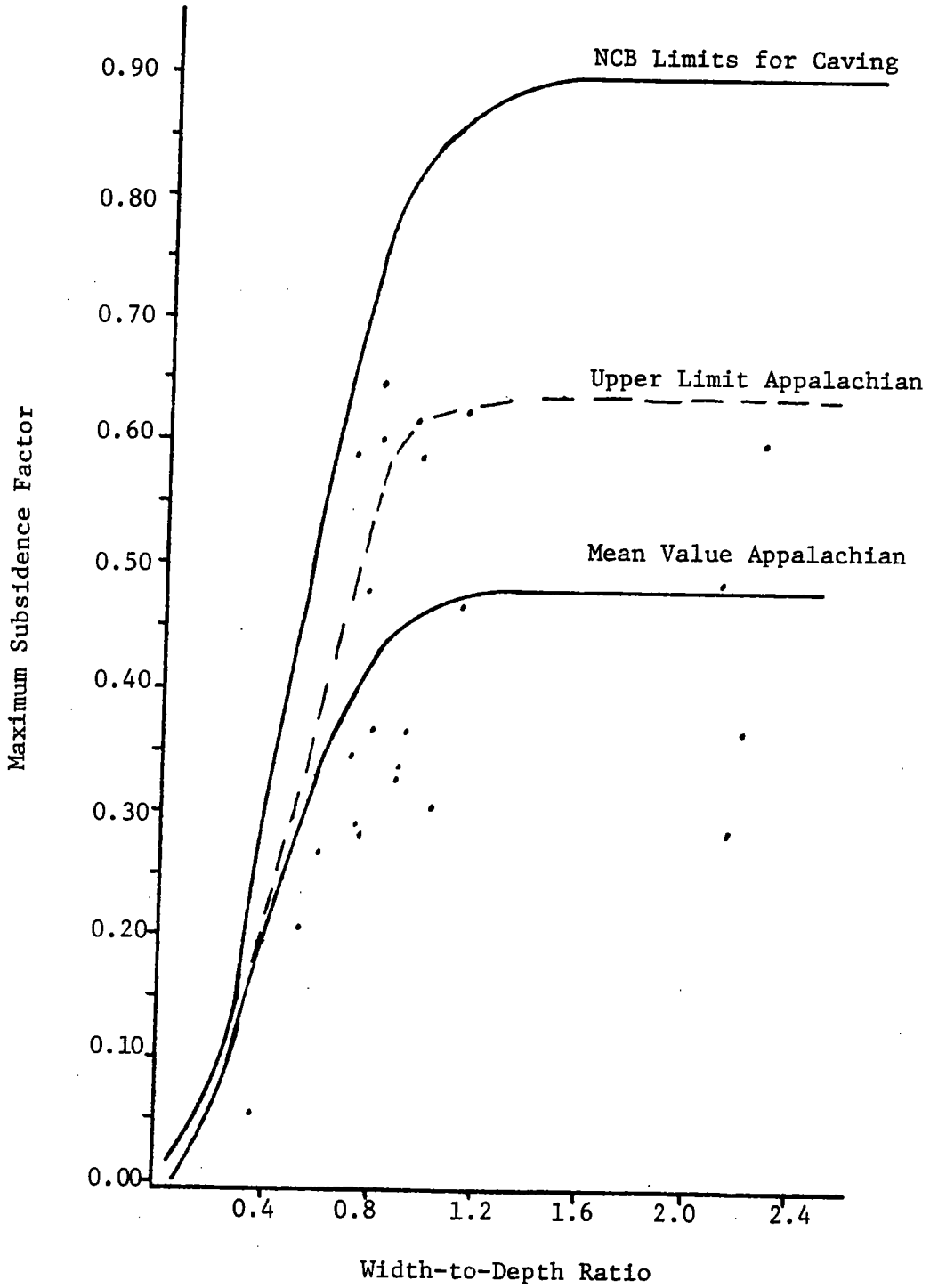


Figure 14: Influence of Width-to-Depth Ratio on the Maximum Subsidence Factor

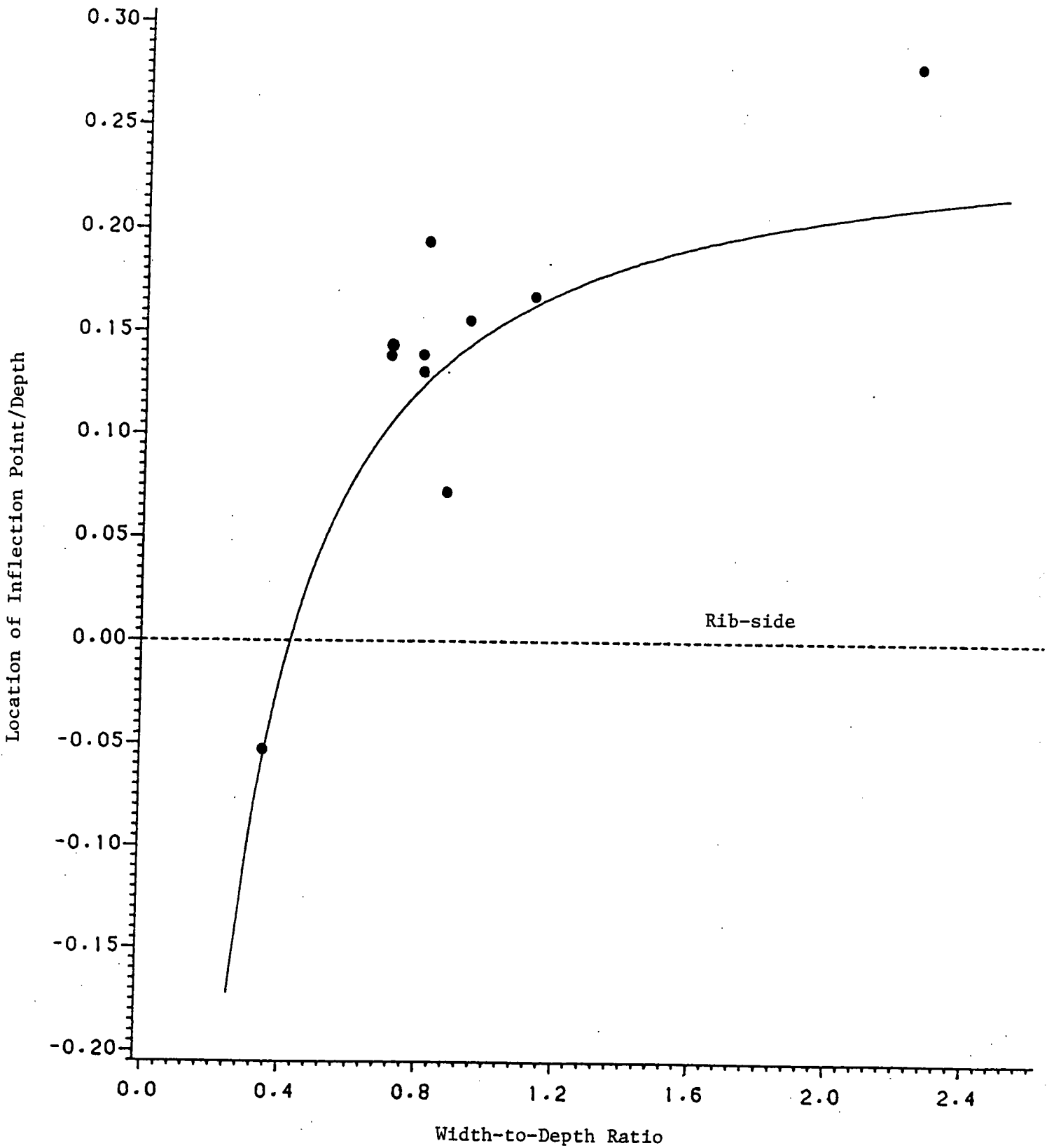


Figure 15: Effect of Width-to-Depth Ratio on the Position of the Inflection Point

supporting the observation of O'Rourke and Turner (1981), that although smaller amounts of subsidence are experienced in the U.S., they can still induce greater curvatures and strains, in fact, as much as two to five times larger.

From the lithological information collected for each case study, the percent hard rock material, such as limestone and sandstone, was calculated for each panel. These values were then plotted against the maximum subsidence factor and draw angle to develop characteristic trends (Figure 16). Analysis of these results indicated that, correlations were difficult to establish because two controls, the lithology as well as the W/h ratio, had a marked influence on the subsidence factor. To overcome this problem, only the critical and supercritical case studies were replotted, thus eliminating the influence of the panel geometry on the maximum subsidence (Figures 17 and 18). These graphs clearly demonstrated that the maximum subsidence factor decreases with an increasing percentage of hard rock in the overlying strata, whereas the opposite effect is, obviously, obtained when its complement, i.e. soft rock content, is considered.

The presence of a massive hard rock bed has been suggested to reduce the magnitude of surface subsidence (Peng and Cheng, 1980) by inhibiting the propagation of caving or sagging strata. The position and thickness of these layers in the overlying strata is also an important consideration. However, the precise effect of these factors on subsidence is difficult to ascertain.

There were no obvious trends suggested from plots of draw angle versus the different lithologic compositions. This is most likely due to the complex fracture mechanisms of the strata and the difficulties encountered in obtaining an accurate measurement of the draw angle.

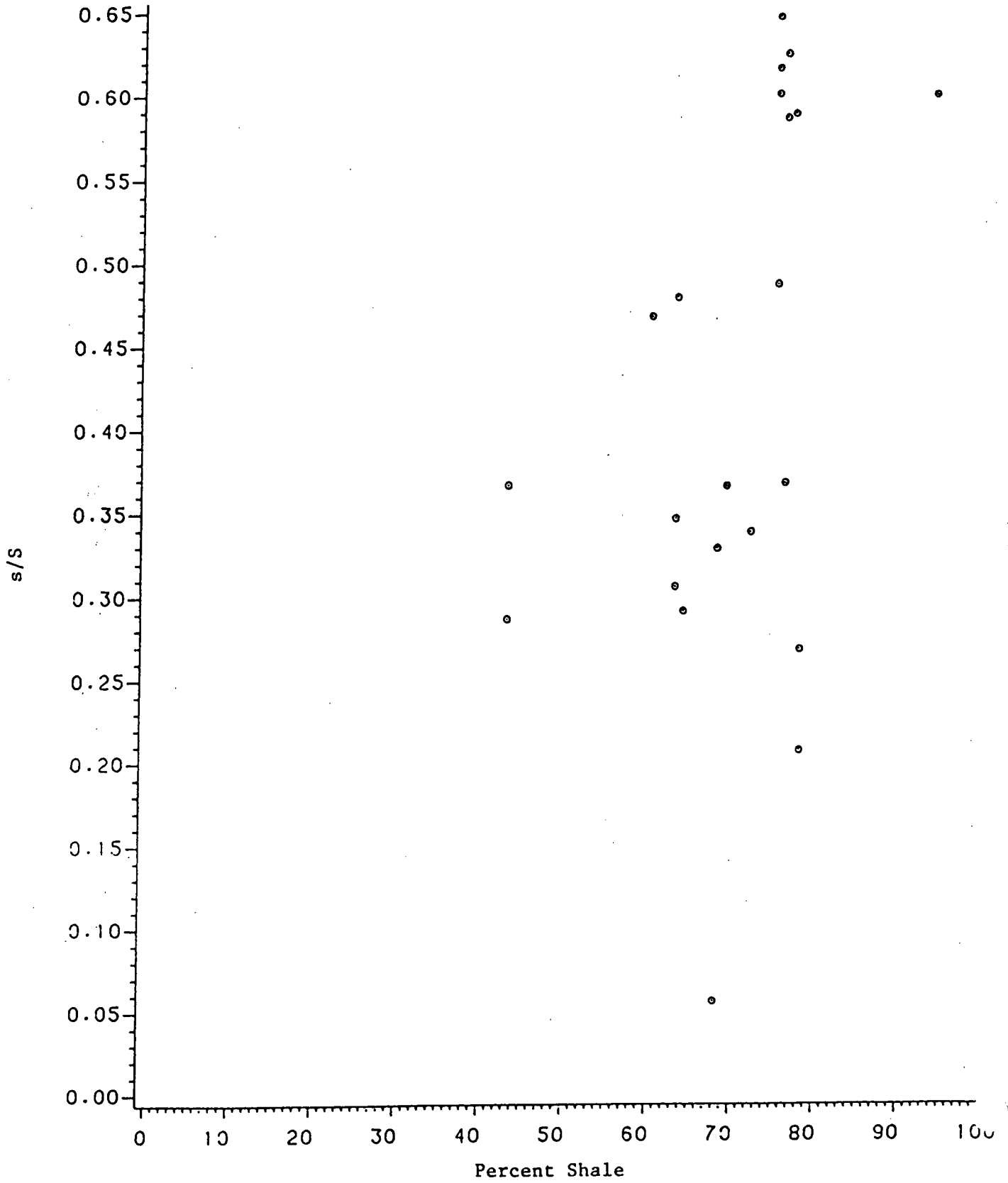


Figure 16: Influence of Shale on s/S for all Case Studies

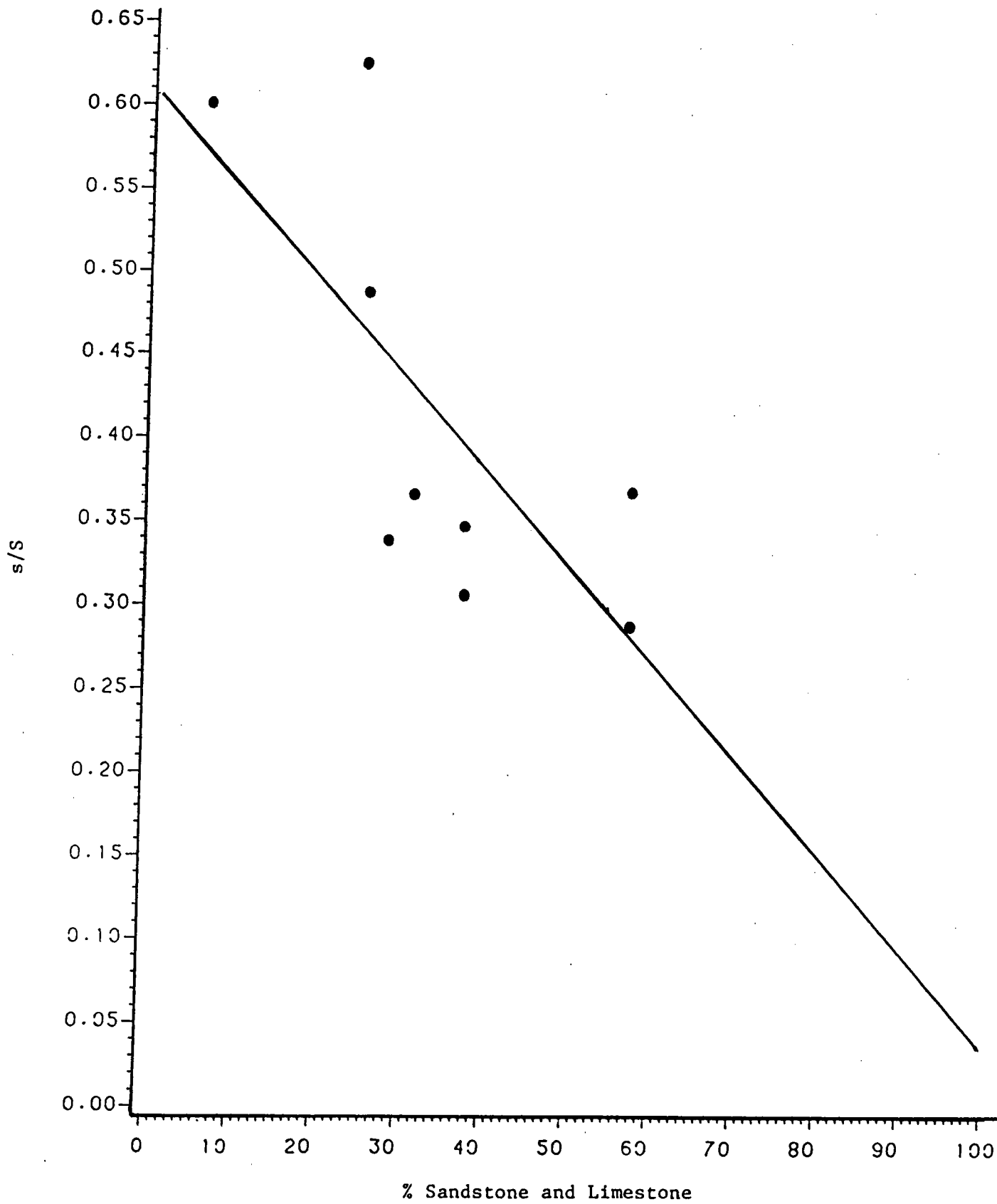


Figure 17: Influence of Sandstone and Limestone on s/S for Critical and Supercritical Panels

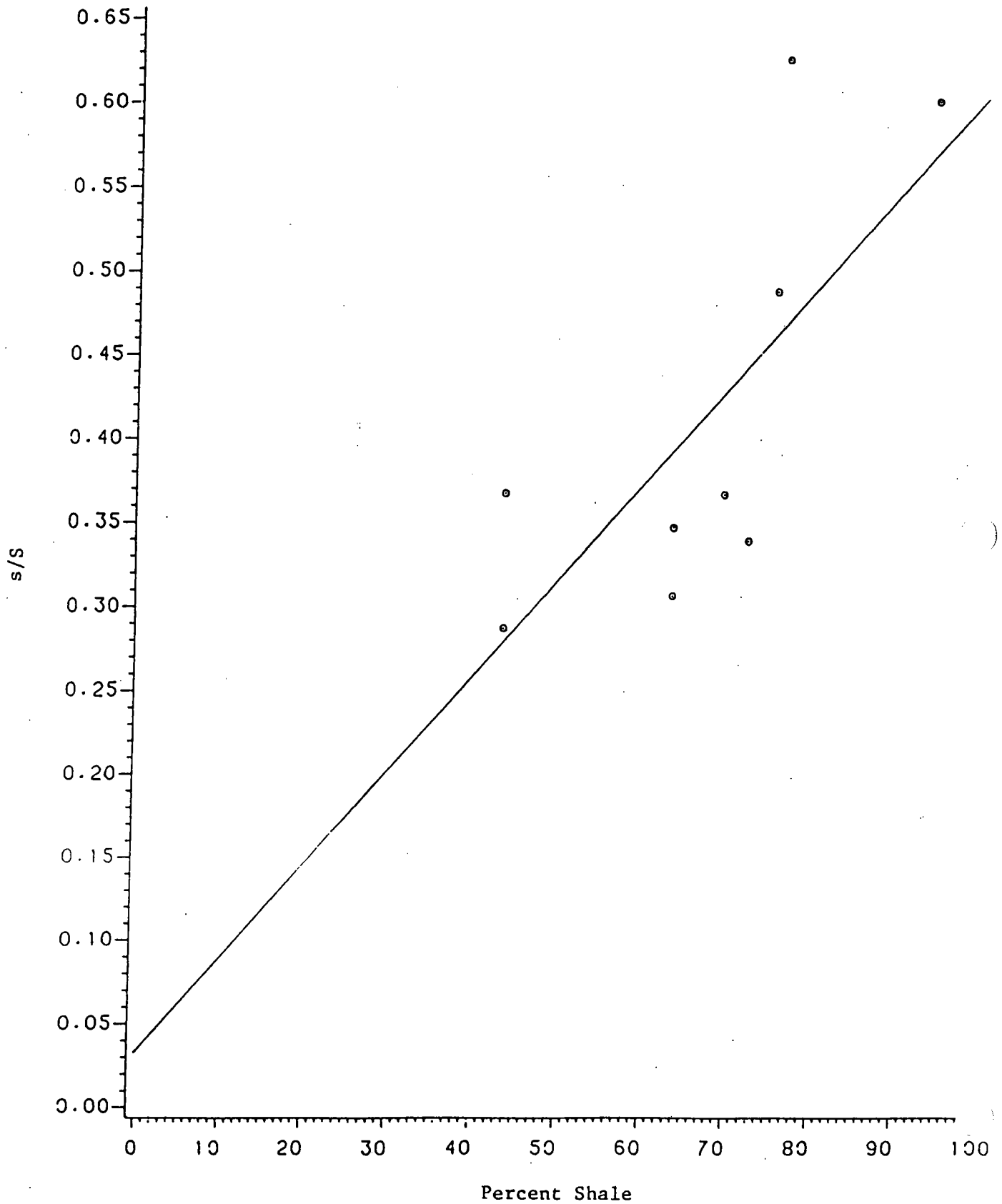


Figure 18: Influence of Shale on s/S for Critical and Supercritical Panels

V. DEVELOPMENT OF AN EMPIRICAL SUBSIDENCE PREDICTION MODEL

Before an empirical prediction model could be developed for the Appalachian region, it was necessary to determine its characteristic subsidence profile. To facilitate this process, all case studies were divided into either sub-critical or critical (including supercritical) extractions. The profiles representing each group are illustrated in Figures 19 and 20.

A hyperbolic tangent function was chosen to mathematically describe these profiles. The referencing system utilized is similar to that detailed by Brauner (1973) and is given in Figure 21. The hyperbolic tangent function expresses the subsidence, s , as:

$$s = \frac{S_{\max}}{2} \left[1 - \tanh \left(\frac{cx}{B} \right) \right] \quad (8)$$

where

S_{\max} = maximum subsidence

c = constant; 1.4 for subcritical panels

1.8 for critical and supercritical panels

x = distance from inflection point to the point in question

B = distance from inflection point to S_{\max}

Comparisons of the characteristic profile and the model curve are given in Figure 22 and 23 along with the upper and lower data bounds.

This relation shows that subsidence is a function of maximum subsidence, which, in turn, is influenced by the W/h ratio and the lithologic characteristics. By integrating, therefore, Figures 14 and 17 a three-dimensional composite graph was established as shown in Figure 24. The calculated family of curves enables the maximum subsidence to be predicted for

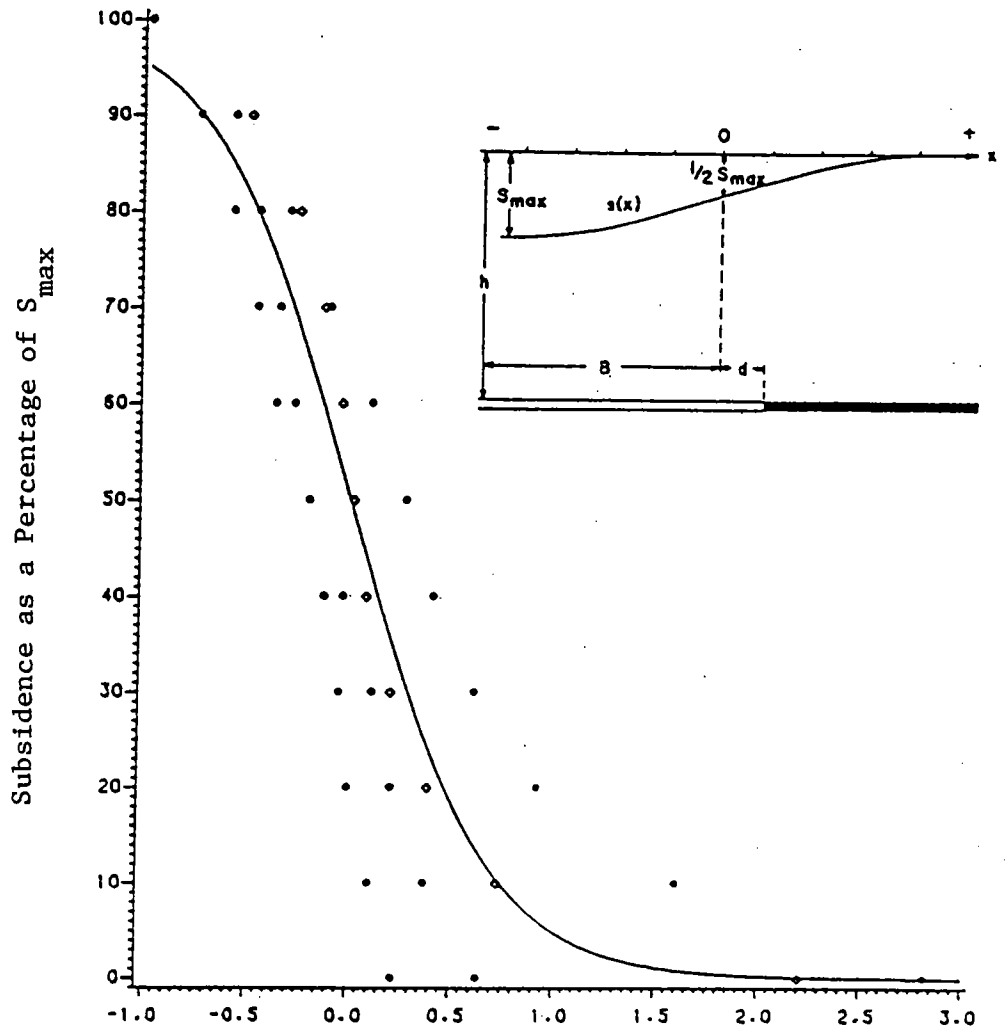


Figure 19: Characteristic Subsidence Profile for Subcritical Extractions

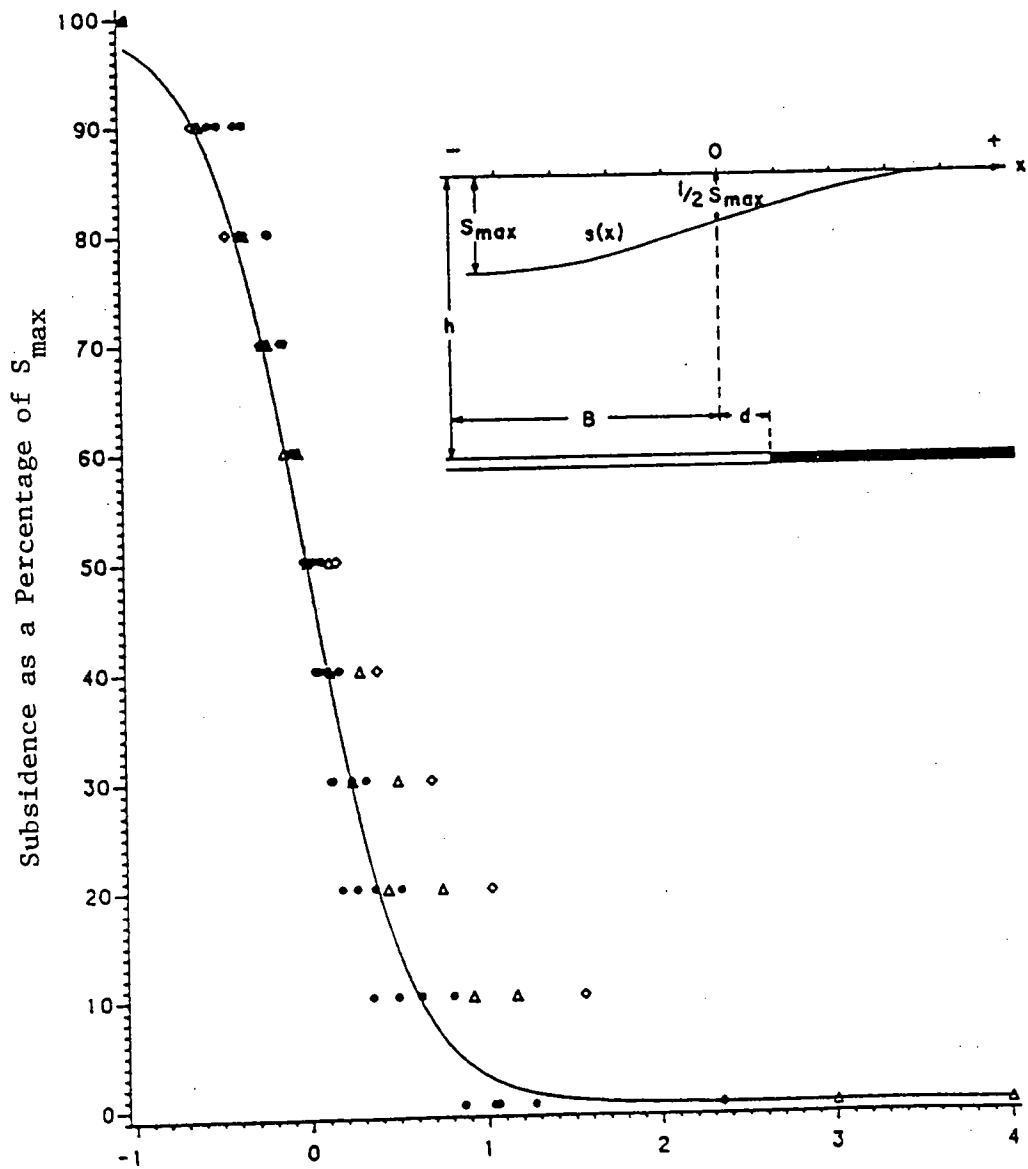


Figure 20: Characteristic Subsidence Profile for Critical and Supercritical Extractions

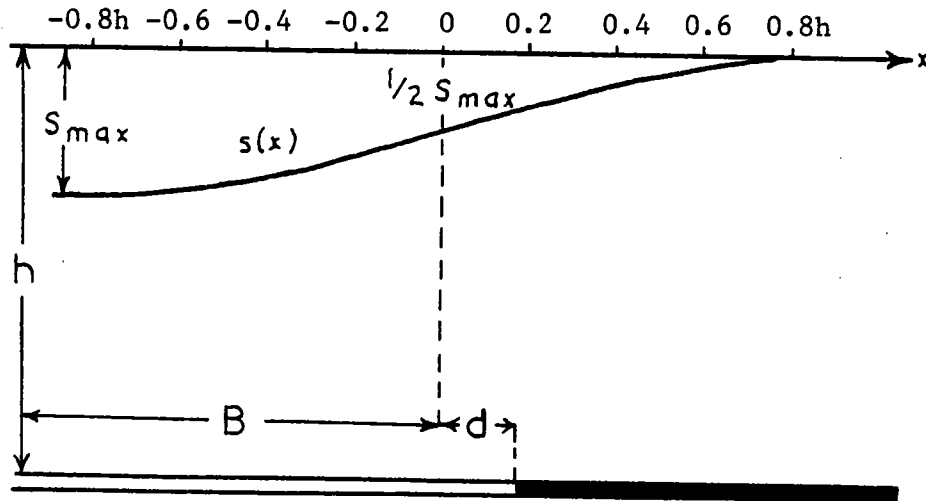


Figure 21: Referencing System (Brauner, 1973)

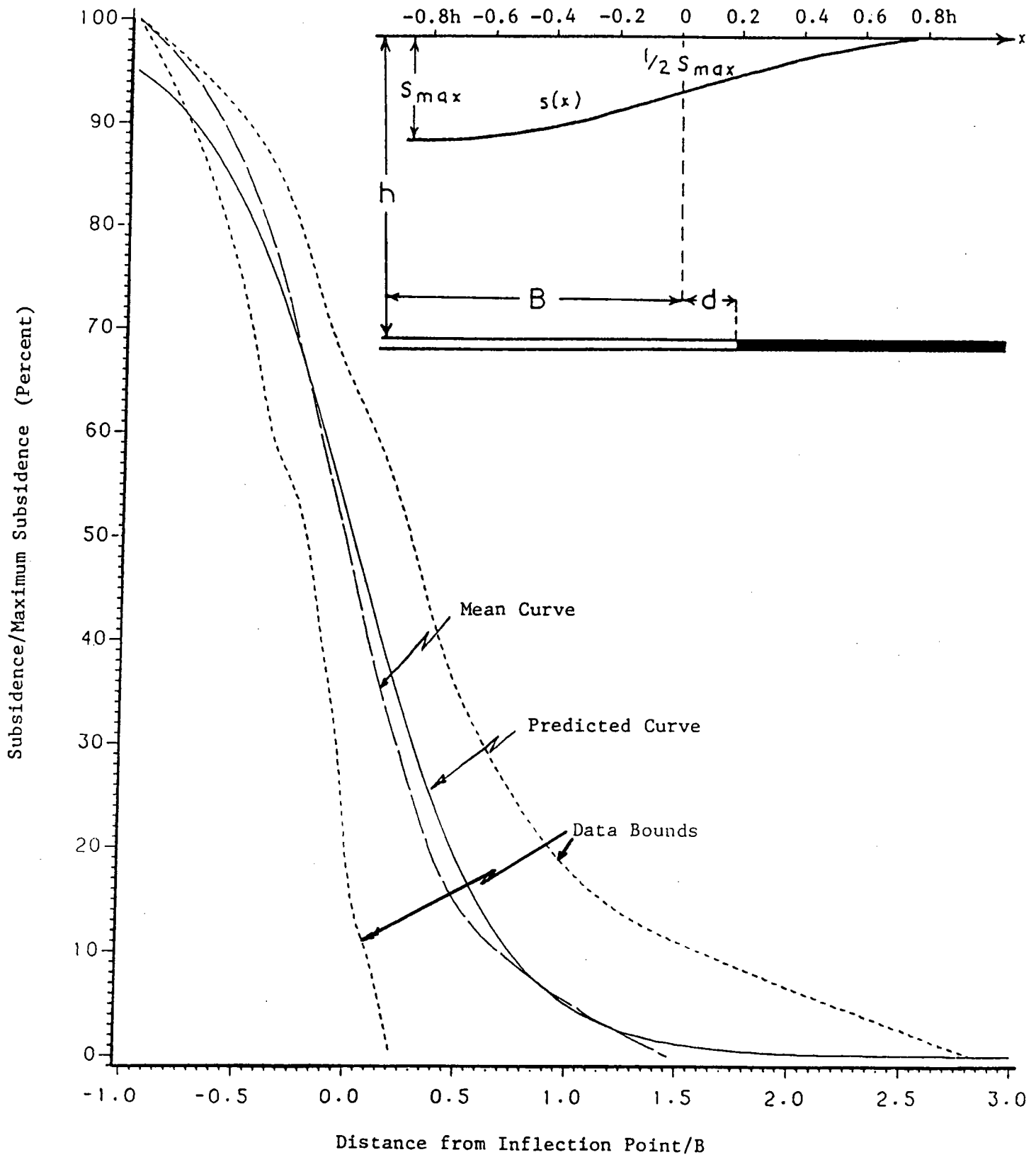


Figure 22: Determination of the Hyperbolic Tangent Profile Function for Subcritical Extractions

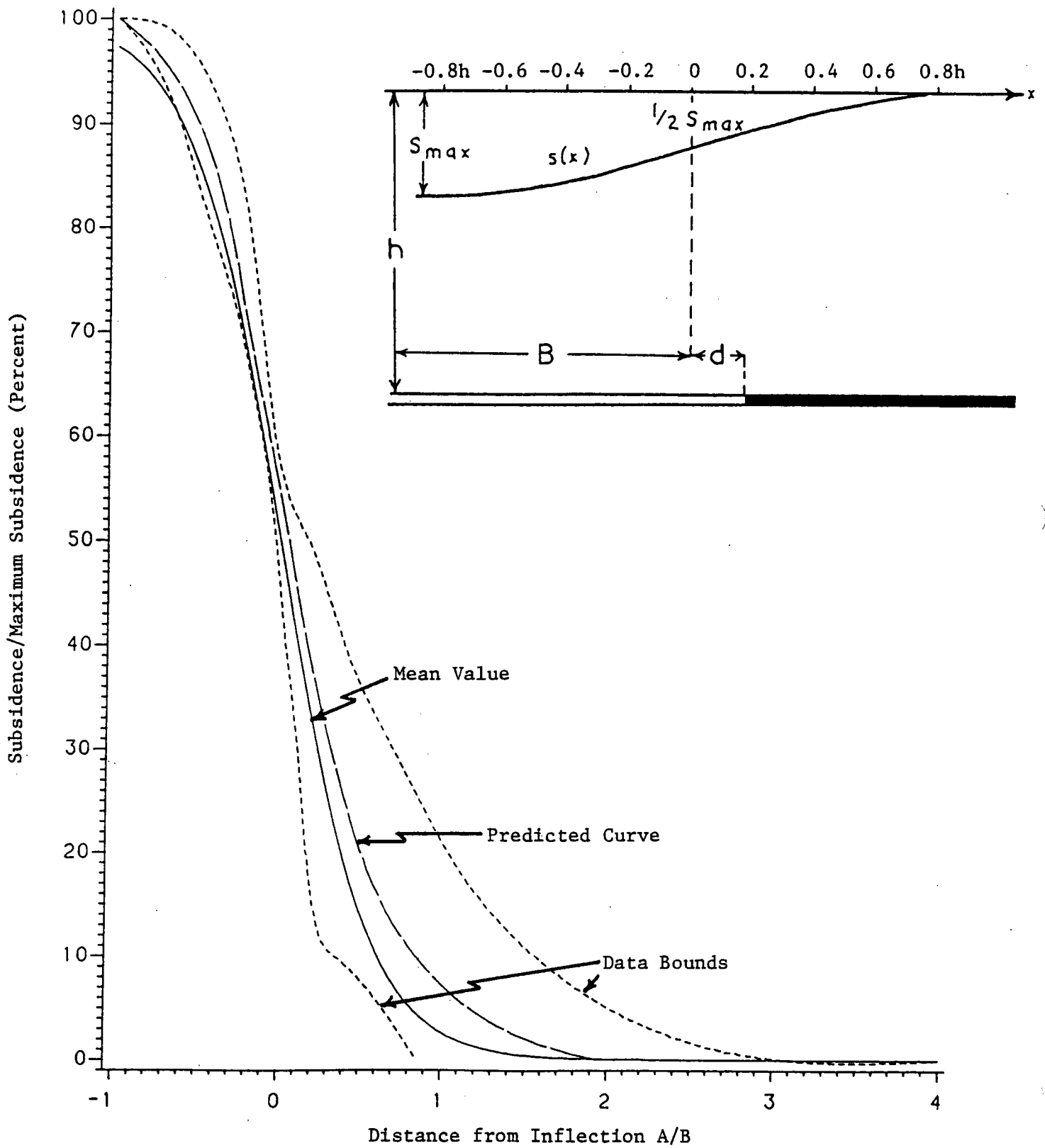


Figure 23: Determination of the Hyperbolic Tangent Profile Function for Critical and Supercritical Extraction

a given panel geometry and then further corrected according to the specific lithologic characteristics.

The complete subsidence profile can now be predicted for mining conditions in Appalachia. From a knowledge of the width-to-depth ratio and the panel lithology the maximum subsidence is found in Figure 24. This value is placed in the hyperbolic tangent function to obtain subsidence values at different distances from the panel centerline. These relationships have been tabulated and are shown in Tables I and II.

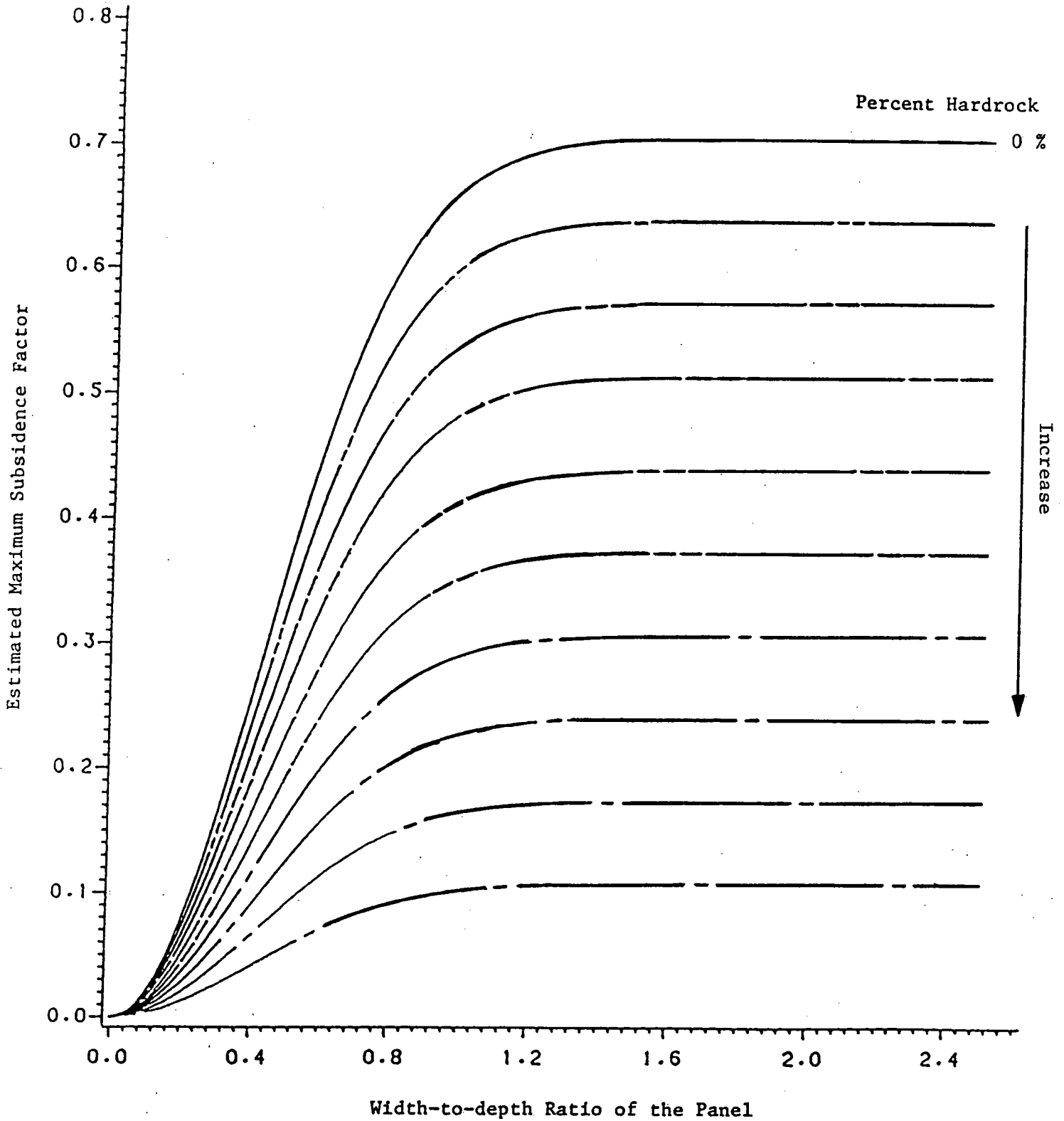


Figure 24: Effect of Panel Lithology and Width-to-Depth Ratio on the Maximum Subsidence

VI APPLICATION OF THE ZONE AREA METHOD

Application of the empirical subsidence prediction method to the zone area computer model requires several modifications. As previously described, the zone area method establishes a series of seven annular rings about a surface point. Given a critical width-to-depth ratio of 1.4 for British mining conditions, each of the seven zones conveniently represents 0.2 of the working depth. For Appalachian mining conditions, a width-to-depth ratio of 1.2 is given for critical extractions. Thus, six zones are utilized in this zone area model, again each zone having a radius of 0.2 of the working depth.

A second modification is the calculation of the influence constant and the zone factors representative of Appalachian mining conditions. Determination of the influence constant, n , follows from Equation 7. Assuming a lithology of 50 percent hard material and a critically extracted panel, the appropriate values of S and s are determined from Tables I and II. Use of Equation 7 yields a value of $n = 3.059$.

Continued investigation of the standard subsidence profiles produced the results shown in Figure 25. Due to this variation of s/S , the previous value of $n = 3.059$ is not applicable to subcritical extractions, and thus must be modified to reflect the changing width-to-depth ratio. By rearranging the hyperbolic tangent function given in Equation 8, the following relationship is formed:

$$s/S = 0.5 [1 - \tanh (cx_r/B)] \quad \dots \dots \dots (9)$$

where

S = subsidence at the center of the panel

s = subsidence at the rib

x_r = distance from inflection point to rib-side.

TABLE I

MAXIMUM SUBSIDENCE AS A PERCENT OF SEAM THICKNESS									
PERCENT HARD ROCK									
W/h	10	20	30	40	50	60	70	80	90
0.00	0.000	0.000	0.000	0.000	0.000	0.000	0.000	0.000	0.000
0.05	0.005	0.005	0.004	0.004	0.003	0.003	0.002	0.002	0.002
0.10	0.020	0.018	0.016	0.015	0.013	0.012	0.010	0.008	0.007
0.15	0.043	0.040	0.036	0.033	0.029	0.025	0.022	0.018	0.015
0.20	0.075	0.069	0.063	0.056	0.050	0.044	0.038	0.031	0.025
0.25	0.113	0.104	0.095	0.085	0.076	0.066	0.057	0.047	0.038
0.30	0.156	0.143	0.130	0.117	0.104	0.091	0.078	0.065	0.052
0.35	0.203	0.186	0.169	0.152	0.135	0.118	0.102	0.085	0.068
0.40	0.251	0.230	0.209	0.188	0.167	0.146	0.126	0.105	0.084
0.45	0.298	0.273	0.249	0.224	0.199	0.174	0.149	0.125	0.100
0.50	0.344	0.316	0.287	0.258	0.230	0.201	0.173	0.144	0.115
0.55	0.388	0.356	0.323	0.291	0.259	0.227	0.194	0.162	0.130
0.60	0.428	0.392	0.357	0.321	0.285	0.250	0.214	0.179	0.143
0.65	0.464	0.425	0.387	0.348	0.309	0.271	0.232	0.194	0.155
0.70	0.495	0.454	0.413	0.372	0.330	0.289	0.248	0.207	0.166
0.75	0.522	0.479	0.435	0.392	0.348	0.305	0.262	0.218	0.175
0.80	0.545	0.499	0.454	0.409	0.364	0.318	0.273	0.228	0.182
0.85	0.563	0.517	0.470	0.423	0.376	0.329	0.282	0.236	0.189
0.90	0.579	0.530	0.482	0.434	0.386	0.338	0.290	0.242	0.194
0.95	0.591	0.541	0.492	0.443	0.394	0.345	0.296	0.247	0.198
1.00	0.600	0.550	0.500	0.450	0.400	0.351	0.301	0.251	0.201
1.10	0.612	0.561	0.511	0.460	0.409	0.358	0.307	0.256	0.205
1.20	0.619	0.568	0.516	0.465	0.413	0.362	0.310	0.259	0.207
1.30	0.623	0.571	0.519	0.467	0.416	0.364	0.312	0.260	0.208
1.40	0.624	0.572	0.520	0.469	0.417	0.365	0.313	0.261	0.209
1.50	0.625	0.573	0.521	0.469	0.417	0.365	0.313	0.261	0.209
1.60	0.625	0.573	0.521	0.469	0.417	0.365	0.313	0.261	0.209
1.70	0.625	0.573	0.521	0.469	0.417	0.365	0.313	0.261	0.209
1.80	0.625	0.573	0.521	0.469	0.417	0.365	0.313	0.261	0.209
1.90	0.625	0.573	0.521	0.469	0.417	0.365	0.313	0.261	0.209
2.00	0.625	0.573	0.521	0.469	0.417	0.365	0.313	0.261	0.209
2.20	0.625	0.573	0.521	0.469	0.417	0.365	0.313	0.261	0.209
2.40	0.625	0.573	0.521	0.469	0.417	0.365	0.313	0.261	0.209
2.60	0.625	0.573	0.521	0.469	0.417	0.365	0.313	0.261	0.209
2.80	0.625	0.573	0.521	0.469	0.417	0.365	0.313	0.261	0.209
3.00	0.625	0.573	0.521	0.469	0.417	0.365	0.313	0.261	0.209

TABLE II

DISTANCE FROM THE CENTER OF THE PANEL IN TERMS OF DEPTH													
SUBSIDENCE AS A PERCENT OF MAXIMUM SUBSIDENCE													
W/h	0	.05	.1	.2	.3	.4	.5	.6	.7	.8	.9	.95	1.00
0.00	0.319	0.221	0.197	0.171	0.154	0.140	0.127	0.114	0.100	0.084	0.061	0.042	0.000
0.05	0.340	0.236	0.210	0.182	0.164	0.149	0.135	0.122	0.107	0.090	0.065	0.044	0.000
0.10	0.362	0.251	0.224	0.194	0.174	0.159	0.144	0.129	0.114	0.095	0.069	0.047	0.000
0.15	0.384	0.266	0.237	0.206	0.185	0.168	0.153	0.137	0.121	0.101	0.073	0.050	0.000
0.20	0.407	0.282	0.251	0.218	0.196	0.178	0.162	0.146	0.128	0.107	0.078	0.053	0.000
0.25	0.431	0.298	0.266	0.231	0.208	0.189	0.171	0.154	0.136	0.113	0.082	0.056	0.000
0.30	0.455	0.315	0.281	0.244	0.219	0.199	0.181	0.163	0.143	0.120	0.087	0.059	0.000
0.35	0.479	0.332	0.296	0.257	0.231	0.210	0.191	0.171	0.151	0.126	0.091	0.063	0.000
0.40	0.505	0.350	0.312	0.270	0.243	0.221	0.201	0.180	0.159	0.133	0.096	0.066	0.000
0.45	0.530	0.367	0.328	0.284	0.256	0.232	0.211	0.190	0.167	0.140	0.101	0.069	0.000
0.50	0.557	0.386	0.344	0.298	0.268	0.244	0.221	0.199	0.175	0.147	0.106	0.073	0.000
0.55	0.584	0.404	0.360	0.313	0.281	0.256	0.232	0.209	0.184	0.154	0.111	0.076	0.000
0.60	0.611	0.423	0.377	0.328	0.295	0.268	0.243	0.219	0.192	0.161	0.116	0.080	0.000
0.65	0.639	0.443	0.395	0.343	0.308	0.280	0.254	0.229	0.201	0.168	0.122	0.084	0.000
0.70	0.668	0.463	0.412	0.358	0.322	0.292	0.266	0.239	0.210	0.176	0.127	0.087	0.000
0.75	0.697	0.483	0.431	0.374	0.336	0.305	0.277	0.249	0.219	0.184	0.133	0.091	0.000
0.80	0.727	0.504	0.449	0.390	0.350	0.318	0.289	0.260	0.229	0.191	0.138	0.095	0.000
0.85	0.757	0.525	0.468	0.406	0.365	0.332	0.301	0.271	0.238	0.199	0.144	0.099	0.000
0.90	0.788	0.546	0.487	0.423	0.380	0.345	0.313	0.282	0.248	0.208	0.150	0.103	0.000
0.95	0.820	0.568	0.506	0.439	0.395	0.359	0.326	0.293	0.258	0.216	0.156	0.107	0.000
1.00	0.852	0.590	0.526	0.457	0.411	0.373	0.339	0.305	0.268	0.224	0.162	0.111	0.000
1.10	0.918	0.636	0.567	0.492	0.442	0.402	0.365	0.328	0.289	0.242	0.175	0.120	0.000
1.20	0.986	0.683	0.609	0.529	0.475	0.432	0.392	0.353	0.310	0.260	0.188	0.129	0.000
1.30	1.057	0.732	0.653	0.566	0.509	0.463	0.420	0.378	0.333	0.278	0.201	0.138	0.000
1.40	1.130	0.783	0.698	0.605	0.544	0.495	0.449	0.404	0.355	0.298	0.215	0.148	0.000
1.50	1.205	0.835	0.744	0.646	0.581	0.528	0.479	0.431	0.379	0.317	0.229	0.158	0.000
1.60	1.282	0.888	0.792	0.687	0.618	0.561	0.510	0.459	0.404	0.338	0.244	0.168	0.000
1.70	1.362	0.944	0.841	0.730	0.657	0.596	0.542	0.487	0.429	0.359	0.259	0.178	0.000
1.80	1.444	1.001	0.892	0.774	0.696	0.632	0.574	0.517	0.454	0.380	0.275	0.189	0.000
1.90	1.529	1.059	0.944	0.819	0.737	0.669	0.608	0.547	0.481	0.403	0.291	0.200	0.000
2.00	1.615	1.119	0.998	0.866	0.779	0.707	0.642	0.578	0.508	0.426	0.308	0.211	0.000
2.20	1.796	1.244	1.109	0.963	0.866	0.786	0.714	0.642	0.565	0.473	0.342	0.235	0.000
2.40	1.985	1.376	1.226	1.064	0.957	0.869	0.789	0.710	0.625	0.523	0.378	0.260	0.000
2.60	2.184	1.513	1.349	1.171	1.053	0.956	0.868	0.781	0.687	0.575	0.416	0.286	0.000
2.80	2.392	1.658	1.477	1.282	1.153	1.047	0.951	0.856	0.753	0.630	0.456	0.313	0.000
3.00	2.610	1.808	1.612	1.399	1.258	1.143	1.038	0.933	0.821	0.687	0.497	0.341	0.000

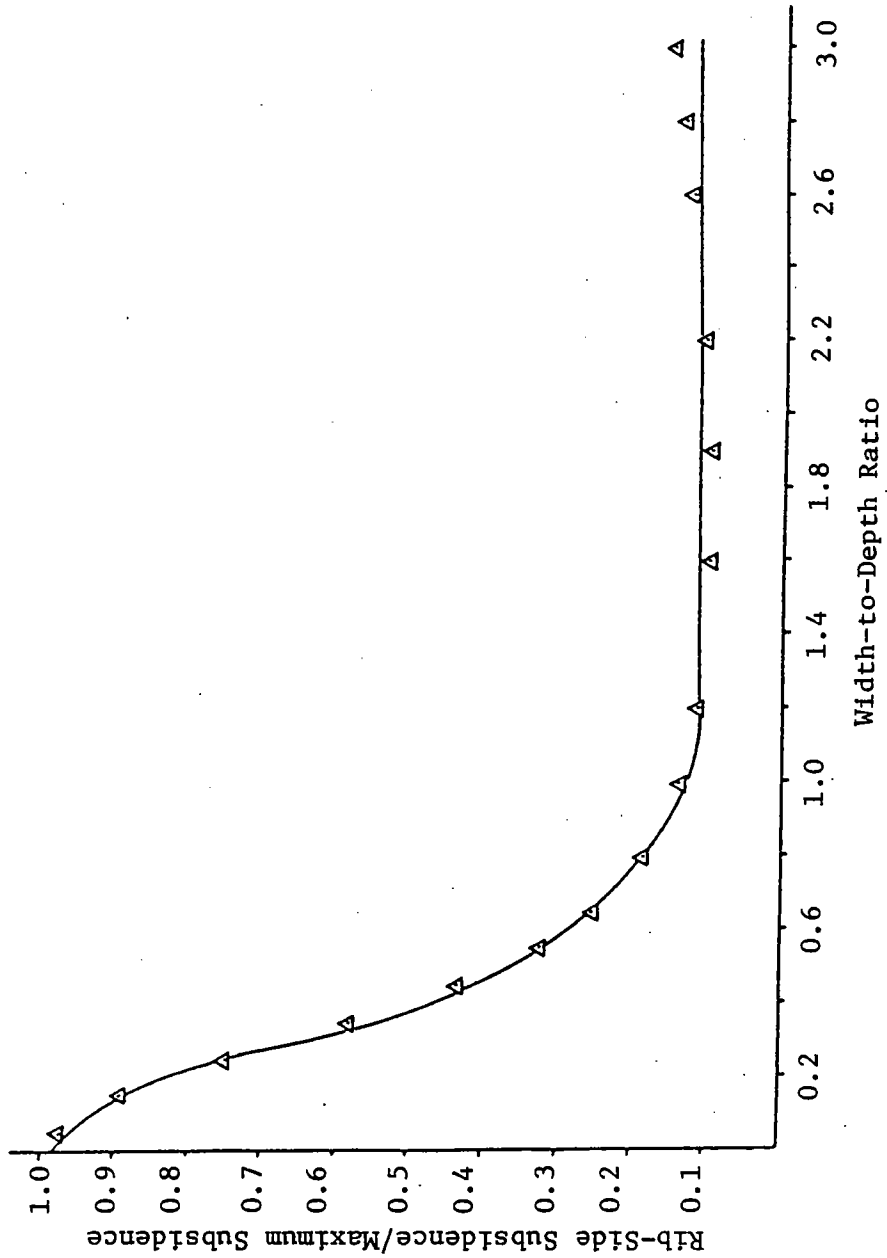


Figure 25: Variation of Rib-Side Subsidence with Width-to-Depth Ratio

For every subcritical ratio, a corresponding value of cx_r/B was found and, through statistical analysis, a fourth power expression was developed relating these two quantities,

$$cx_r/B = -2.838(W/h)^4 + 9.910(W/h)^3 - 13.576(W/h)^2 + 9.704(W/h) - 2.233 \dots (10)$$

Substitution of Equation 10 into Equation 9 yields an expression necessary for calculation of rib-side subsidence in the sub-critical range:

$$s/S = 0.5(1 - \tanh[-2.838(W/h)^4 + 9.910(W/h)^3 - 13.576(W/h)^2 + 9.704(W/h) - 2.233]) \dots (11)$$

Use of this expression allows determination of the influence constant, n , from Equation 7, therefore extending the applicability of the zone area method into subcritical extractions.

In order to predict subsidence profiles in the Appalachian coal field more accurately, efforts were undertaken to express zone factors in terms of panel lithology. This is important because, due to the variability of subsidence with geology, a single set of zone factors cannot describe accurately all conditions.

Assuming a critically extracted panel, six proportional extracted areas were calculated for each distance from the panel center (Table II). For each six zone system an expression similar to Equation 4 was developed. This process was continued for all critically extracted panels having lithologic properties between 10 to 90 percent hard rock, as shown in Table I. By statistically analyzing all six term equations a linear relationship was found, as illustrated in Figures 26 and 27, relating zone factors to the amount of hard rock in overburden.

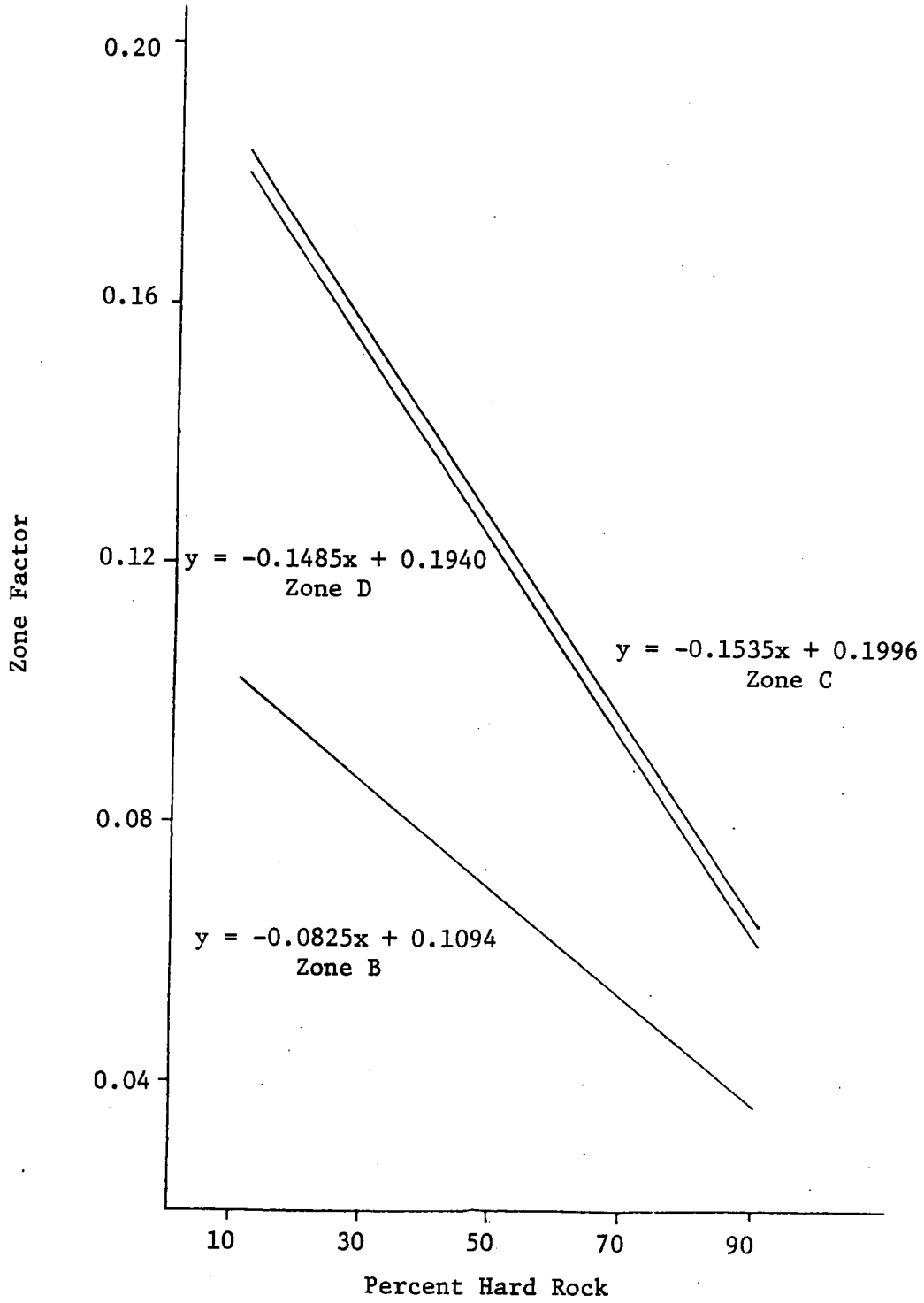


Figure 26: Variation of Zone Factors with Percent Hard Rock for Zones B, C, D

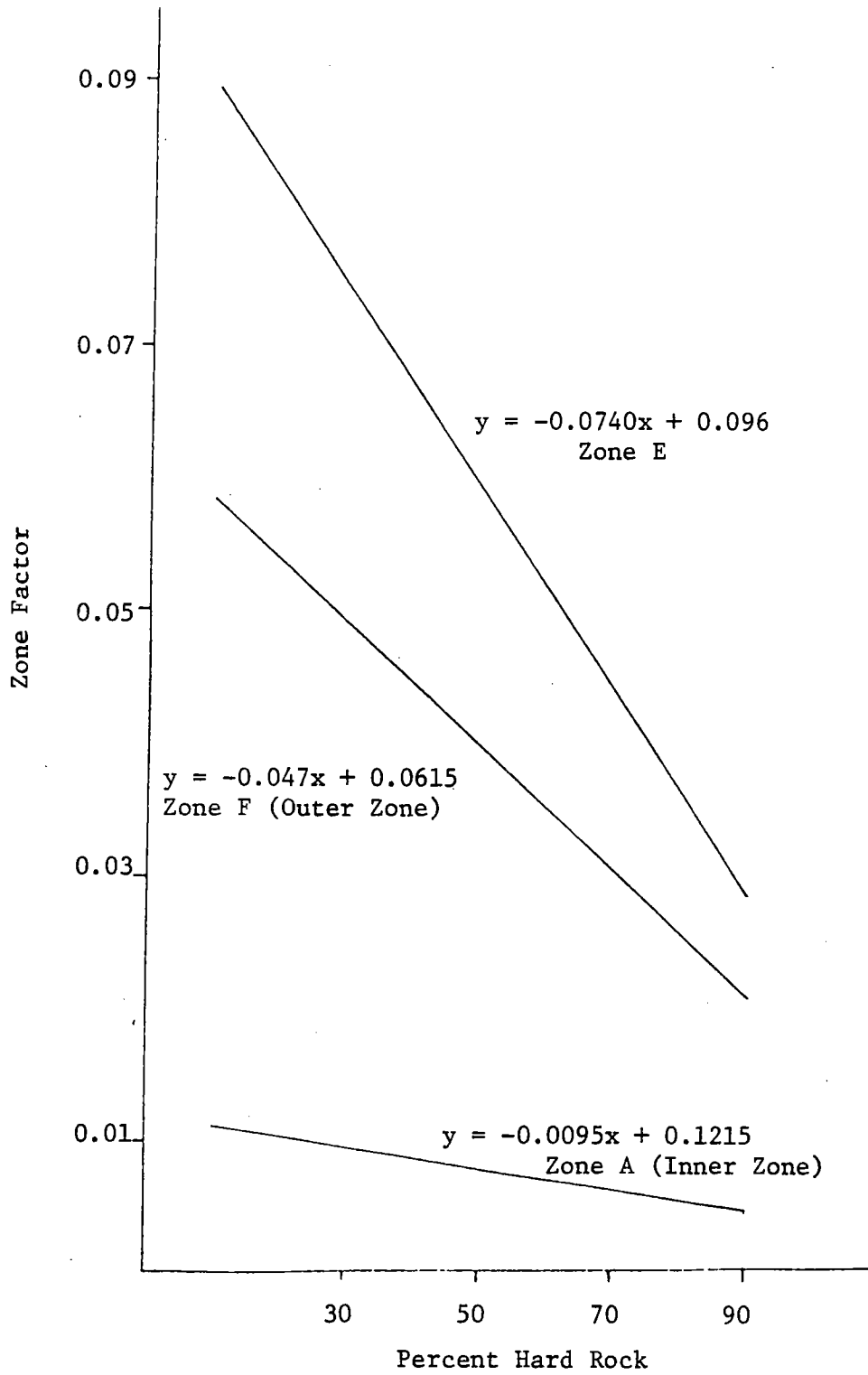


Figure 27: Variation of Zone Factor with Percent Hard Rock for Zone A, E, F

To validate the accuracy of the zone area model and consequently the zone factor relationships, the computer generated subsidence values were tested against known profiles. The values of width-to-depth ratio and percent hard rock were varied for each panel to provide an adequate number of comparisons. As shown in Figures 28, 29 and 30, excellent correlation was achieved over the entire subsidence profile, using the modified zone factor relationships.

Due to the regional variation of subsidence characteristics, the values of the influence constant and of the zone factors found for Appalachian mining conditions are not directly applicable to those situations in other parts of the country.

Considering the instance of subsidence in the Illinois Basin, O'Rourke and Turner (1979) commented on the striking similarities between the British Midlands and Yorkshire coalfields and this region. In light of this, the National Coal Board values for the influence constant and the zone factors can be expected to accurately predict the field measurements.

The Appalachian values of the influence constant and the zone factors are seen to adequately model the field data from a case study located in the Colorado Plateau region (Figure 31). Due to the lack of adequate field data for this area, the values determined for the Appalachian mining conditions can be utilized for preliminary subsidence approximations.

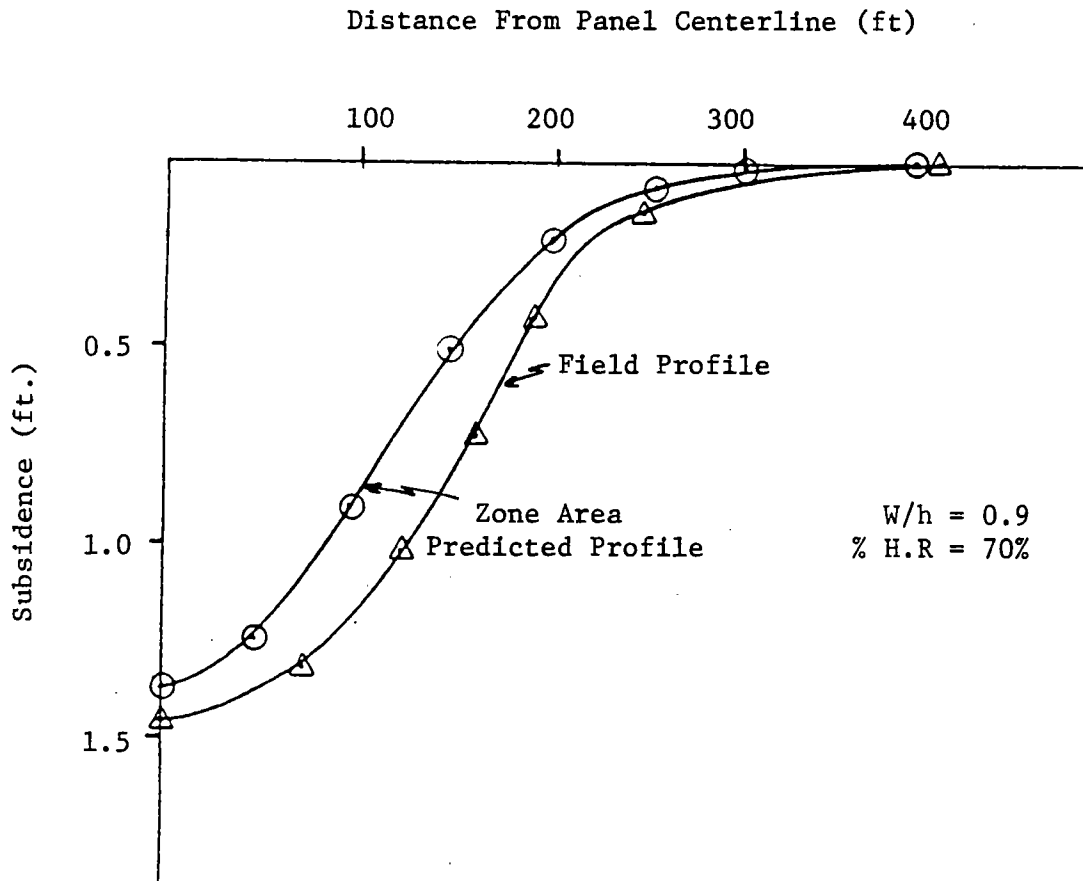
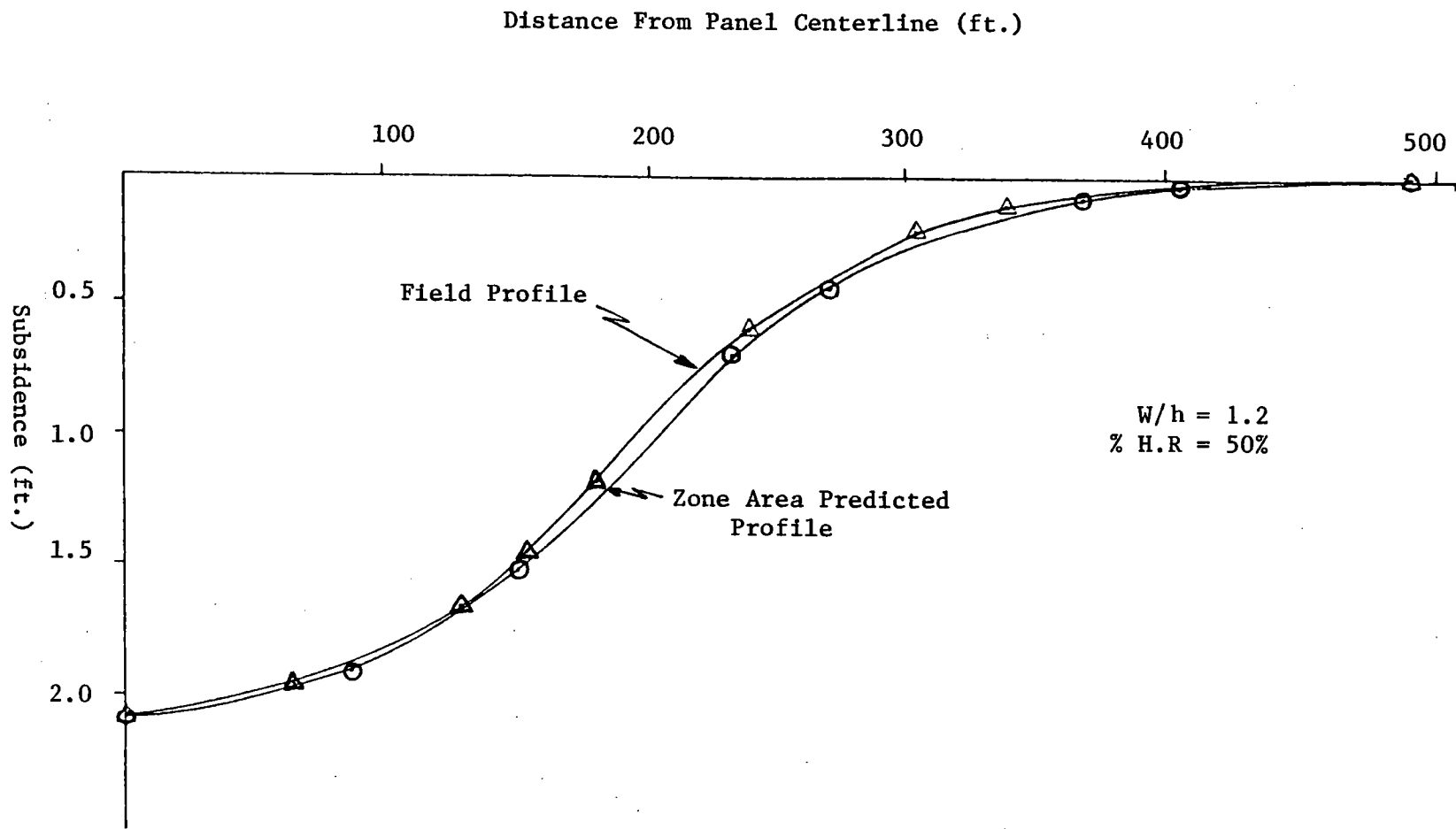


Figure 28: Field Profile vs Zone Area Predicted Profile

Figure 29: Field Profile vs Zone Area Predicted Profile



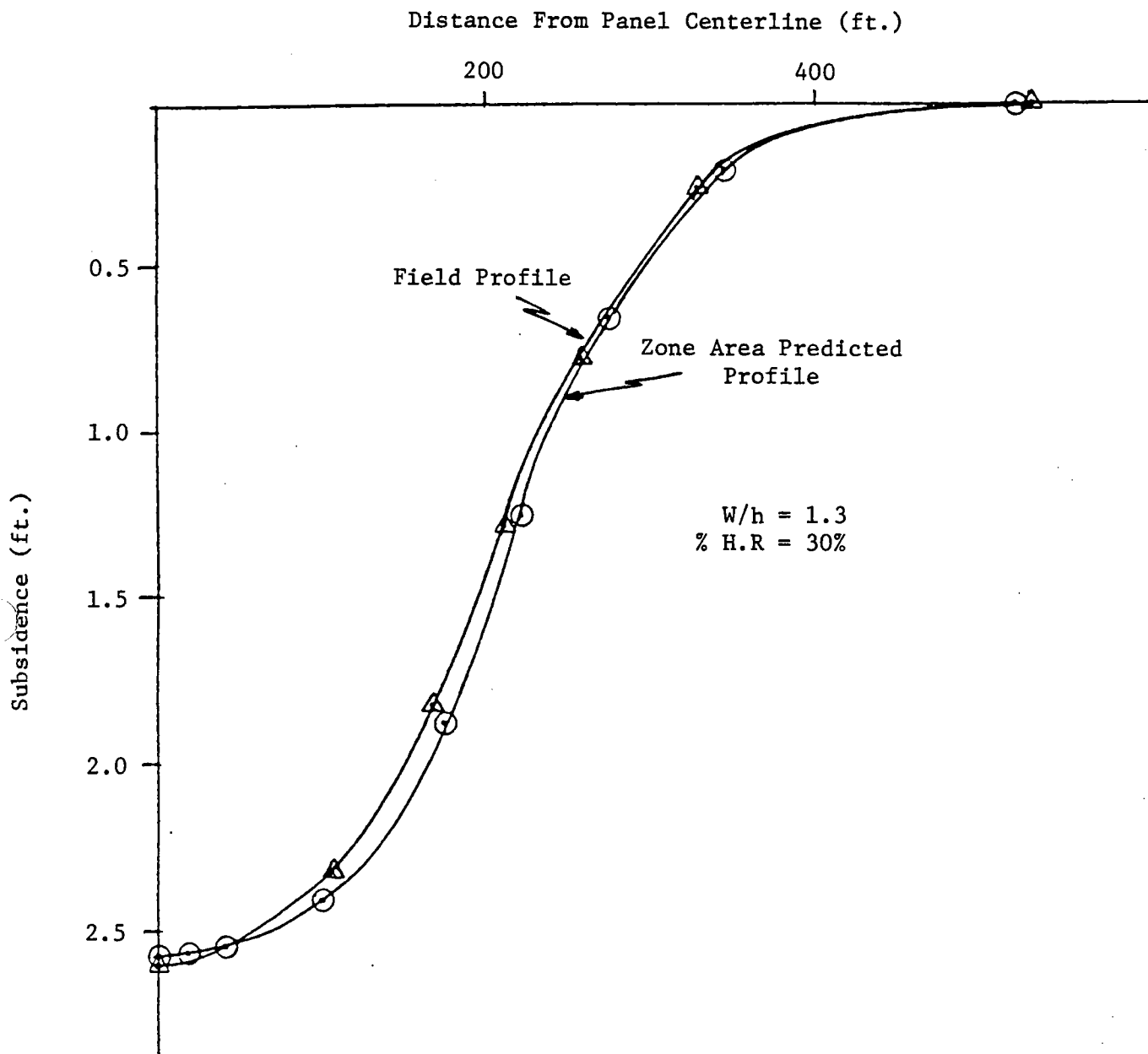


Figure 30: Field Profile vs Zone Area Predicted Profile

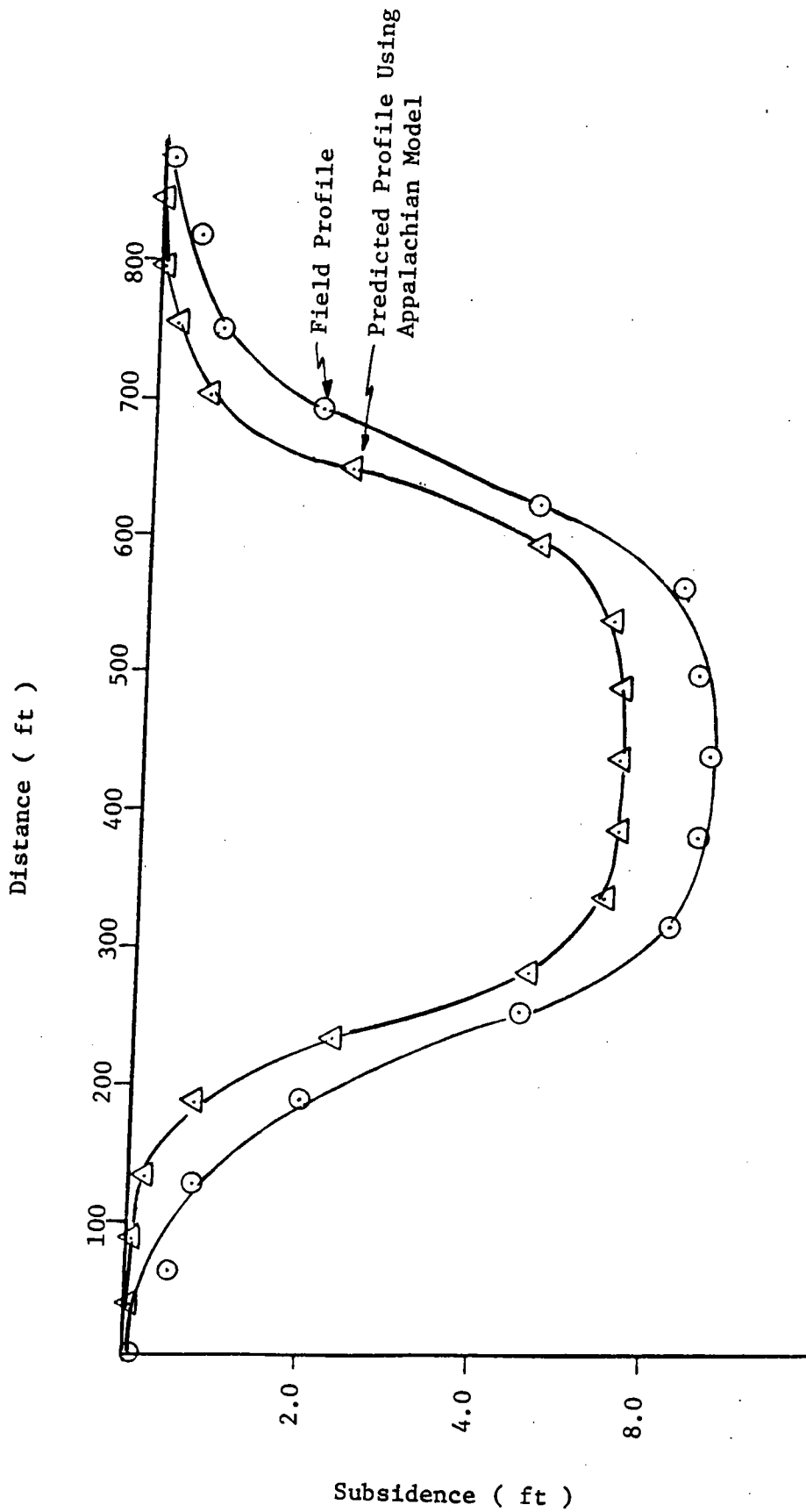


Figure 31: Field Profile vs. Predicted Profiles Using Appalachian Model

VII CONCLUSIONS

The need for coal as a viable energy resource will continue to increase in the future. As production increases to meet this demand, ground subsidence will become a major concern for the mining industry. In response to this, the industry will be faced with the problem of subsidence control.

In order to develop the zone area model, numerous case studies, both published and unpublished, were collected. These data were subsequently analyzed according to a variety of subsidence characteristics such as draw angle, inflection point, maximum subsidence, panel geology, and final profile shape. The results of this analysis included development of an empirical subsidence model incorporating panel lithology into its calculations.

The zone area method was adapted to this empirical model by first investigating the effects of panel lithology on the magnitude of the zone factors. The research indicated a linear relationship between percent hard rock and magnitude of zone factors, which was appropriately coded into the computer model. However, this constant was affected by variations in the width-to-depth ratio of the panel, which in turn affected the value of rib-side subsidence. Although the value of the influence constant remained unchanged in the critical and supercritical range, efforts were undertaken to define its value in the subcritical range. A hyperbolic tangent function was found to most accurately represent the influence constant for these panels.

Verification of the zone area model was conducted for numerous field studies. In all cases, good agreement was found between field and model values, such that the maximum error was less than 25 percent. This indicated that the developed model could predict both accurately and efficiently the complete subsidence profile for any geologic area, given the representative constants for that region.

Future research might include refinement of the computer model to include the predictive capabilities of strain and curvature. To accomplish this task, more case studies are needed to investigate the interaction of these variables with respect to panel geometry and overburden lithology.

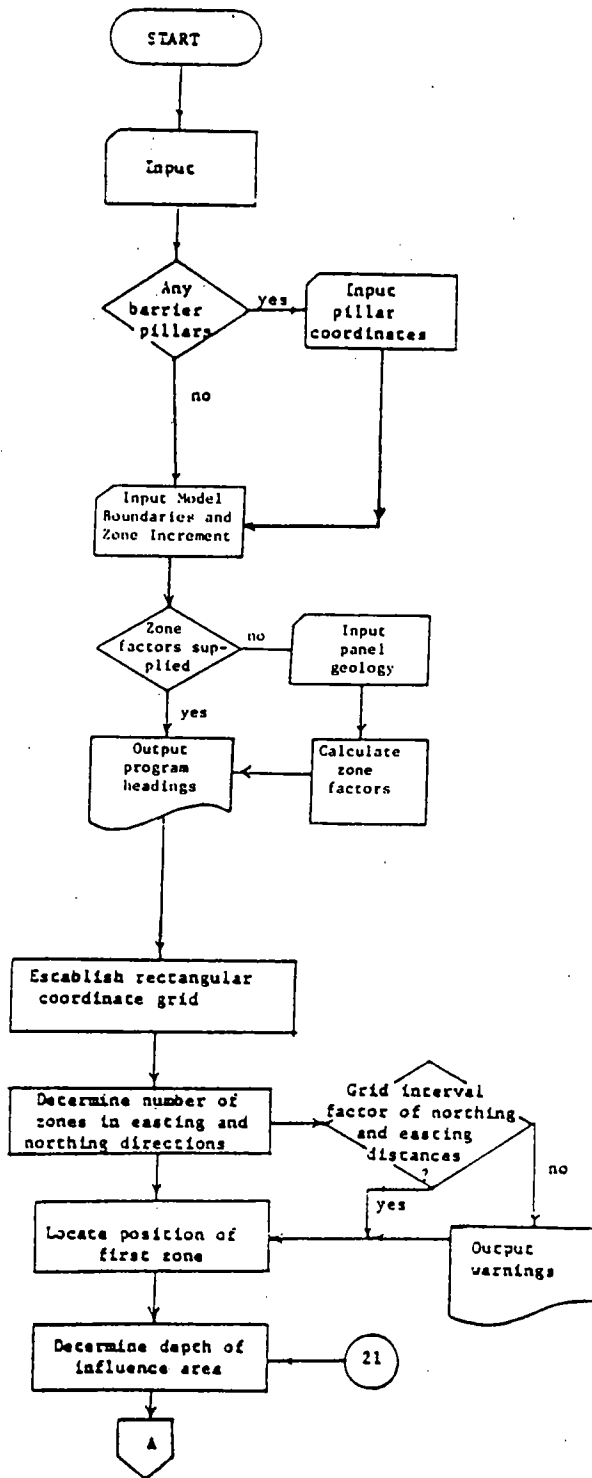
REFERENCES

1. Adamek, V. and Jeran, P. W. (1981), "Evaluation of Existing Predictive Methods for Mine Subsidence in the U.S.," Proceedings, 1st Annual Conf. Ground Control in Mining, West Virginia Univ., Morgantown, pp. 209-219.
2. Bals, R. (1932), "A Contribution to the Problem of Precalculating Mining Subsidences," Mitteilungen aus dem Markscheidewesen, Vol. 42/43, pp. 98-111 (in German).
3. Brauner, G. (1973), "Subsidence Due to Underground Mining (in two parts)," U.S. Bureau of Mines, Information Circulars 8571, 8572.
4. Flaschentrager, H. (1975), "Considerations on Ground Movement Phenomena Based on Observations Made in the Left Bank Lower Rhine Region," Proc., European Congress on Ground Movement, pp. 58-73.
5. Gonot, J. (1871), "Des Affaisements du sol Produits par l' Exploitation Hullyere," Liege.
6. Grond, C. J. A. (1957), "Ground Movements Due to Mining with Different Types of Strata and at Different Depths," Proc., European Congress on Ground Movement, University of Leeds, pp. 115-127.
7. Johnson, W. and Miller G. C. (1979), "Abandoned Coal-Mined Lands: Nature, Extent, and Cost of Reclamation," U.S. Bureau of Mines, Special Publications, 6-79, No. 3.
8. Keinhorst, H. (1928), "Considerations on the Problem of Mining Damages," Gluckauf (in German).
9. Marr, J. E. (1959), "The Estimation of Mining Subsidence," Colliery Guardian, Vol. 198, No. 5116, pp. 345-352.
10. Marr, J. E. (1975), "The Application of the Zone Area System to the Prediction of Mining Subsidence," Min. Eng., Vol. 135, No. 176, pp. 53-62.
11. National Coal Board-Production Department (1975), "Subsidence Engineers' Handbook," 2nd (Revised) Edition, 111 pp.
12. O'Rourke, T. D. and Turner, S. M. (1979), "Longwall Subsidence Patterns: A Review of Observed Movements, Controlling Parameters and Empirical Relationships," U.S. Bureau of Mines, Geotechnical Engineering Report, 79-6, 82 pp.
13. O'Rourke, T. D. and Turner, S. M. (1981), "Empirical Methods for Estimating Subsidence in U.S. Coal Fields," Proceedings, 22nd U.S. Symp. on Rock Mech., Massachusetts Institute of Technology, Cambridge, Massachusetts, pp. 322-327.

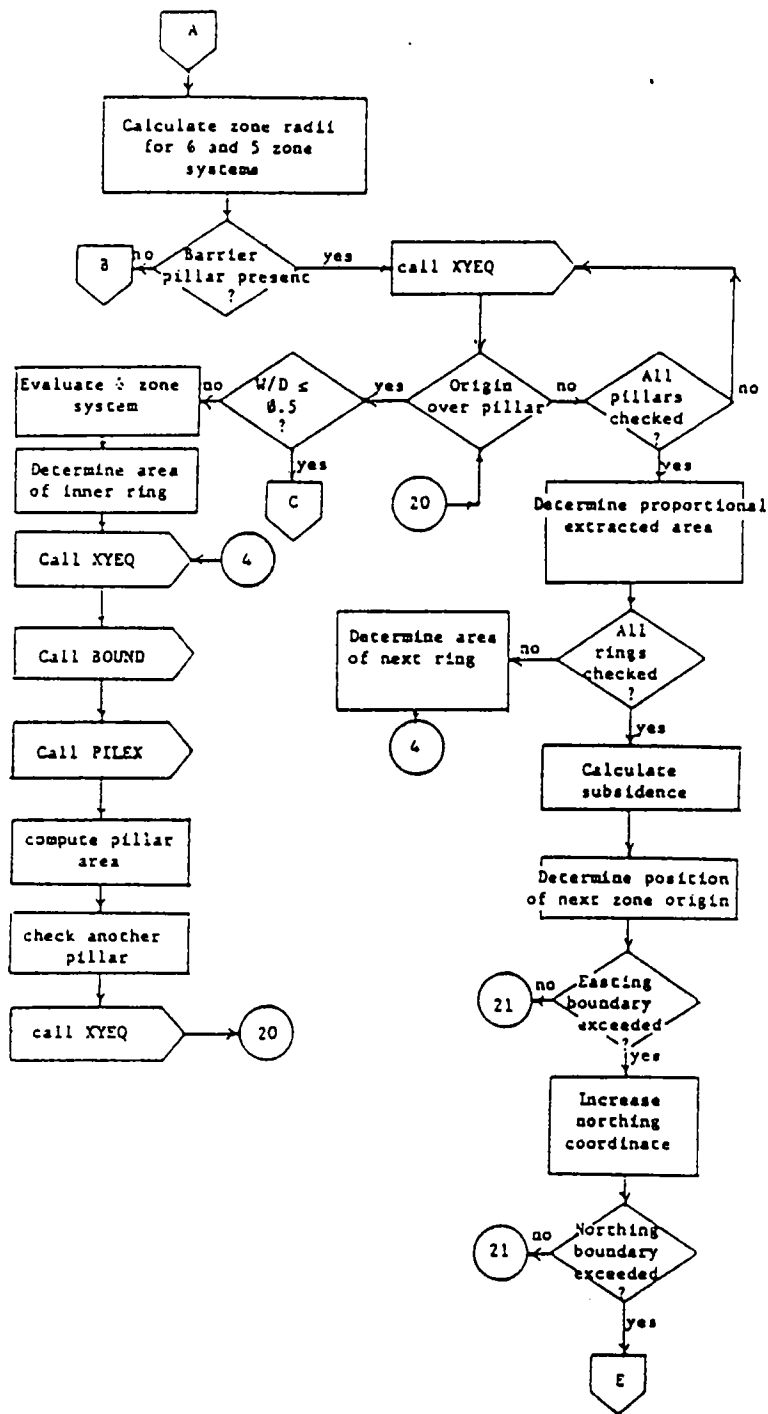
14. Peng, S. S. and Cheng, S. L. (1980), "Prediction of Surface Subsidence Profile Due to Underground Coal Mining," Tech. Report No. TR80-5, Dept. of Min. Eng., West Virginia Univ., Morgantown, West Virginia, 10 pp.
15. Shadbolt, C. H. (1978), "Mining Subsidence-Historical Review and State of the Art," Proceedings, Conf. Large Ground Movements and Structures, Cardiff, Wales, pp. 705-748.
16. Sinclair, J. (1963), Ground Movement and Control at Collieries, Sir Issac Pitman and Sons, Ltd.: London, 349 pp.
17. Singh, L. N., Rafeigui, M. A. and Singh, B. (1976), "Angle of Fracture in Mine Subsidence," J. Mines Met. Fuels, Vol. 24, pp. 375-385.
18. Virginia Polytechnic Institute and State University (1980), "The Prediction of Mining Subsidence and Related Parameters over Longwall Mining Operations," Final Report, DOE, Vol. VII, Contract No. EX-76-C-01-1231.
19. Voight, B. and Pariseau, W. (1970, "State of Predictive Art in Subsidence Engineering," Journal of the Soil Mechanics and Foundations Division, Proceedings, ASCE, Vol. 96, No. SM2.
20. Zenc, M. (1969), "Comparison of Bals' and Knothes' Methods of Calculating Surface Movements Due to Underground Mining," Inter. Jour. Rock Mech., Vol. 6, pp. 159-90.

APPENDIX A

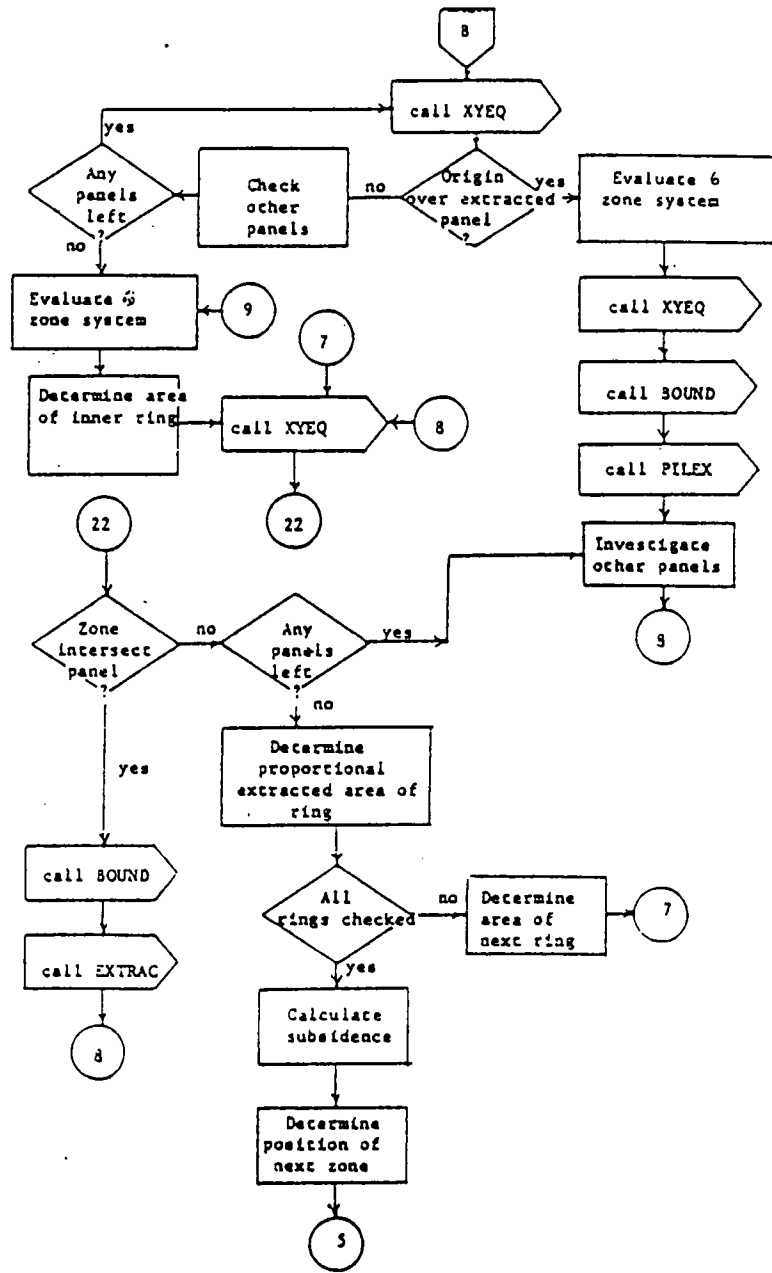
PROGRAM FLOWCHARTS



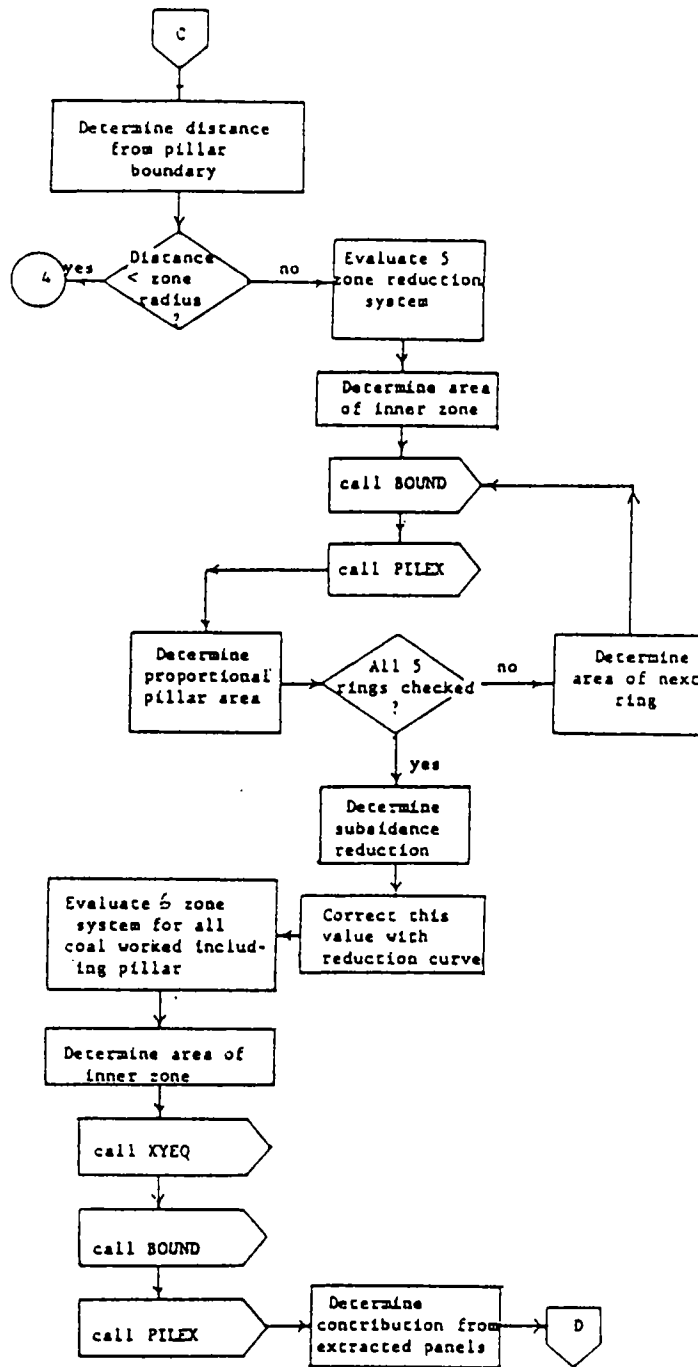
Flowchart of MAIN Program



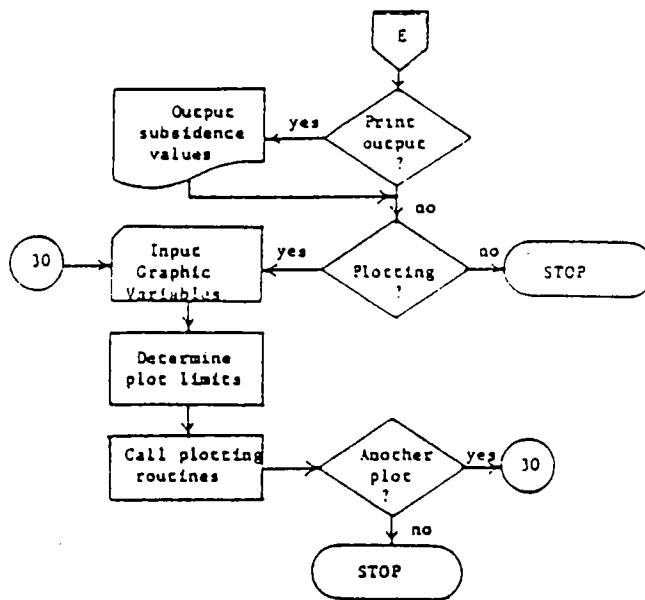
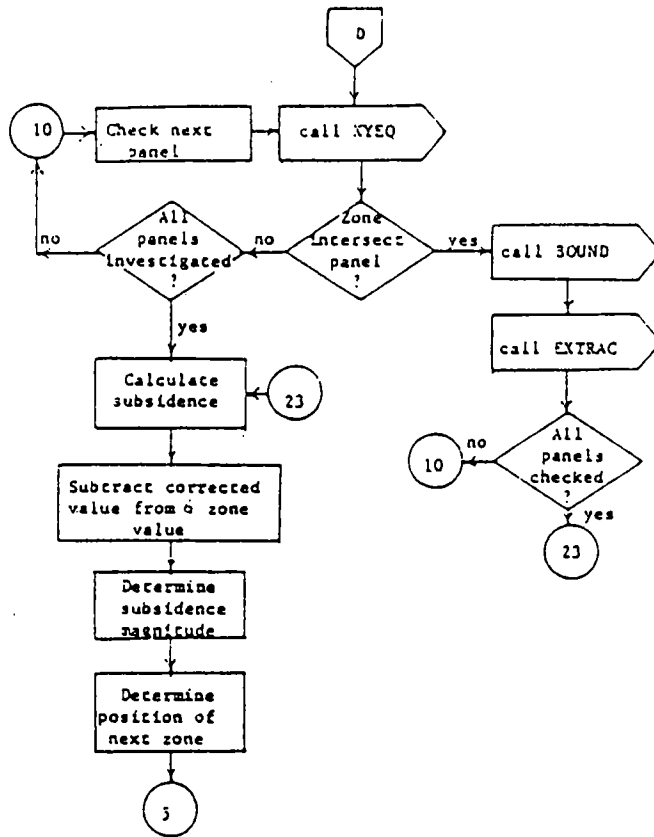
MAIN Program (continued)



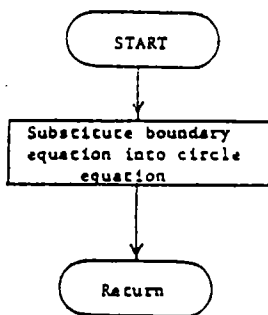
MAIN Program (continued)



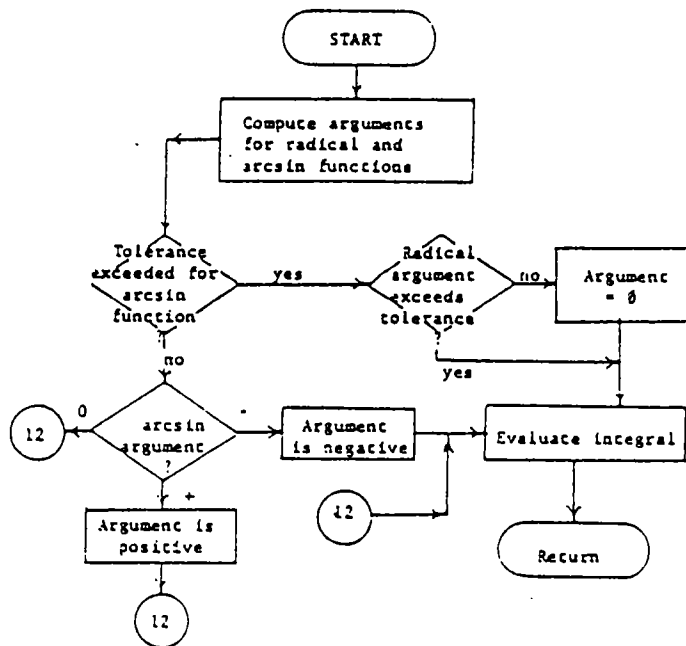
MAIN Program (continued)



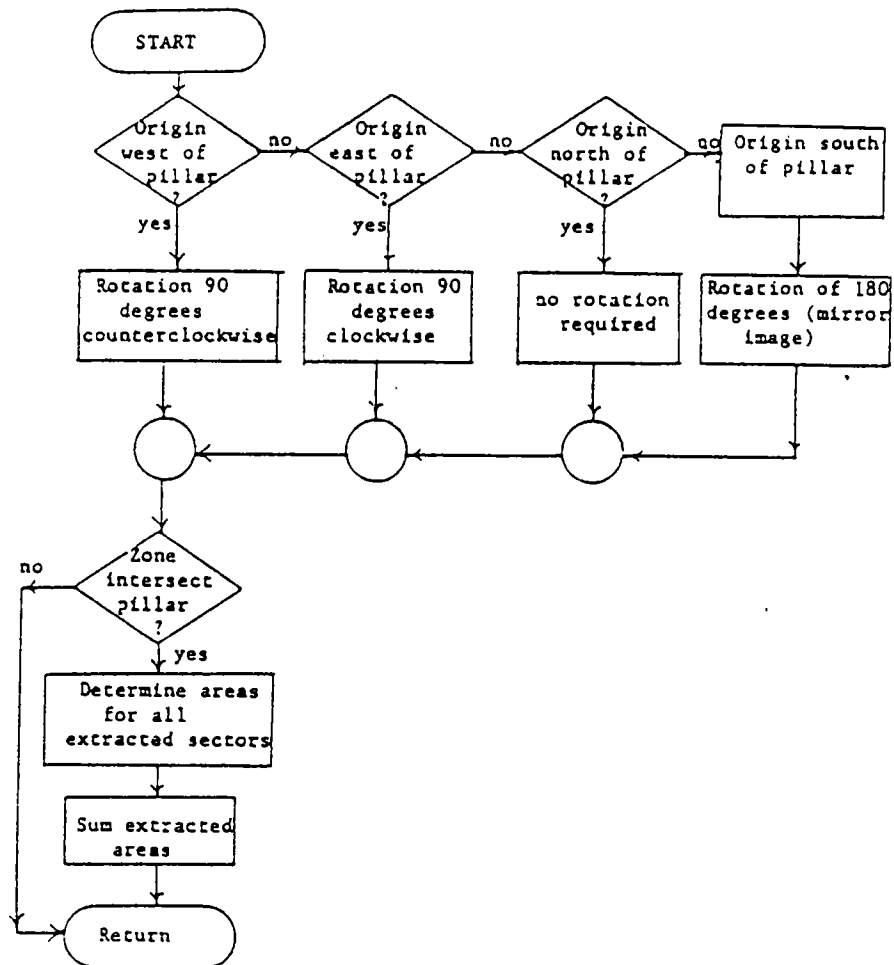
MAIN Program (continued)



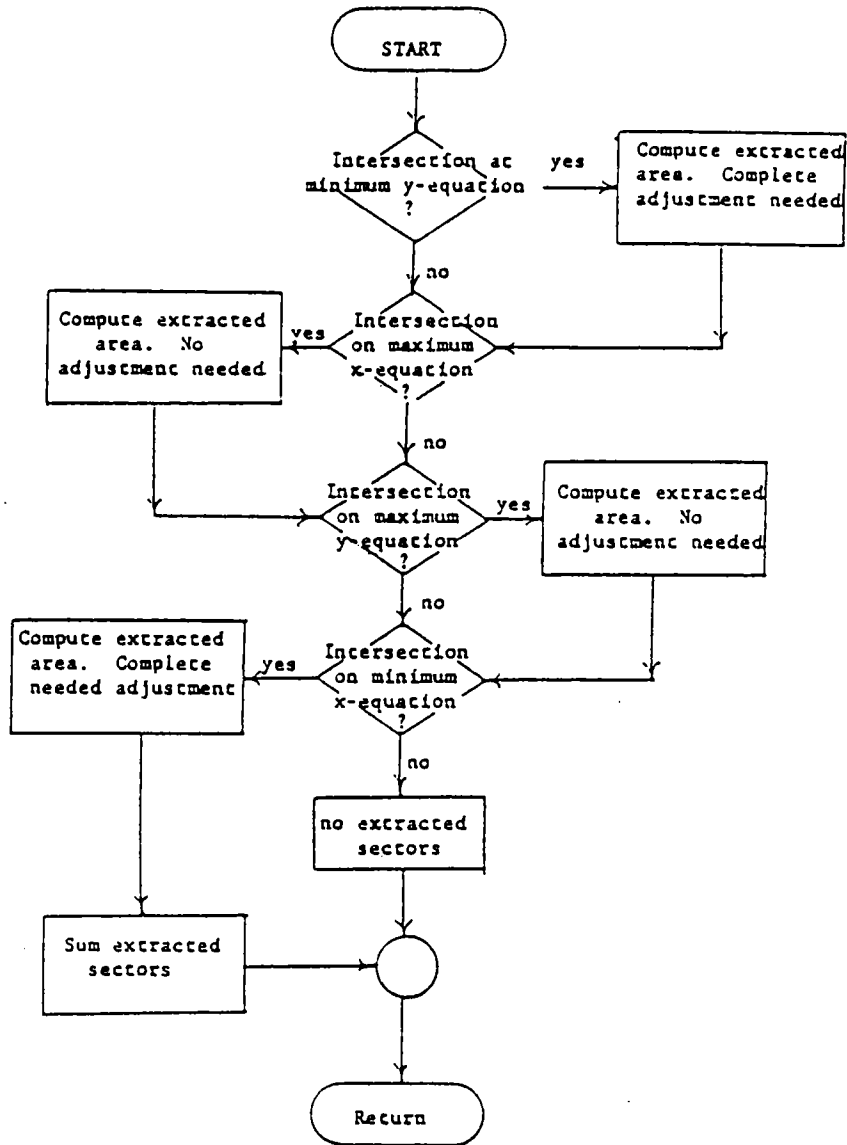
Flowchart of DYDX and DXDY Subroutines



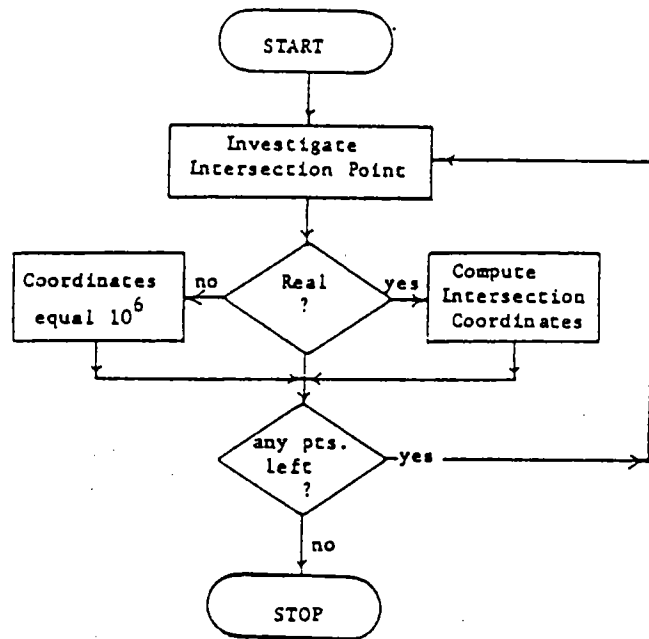
Flowchart of SUB1 and SUB2 Subroutines



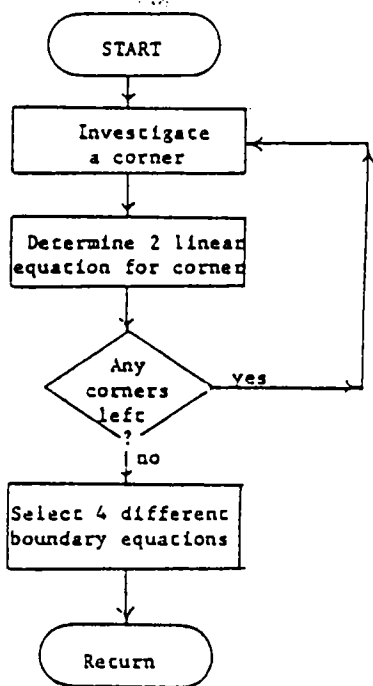
Flowchart of EXTRAC Subroutine



Flowchart of PILEX Subroutine



Flowchart of Subroutine BOUND



Flowchart of Subroutine XYEQ

APPENDIX B

INPUT DATA

TEST DATA FOR CONTOUR PROGRAM
 MULTI-PANEL EXTRACTION EXAMPLE
 WIDTH-TO-DEPTH RATIO=1.2
 DEPTH=500 FEET

0
 1200,600,,
 1600,600,,
 1600,3600,,
 1200,3600,2
 600,1200,,
 1200,1200,,
 1200,3600,,
 600,3600,,
 1600,600,,
 2200,600,,
 2200,3600,,
 1600,3600,1
 2800,0,4200,0,50
 0
 0.7,3.059
 31,500,1.5,30,0.5,135,5
 FEET
 0,-1,0
 TITLE SUBSIDENCE CONTOURS
 DEVICE 1,GOODMAN,100.,60.,4,4
 IDXY 4845,11,3,1,2,3,0,0,0,0,(2F5.0,F4.2)
 GRID 1,400,400,0,0,0,0
 EXTR 0,2800,0,4200
 PERF
 BOX 400,5,400,5,0,0,0,2,0.1
 SIZC 0,400,400
 CONT
 CINT 0,0,0.05,0,5,0.1,2,7,5
 BXEX
 PERF
 STOP

APPENDIX C

PROGRAM OUTPUT

TEST DATA FOR CONTOUR PROGRAM
MULTI-PANEL EXTRACTION EXAMPLE
WIDTH-TO-DEPTH RATIO=1.2
DEPTH=500 FEET

*****USER INPUT DATA*****

SEAM HEIGHT	= 5.0	FEET	WORKING DEPTH	= 500.	FEET
DRAW ANGLE	=31.0	DEGREES	ZONE INCREMENT	= 50	FEET
SURFACE GRADIENT	= 30.0	DEGREES	SURFACE DIP	= 1.5	DEGREES
SEAM GRADIENT	=135.0	DEGREES	SEAM DIP	= 0.5	DEGREES
MINIMUM EASTING	= 0	FEET	MAXIMUM EASTING	= 2800	FEET
MINIMUM NORTHING	= 0	FEET	MAXIMUM NORTHING	= 4200	FEET
INFLUENCE CONSTANT	= 3.059		% HARD MATERIAL	= 70.0	

ZONE FACTORS (INNER ZONE FIRST)

0.006 0.052 0.092 0.090 0.044 0.029

PANEL AND PILLAR COORDINATES

EASTING	NORTHING	PILLAR	1
1200.	600.		
1600.	600.		
1600.	3600.		
1200.	3600.		

EASTING	NORTHING	WORKING	1
600.	1200.		
1200.	1200.		
1200.	3600.		
600.	3600.		

EASTING	NORTHING	WORKING	2
1600.	600.		
2200.	600.		
2200.	3600.		
1600.	3600.		

*****USER OUTPUT REQUESTED*****

***** SUBSIDENCE VALUES CALCULATED BY ZONE AREA MODELING *****

NORTHING	EASTING --->											
0.	0.0	0.0	0.0	0.0	0.0	0.0	0.0	0.0	0.0	0.0	0.0	0.0
	0.0	0.0	0.0	0.0	0.0	0.0	0.0	0.0	0.0	0.0	0.0	0.0
	0.0	0.0	0.0	0.0	0.0	0.0	0.0	0.0	0.0	0.0	0.0	0.0
	0.0	0.0	0.0	0.0	0.0	0.0	0.0	0.0	0.0	0.0	0.0	0.0
	0.0	0.0	0.0	0.0	0.0	0.0	0.0	0.0	0.0	0.0	0.0	0.0
50.	0.0	0.0	0.0	0.0	0.0	0.0	0.0	0.0	0.0	0.0	0.0	0.0
	0.0	0.0	0.0	0.0	0.0	0.0	0.0	0.0	0.0	0.0	0.0	0.0
	0.0	0.0	0.0	0.0	0.0	0.0	0.0	0.0	0.0	0.0	0.0	0.0
	0.0	0.0	0.0	0.0	0.0	0.0	0.0	0.0	0.0	0.0	0.0	0.0
	0.0	0.0	0.0	0.0	0.0	0.0	0.0	0.0	0.0	0.0	0.0	0.0
100.	0.0	0.0	0.0	0.0	0.0	0.0	0.0	0.0	0.0	0.0	0.0	0.0
	0.0	0.0	0.0	0.0	0.0	0.0	0.0	0.0	0.0	0.0	0.0	0.0
	0.0	0.0	0.0	0.0	0.0	0.0	0.0	0.0	0.0	0.0	0.0	0.0
	0.0	0.0	0.0	0.0	0.0	0.0	0.0	0.0	0.0	0.0	0.0	0.0
	0.0	0.0	0.0	0.0	0.0	0.0	0.0	0.0	0.0	0.0	0.0	0.0

400.	0.0	0.0	0.0	0.0	0.0	0.0	0.0	0.0	0.0	0.0	0.0	0.0
	0.0	0.0	0.0	0.0	0.0	0.0	0.0	0.0	0.0	0.0	0.0	0.0
	0.0	0.0	0.0	0.0	0.0	0.0	0.0	0.0	0.0	0.0	0.0	0.0
	0.0	0.0	0.0	0.0	0.0	0.0	0.0	0.0	0.0	0.0	0.0	0.0
	0.0	0.0	0.0	0.0	0.0	0.0	0.0	0.0	0.0			
450.	0.0	0.0	0.0	0.0	0.0	0.0	0.0	0.0	0.0	0.0	0.0	0.0
	0.0	0.0	0.0	0.0	0.0	0.0	0.0	0.0	0.0	0.0	0.0	0.0
	0.0	0.0	0.0	0.0	0.0	0.0	0.0	0.0	0.0	0.0	0.0	0.01
	0.01	0.01	0.01	0.01	0.01	0.01	0.0	0.0	0.0	0.0	0.0	0.0
	0.0	0.0	0.0	0.0	0.0	0.0	0.0	0.0	0.0			
500.	0.0	0.0	0.0	0.0	0.0	0.0	0.0	0.0	0.0	0.0	0.0	0.0
	0.0	0.0	0.0	0.0	0.0	0.0	0.0	0.0	0.0	0.0	0.0	0.0
	0.0	0.0	0.0	0.0	0.0	0.0	0.0	0.0	0.0	0.01	0.02	0.02
	0.03	0.03	0.03	0.03	0.03	0.02	0.01	0.01	0.0	0.0	0.0	0.0
	0.0	0.0	0.0	0.0	0.0	0.0	0.0	0.0	0.0			
550.	0.0	0.0	0.0	0.0	0.0	0.0	0.0	0.0	0.0	0.0	0.0	0.0
	0.0	0.0	0.0	0.0	0.0	0.0	0.0	0.0	0.0	0.0	0.0	0.0
	0.0	0.0	0.0	0.0	0.0	0.0	0.0	0.0	0.01	0.02	0.04	0.06
	0.07	0.08	0.08	0.08	0.07	0.06	0.04	0.02	0.01	0.0	0.0	0.0
	0.0	0.0	0.0	0.0	0.0	0.0	0.0	0.0	0.0			
600.	0.0	0.0	0.0	0.0	0.0	0.0	0.0	0.0	0.0	0.0	0.0	0.0
	0.0	0.0	0.0	0.0	0.0	0.0	0.0	0.0	0.0	0.0	0.0	0.0
	0.0	0.0	0.0	0.0	0.0	0.0	0.0	0.01	0.02	0.05	0.09	0.14
	0.17	0.18	0.19	0.18	0.17	0.14	0.09	0.05	0.02	0.01	0.0	0.0
	0.0	0.0	0.0	0.0	0.0	0.0	0.0	0.0	0.0			

650. 0.0 0.0 0.0 0.0 0.0 0.0 0.0 0.0 0.0 0.0 0.0 0.0
0.0 0.0 0.0 0.0 0.0 0.0 0.0 0.0 0.0 0.0 0.0 0.0
0.0 0.0 0.0 0.0 0.0 0.0 0.01 0.02 0.05 0.11 0.21 0.30
0.36 0.38 0.39 0.38 0.36 0.30 0.21 0.11 0.05 0.02 0.01 0.0
0.0 0.0 0.0 0.0 0.0 0.0 0.0 0.0 0.0

700. 0.0 0.0 0.0 0.0 0.0 0.0 0.0 0.0 0.0 0.0 0.0 0.0
0.0 0.0 0.0 0.0 0.0 0.0 0.0 0.0 0.0 0.0 0.0 0.0
0.0 0.0 0.0 0.0 0.0 0.01 0.02 0.04 0.09 0.21 0.43 0.60
0.69 0.73 0.75 0.73 0.70 0.60 0.43 0.21 0.09 0.04 0.02 0.0
0.0 0.0 0.0 0.0 0.0 0.0 0.0 0.0 0.0

750. 0.0 0.0 0.0 0.0 0.0 0.0 0.0 0.0 0.0 0.0 0.0 0.0
0.0 0.0 0.0 0.0 0.0 0.0 0.0 0.0 0.0 0.0 0.0 0.0
0.0 0.0 0.0 0.0 0.0 0.01 0.02 0.06 0.13 0.30 0.59 0.89
1.04 1.09 1.12 1.10 1.04 0.90 0.60 0.30 0.13 0.06 0.02 0.01
0.0 0.0 0.0 0.0 0.0 0.0 0.0 0.0 0.0

800. 0.0 0.0 0.0 0.0 0.0 0.0 0.0 0.0 0.0 0.0 0.0 0.0
0.0 0.0 0.0 0.0 0.0 0.0 0.0 0.0 0.0 0.0 0.0 0.0
0.0 0.0 0.0 0.0 0.0 0.01 0.03 0.07 0.17 0.35 0.69 1.04
1.27 1.35 1.38 1.35 1.27 1.04 0.69 0.36 0.17 0.07 0.03 0.01
0.0 0.0 0.0 0.0 0.0 0.0 0.0 0.0 0.0

850. 0.0 0.0 0.0 0.0 0.0 0.0 0.0 0.0 0.0 0.0 0.0 0.0
0.0 0.0 0.0 0.0 0.0 0.0 0.0 0.0 0.0 0.0 0.0 0.0
0.0 0.0 0.0 0.0 0.0 0.01 0.03 0.08 0.18 0.38 0.72 1.09
1.35 1.46 1.50 1.46 1.35 1.09 0.73 0.38 0.18 0.08 0.03 0.01
0.0 0.0 0.0 0.0 0.0 0.0 0.0 0.0 0.0

1150. 0.0 0.0 0.0 0.0 0.0 0.0 0.0 0.0 0.0 0.0 0.0 0.0
0.01 0.02 0.04 0.06 0.07 0.08 0.09 0.08 0.07 0.06 0.04 0.02
0.01 0.0 0.0 0.0 0.01 0.01 0.04 0.09 0.19 0.38 0.73 1.10
1.36 1.49 1.55 1.49 1.37 1.10 0.73 0.39 0.19 0.09 0.03 0.01
0.0 0.0 0.0 0.0 0.0 0.0 0.0 0.0 0.0

1200. 0.0 0.0 0.0 0.0 0.0 0.0 0.0 0.0 0.0 0.0 0.0 0.01
0.02 0.05 0.09 0.13 0.16 0.18 0.18 0.18 0.16 0.13 0.09 0.05
0.02 0.01 0.0 0.01 0.01 0.02 0.04 0.09 0.19 0.38 0.73 1.09
1.36 1.49 1.55 1.49 1.36 1.10 0.73 0.39 0.19 0.09 0.03 0.01
0.0 0.0 0.0 0.0 0.0 0.0 0.0 0.0 0.0

1250. 0.0 0.0 0.0 0.0 0.0 0.0 0.0 0.0 0.0 0.0 0.01 0.02
0.05 0.10 0.19 0.28 0.34 0.36 0.38 0.37 0.34 0.28 0.20 0.10
0.05 0.02 0.01 0.01 0.02 0.02 0.04 0.09 0.19 0.38 0.72 1.09
1.36 1.49 1.55 1.49 1.36 1.09 0.73 0.39 0.19 0.09 0.03 0.01
0.0 0.0 0.0 0.0 0.0 0.0 0.0 0.0 0.0

1300. 0.0 0.0 0.0 0.0 0.0 0.0 0.0 0.0 0.0 0.01 0.02 0.04
0.09 0.19 0.40 0.55 0.65 0.69 0.71 0.69 0.65 0.56 0.40 0.20
0.09 0.04 0.02 0.01 0.02 0.02 0.04 0.09 0.19 0.38 0.72 1.09
1.36 1.49 1.54 1.49 1.36 1.09 0.73 0.38 0.19 0.09 0.04 0.01
0.0 0.0 0.0 0.0 0.0 0.0 0.0 0.0 0.0

1350. 0.0 0.0 0.0 0.0 0.0 0.0 0.0 0.0 0.0 0.01 0.02 0.06
0.13 0.28 0.55 0.82 0.98 1.04 1.06 1.04 0.98 0.83 0.55 0.28
0.13 0.06 0.03 0.02 0.02 0.03 0.04 0.09 0.19 0.38 0.72 1.08
1.35 1.49 1.54 1.49 1.36 1.09 0.72 0.38 0.19 0.09 0.04 0.01
0.0 0.0 0.0 0.0 0.0 0.0 0.0 0.0 0.0

1400.	0.0	0.0	0.0	0.0	0.0	0.0	0.0	0.0	0.0	0.01	0.03	0.08
	0.16	0.33	0.64	0.97	1.21	1.30	1.33	1.30	1.21	0.98	0.65	0.34
	0.16	0.07	0.03	0.02	0.03	0.03	0.04	0.09	0.19	0.38	0.72	1.08
	1.35	1.49	1.54	1.49	1.35	1.09	0.72	0.38	0.19	0.09	0.04	0.01
	0.0	0.0	0.0	0.0	0.0	0.0	0.0	0.0	0.0			
1450.	0.0	0.0	0.0	0.0	0.0	0.0	0.0	0.0	0.0	0.01	0.04	0.08
	0.18	0.36	0.68	1.03	1.29	1.42	1.46	1.42	1.30	1.04	0.69	0.36
	0.18	0.08	0.04	0.03	0.03	0.03	0.04	0.09	0.19	0.38	0.72	1.08
	1.35	1.48	1.54	1.49	1.35	1.08	0.72	0.38	0.19	0.09	0.04	0.01
	0.0	0.0	0.0	0.0	0.0	0.0	0.0	0.0	0.0			
1500.	0.0	0.0	0.0	0.0	0.0	0.0	0.0	0.0	0.0	0.01	0.04	0.09
	0.19	0.37	0.70	1.06	1.33	1.47	1.52	1.47	1.33	1.06	0.70	0.37
	0.19	0.09	0.04	0.03	0.03	0.03	0.04	0.09	0.19	0.38	0.71	1.08
	1.35	1.48	1.54	1.48	1.35	1.08	0.72	0.38	0.19	0.09	0.04	0.01
	0.0	0.0	0.0	0.0	0.0	0.0	0.0	0.0	0.0			
1550.	0.0	0.0	0.0	0.0	0.0	0.0	0.0	0.0	0.0	0.01	0.04	0.09
	0.19	0.38	0.70	1.06	1.33	1.47	1.53	1.48	1.33	1.06	0.71	0.38
	0.19	0.09	0.04	0.03	0.03	0.03	0.04	0.09	0.19	0.38	0.71	1.07
	1.34	1.48	1.54	1.48	1.35	1.08	0.72	0.38	0.19	0.09	0.04	0.01
	0.0	0.0	0.0	0.0	0.0	0.0	0.0	0.0	0.0			
1600.	0.0	0.0	0.0	0.0	0.0	0.0	0.0	0.0	0.0	0.01	0.04	0.09
	0.19	0.38	0.70	1.06	1.33	1.47	1.53	1.47	1.33	1.06	0.70	0.38
	0.19	0.09	0.04	0.03	0.03	0.03	0.04	0.09	0.19	0.38	0.71	1.07
	1.34	1.48	1.54	1.48	1.34	1.07	0.71	0.38	0.19	0.09	0.04	0.01
	0.0	0.0	0.0	0.0	0.0	0.0	0.0	0.0	0.0			

1650. 0.0 0.0 0.0 0.0 0.0 0.0 0.0 0.0 0.0 0.01 0.04 0.09
0.19 0.37 0.70 1.05 1.33 1.47 1.53 1.47 1.33 1.06 0.70 0.38
0.19 0.09 0.04 0.03 0.03 0.03 0.04 0.09 0.19 0.38 0.71 1.07
1.34 1.48 1.53 1.48 1.34 1.07 0.71 0.38 0.19 0.09 0.04 0.01
0.0 0.0 0.0 0.0 0.0 0.0 0.0 0.0 0.0

1700. 0.0 0.0 0.0 0.0 0.0 0.0 0.0 0.0 0.0 0.01 0.04 0.09
0.19 0.37 0.70 1.05 1.32 1.47 1.53 1.47 1.33 1.05 0.70 0.38
0.19 0.09 0.04 0.03 0.03 0.03 0.04 0.09 0.19 0.38 0.71 1.06
1.34 1.48 1.53 1.48 1.34 1.07 0.71 0.38 0.19 0.09 0.04 0.01
0.0 0.0 0.0 0.0 0.0 0.0 0.0 0.0 0.0

1750. 0.0 0.0 0.0 0.0 0.0 0.0 0.0 0.0 0.0 0.01 0.04 0.09
0.19 0.37 0.69 1.05 1.32 1.47 1.52 1.47 1.32 1.05 0.70 0.37
0.19 0.09 0.04 0.03 0.03 0.03 0.04 0.09 0.19 0.38 0.70 1.06
1.33 1.48 1.53 1.48 1.34 1.07 0.71 0.38 0.19 0.09 0.04 0.01
0.0 0.0 0.0 0.0 0.0 0.0 0.0 0.0 0.0

1800. 0.0 0.0 0.0 0.0 0.0 0.0 0.0 0.0 0.0 0.01 0.04 0.09
0.19 0.37 0.69 1.05 1.32 1.47 1.52 1.47 1.32 1.05 0.70 0.37
0.19 0.09 0.04 0.03 0.03 0.03 0.04 0.09 0.19 0.38 0.70 1.06
1.33 1.47 1.53 1.48 1.33 1.06 0.71 0.38 0.19 0.09 0.04 0.01
0.0 0.0 0.0 0.0 0.0 0.0 0.0 0.0 0.0

1850. 0.0 0.0 0.0 0.0 0.0 0.0 0.0 0.0 0.0 0.01 0.04 0.09
0.19 0.37 0.69 1.04 1.32 1.47 1.52 1.47 1.32 1.05 0.69 0.37
0.19 0.09 0.04 0.03 0.03 0.03 0.04 0.09 0.19 0.38 0.70 1.06
1.33 1.47 1.53 1.47 1.33 1.06 0.70 0.38 0.19 0.09 0.04 0.01
0.0 0.0 0.0 0.0 0.0 0.0 0.0 0.0 0.0

1900. 0.0 0.0 0.0 0.0 0.0 0.0 0.0 0.0 0.0 0.01 0.04 0.09
0.19 0.37 0.69 1.04 1.31 1.46 1.52 1.47 1.32 1.04 0.69 0.37
0.19 0.09 0.04 0.03 0.03 0.03 0.04 0.09 0.19 0.37 0.70 1.05
1.33 1.47 1.53 1.47 1.33 1.06 0.70 0.38 0.19 0.09 0.04 0.01
0.0 0.0 0.0 0.0 0.0 0.0 0.0 0.0 0.0

1950. 0.0 0.0 0.0 0.0 0.0 0.0 0.0 0.0 0.0 0.01 0.04 0.09
0.19 0.37 0.69 1.04 1.31 1.46 1.52 1.46 1.31 1.04 0.69 0.37
0.19 0.09 0.04 0.03 0.03 0.03 0.04 0.09 0.19 0.37 0.70 1.05
1.32 1.47 1.53 1.47 1.33 1.05 0.70 0.38 0.19 0.09 0.04 0.01
0.0 0.0 0.0 0.0 0.0 0.0 0.0 0.0 0.0

2000. 0.0 0.0 0.0 0.0 0.0 0.0 0.0 0.0 0.0 0.01 0.04 0.09
0.19 0.37 0.69 1.03 1.31 1.46 1.52 1.46 1.31 1.04 0.69 0.37
0.19 0.09 0.04 0.03 0.03 0.03 0.04 0.09 0.19 0.37 0.69 1.05
1.32 1.47 1.52 1.47 1.32 1.05 0.70 0.37 0.19 0.09 0.04 0.01
0.0 0.0 0.0 0.0 0.0 0.0 0.0 0.0 0.0

2050. 0.0 0.0 0.0 0.0 0.0 0.0 0.0 0.0 0.0 0.01 0.04 0.09
0.19 0.37 0.68 1.03 1.31 1.46 1.52 1.46 1.31 1.04 0.69 0.37
0.19 0.09 0.04 0.03 0.04 0.03 0.04 0.09 0.19 0.37 0.69 1.04
1.32 1.47 1.52 1.47 1.32 1.05 0.70 0.37 0.19 0.09 0.04 0.01
0.0 0.0 0.0 0.0 0.0 0.0 0.0 0.0 0.0

2100. 0.0 0.0 0.0 0.0 0.0 0.0 0.0 0.0 0.0 0.01 0.04 0.09
0.19 0.37 0.68 1.03 1.30 1.46 1.51 1.46 1.31 1.03 0.69 0.37
0.19 0.09 0.04 0.03 0.04 0.03 0.04 0.09 0.19 0.37 0.69 1.04
1.32 1.47 1.52 1.47 1.32 1.05 0.69 0.37 0.19 0.09 0.04 0.01
0.0 0.0 0.0 0.0 0.0 0.0 0.0 0.0 0.0

2150. 0.0 0.0 0.0 0.0 0.0 0.0 0.0 0.0 0.0 0.01 0.04 0.09
0.19 0.37 0.68 1.03 1.30 1.46 1.51 1.46 1.30 1.03 0.68 0.37
0.19 0.09 0.04 0.03 0.04 0.03 0.04 0.09 0.19 0.37 0.69 1.04
1.31 1.46 1.52 1.46 1.32 1.04 0.69 0.37 0.19 0.09 0.04 0.01
0.0 0.0 0.0 0.0 0.0 0.0 0.0 0.0 0.0

2200. 0.0 0.0 0.0 0.0 0.0 0.0 0.0 0.0 0.0 0.02 0.04 0.09
0.19 0.37 0.68 1.02 1.30 1.46 1.51 1.46 1.30 1.03 0.68 0.37
0.19 0.09 0.04 0.03 0.04 0.03 0.04 0.09 0.19 0.37 0.69 1.04
1.31 1.46 1.52 1.46 1.31 1.04 0.69 0.37 0.19 0.09 0.04 0.01
0.0 0.0 0.0 0.0 0.0 0.0 0.0 0.0 0.0

2250. 0.0 0.0 0.0 0.0 0.0 0.0 0.0 0.0 0.0 0.02 0.04 0.09
0.19 0.37 0.68 1.02 1.30 1.45 1.51 1.46 1.30 1.02 0.68 0.37
0.19 0.09 0.04 0.03 0.04 0.03 0.04 0.09 0.19 0.37 0.69 1.03
1.31 1.46 1.52 1.46 1.31 1.04 0.69 0.37 0.19 0.09 0.04 0.01
0.0 0.0 0.0 0.0 0.0 0.0 0.0 0.0 0.0

2300. 0.0 0.0 0.0 0.0 0.0 0.0 0.0 0.0 0.0 0.02 0.04 0.09
0.19 0.37 0.67 1.02 1.29 1.45 1.51 1.45 1.30 1.02 0.68 0.37
0.19 0.09 0.04 0.03 0.04 0.03 0.04 0.09 0.19 0.37 0.68 1.03
1.31 1.46 1.52 1.46 1.31 1.04 0.69 0.37 0.19 0.09 0.04 0.01
0.0 0.0 0.0 0.0 0.0 0.0 0.0 0.0 0.0

2350. 0.0 0.0 0.0 0.0 0.0 0.0 0.0 0.0 0.0 0.02 0.04 0.09
0.19 0.37 0.67 1.02 1.29 1.45 1.51 1.45 1.29 1.02 0.68 0.37
0.19 0.09 0.05 0.03 0.04 0.03 0.04 0.09 0.19 0.37 0.68 1.03
1.30 1.46 1.51 1.46 1.31 1.03 0.69 0.37 0.19 0.09 0.04 0.01
0.0 0.0 0.0 0.0 0.0 0.0 0.0 0.0 0.0

2400. 0.0 0.0 0.0 0.0 0.0 0.0 0.0 0.0 0.0 0.02 0.04 0.09
0.19 0.36 0.67 1.01 1.29 1.45 1.51 1.45 1.29 1.02 0.67 0.37
0.19 0.09 0.05 0.04 0.04 0.03 0.05 0.09 0.19 0.37 0.68 1.03
1.30 1.46 1.51 1.46 1.30 1.03 0.68 0.37 0.19 0.09 0.04 0.01
0.0 0.0 0.0 0.0 0.0 0.0 0.0 0.0 0.0

2450. 0.0 0.0 0.0 0.0 0.0 0.0 0.0 0.0 0.0 0.02 0.04 0.09
0.19 0.36 0.67 1.01 1.29 1.45 1.50 1.45 1.29 1.01 0.67 0.37
0.19 0.09 0.05 0.04 0.04 0.04 0.05 0.09 0.19 0.37 0.68 1.02
1.30 1.46 1.51 1.46 1.30 1.03 0.68 0.37 0.19 0.09 0.04 0.01
0.0 0.0 0.0 0.0 0.0 0.0 0.0 0.0 0.0

2500. 0.0 0.0 0.0 0.0 0.0 0.0 0.0 0.0 0.0 0.02 0.04 0.09
0.19 0.36 0.67 1.01 1.28 1.45 1.50 1.45 1.29 1.01 0.67 0.37
0.19 0.09 0.05 0.04 0.04 0.04 0.05 0.09 0.19 0.37 0.68 1.02
1.30 1.45 1.51 1.45 1.30 1.02 0.68 0.37 0.19 0.09 0.04 0.01
0.0 0.0 0.0 0.0 0.0 0.0 0.0 0.0 0.0

2550. 0.0 0.0 0.0 0.0 0.0 0.0 0.0 0.0 0.01 0.02 0.04 0.09
0.19 0.36 0.67 1.01 1.28 1.45 1.50 1.45 1.28 1.01 0.67 0.36
0.19 0.09 0.05 0.04 0.04 0.04 0.05 0.09 0.19 0.37 0.67 1.02
1.29 1.45 1.51 1.45 1.30 1.02 0.68 0.37 0.19 0.09 0.04 0.01
0.0 0.0 0.0 0.0 0.0 0.0 0.0 0.0 0.0

2600. 0.0 0.0 0.0 0.0 0.0 0.0 0.0 0.0 0.01 0.02 0.04 0.09
0.19 0.36 0.66 1.00 1.28 1.44 1.50 1.45 1.28 1.01 0.67 0.36
0.19 0.09 0.05 0.04 0.04 0.04 0.05 0.09 0.19 0.37 0.67 1.02
1.29 1.45 1.51 1.45 1.29 1.02 0.68 0.37 0.19 0.09 0.04 0.01
0.0 0.0 0.0 0.0 0.0 0.0 0.0 0.0 0.0

2650. 0.0 0.0 0.0 0.0 0.0 0.0 0.0 0.0 0.01 0.02 0.04 0.09
0.19 0.36 0.66 1.00 1.28 1.44 1.50 1.44 1.28 1.00 0.67 0.36
0.19 0.09 0.05 0.04 0.04 0.04 0.05 0.09 0.19 0.36 0.67 1.01
1.29 1.45 1.51 1.45 1.29 1.02 0.67 0.37 0.19 0.09 0.04 0.02
0.0 0.0 0.0 0.0 0.0 0.0 0.0 0.0 0.0 0.0

2700. 0.0 0.0 0.0 0.0 0.0 0.0 0.0 0.0 0.01 0.02 0.04 0.09
0.19 0.36 0.66 1.00 1.27 1.44 1.50 1.44 1.28 1.00 0.66 0.36
0.19 0.09 0.05 0.04 0.04 0.04 0.05 0.09 0.19 0.36 0.67 1.01
1.29 1.45 1.50 1.45 1.29 1.01 0.67 0.37 0.19 0.09 0.04 0.02
0.0 0.0 0.0 0.0 0.0 0.0 0.0 0.0 0.0 0.0

2750. 0.0 0.0 0.0 0.0 0.0 0.0 0.0 0.0 0.01 0.02 0.04 0.09
0.19 0.36 0.66 0.99 1.27 1.44 1.50 1.44 1.27 1.00 0.66 0.36
0.19 0.09 0.05 0.04 0.04 0.04 0.05 0.09 0.19 0.36 0.67 1.01
1.28 1.45 1.50 1.45 1.29 1.01 0.67 0.37 0.19 0.09 0.04 0.02
0.0 0.0 0.0 0.0 0.0 0.0 0.0 0.0 0.0 0.0

2800. 0.0 0.0 0.0 0.0 0.0 0.0 0.0 0.0 0.01 0.02 0.04 0.09
0.19 0.36 0.66 0.99 1.27 1.44 1.50 1.44 1.27 1.00 0.66 0.36
0.19 0.09 0.05 0.04 0.04 0.04 0.05 0.09 0.19 0.36 0.67 1.00
1.28 1.45 1.50 1.45 1.28 1.01 0.67 0.36 0.19 0.09 0.04 0.02
0.0 0.0 0.0 0.0 0.0 0.0 0.0 0.0 0.0 0.0

2850. 0.0 0.0 0.0 0.0 0.0 0.0 0.0 0.0 0.01 0.02 0.04 0.09
0.19 0.36 0.66 0.99 1.27 1.44 1.49 1.44 1.27 0.99 0.66 0.36
0.19 0.09 0.05 0.04 0.04 0.04 0.05 0.09 0.19 0.36 0.66 1.00
1.28 1.44 1.50 1.45 1.28 1.01 0.67 0.36 0.19 0.09 0.04 0.02
0.0 0.0 0.0 0.0 0.0 0.0 0.0 0.0 0.0 0.0

2900. 0.0 0.0 0.0 0.0 0.0 0.0 0.0 0.0 0.01 0.02 0.04 0.09
0.19 0.36 0.65 0.99 1.26 1.44 1.49 1.44 1.27 0.99 0.66 0.36
0.19 0.09 0.05 0.04 0.04 0.04 0.05 0.09 0.19 0.36 0.66 1.00
1.28 1.44 1.50 1.44 1.28 1.00 0.67 0.36 0.19 0.09 0.04 0.02
0.0 0.0 0.0 0.0 0.0 0.0 0.0 0.0 0.0

2950. 0.0 0.0 0.0 0.0 0.0 0.0 0.0 0.0 0.01 0.02 0.04 0.09
0.19 0.36 0.65 0.98 1.26 1.44 1.49 1.44 1.26 0.99 0.66 0.36
0.19 0.09 0.05 0.04 0.04 0.04 0.05 0.09 0.19 0.36 0.66 1.00
1.27 1.44 1.50 1.44 1.28 1.00 0.66 0.36 0.19 0.09 0.04 0.02
0.0 0.0 0.0 0.0 0.0 0.0 0.0 0.0 0.0

3000. 0.0 0.0 0.0 0.0 0.0 0.0 0.0 0.0 0.01 0.02 0.04 0.09
0.19 0.36 0.65 0.98 1.26 1.43 1.49 1.43 1.26 0.99 0.65 0.36
0.19 0.09 0.05 0.04 0.04 0.04 0.05 0.09 0.19 0.36 0.66 0.99
1.27 1.44 1.50 1.44 1.27 1.00 0.66 0.36 0.19 0.09 0.04 0.02
0.0 0.0 0.0 0.0 0.0 0.0 0.0 0.0 0.0

3050. 0.0 0.0 0.0 0.0 0.0 0.0 0.0 0.0 0.01 0.02 0.04 0.09
0.19 0.36 0.65 0.98 1.26 1.43 1.49 1.43 1.26 0.98 0.65 0.36
0.19 0.09 0.05 0.04 0.04 0.04 0.05 0.09 0.19 0.36 0.66 0.99
1.27 1.44 1.49 1.44 1.27 1.00 0.66 0.36 0.19 0.09 0.04 0.02
0.01 0.0 0.0 0.0 0.0 0.0 0.0 0.0 0.0

3100. 0.0 0.0 0.0 0.0 0.0 0.0 0.0 0.0 0.01 0.02 0.04 0.09
0.19 0.36 0.65 0.98 1.26 1.43 1.49 1.43 1.26 0.98 0.65 0.36
0.19 0.09 0.05 0.04 0.04 0.04 0.05 0.09 0.19 0.36 0.66 0.99
1.27 1.44 1.49 1.44 1.27 0.99 0.66 0.36 0.19 0.09 0.04 0.02
0.01 0.0 0.0 0.0 0.0 0.0 0.0 0.0 0.0

3150. 0.0 0.0 0.0 0.0 0.0 0.0 0.0 0.0 0.01 0.02 0.04 0.10
0.19 0.36 0.65 0.97 1.25 1.43 1.49 1.43 1.26 0.98 0.65 0.36
0.19 0.09 0.05 0.04 0.05 0.04 0.05 0.09 0.19 0.36 0.65 0.99
1.26 1.44 1.49 1.44 1.27 0.99 0.66 0.36 0.19 0.09 0.04 0.02
0.01 0.0 0.0 0.0 0.0 0.0 0.0 0.0 0.0

3200. 0.0 0.0 0.0 0.0 0.0 0.0 0.0 0.0 0.01 0.02 0.04 0.10
0.19 0.36 0.64 0.97 1.25 1.43 1.49 1.43 1.25 0.98 0.65 0.36
0.19 0.09 0.05 0.04 0.05 0.04 0.05 0.09 0.19 0.36 0.65 0.98
1.26 1.43 1.49 1.44 1.26 0.99 0.66 0.36 0.19 0.09 0.04 0.02
0.01 0.0 0.0 0.0 0.0 0.0 0.0 0.0 0.0

3250. 0.0 0.0 0.0 0.0 0.0 0.0 0.0 0.0 0.01 0.02 0.04 0.10
0.19 0.35 0.64 0.97 1.25 1.43 1.48 1.43 1.25 0.97 0.65 0.36
0.19 0.09 0.05 0.04 0.05 0.04 0.05 0.09 0.19 0.36 0.65 0.98
1.26 1.43 1.49 1.43 1.26 0.99 0.65 0.36 0.19 0.09 0.04 0.02
0.01 0.0 0.0 0.0 0.0 0.0 0.0 0.0 0.0

3300. 0.0 0.0 0.0 0.0 0.0 0.0 0.0 0.0 0.01 0.02 0.04 0.09
0.18 0.35 0.63 0.95 1.22 1.40 1.46 1.40 1.23 0.95 0.63 0.35
0.18 0.09 0.05 0.04 0.05 0.04 0.05 0.09 0.18 0.35 0.64 0.96
1.24 1.41 1.46 1.41 1.24 0.97 0.64 0.35 0.18 0.09 0.04 0.02
0.01 0.0 0.0 0.0 0.0 0.0 0.0 0.0 0.0

3350. 0.0 0.0 0.0 0.0 0.0 0.0 0.0 0.0 0.01 0.02 0.04 0.09
0.17 0.33 0.60 0.91 1.18 1.33 1.38 1.33 1.18 0.92 0.60 0.33
0.17 0.09 0.05 0.04 0.04 0.04 0.05 0.09 0.17 0.33 0.61 0.93
1.19 1.34 1.39 1.34 1.19 0.93 0.61 0.33 0.17 0.09 0.04 0.02
0.01 0.0 0.0 0.0 0.0 0.0 0.0 0.0 0.0

3400. 0.0 0.0 0.0 0.0 0.0 0.0 0.0 0.0 0.0 0.01 0.03 0.08
0.15 0.29 0.54 0.83 1.05 1.17 1.21 1.17 1.05 0.83 0.55 0.29
0.15 0.08 0.04 0.03 0.04 0.03 0.04 0.08 0.15 0.29 0.55 0.84
1.07 1.19 1.22 1.19 1.07 0.85 0.56 0.30 0.15 0.08 0.03 0.01
0.0 0.0 0.0 0.0 0.0 0.0 0.0 0.0 0.0

3450. 0.0 0.0 0.0 0.0 0.0 0.0 0.0 0.0 0.0 0.01 0.03 0.06
0.11 0.23 0.45 0.67 0.83 0.91 0.93 0.91 0.83 0.67 0.45 0.23
0.12 0.06 0.03 0.03 0.03 0.03 0.03 0.06 0.12 0.23 0.46 0.69
0.84 0.92 0.95 0.92 0.85 0.69 0.46 0.24 0.12 0.06 0.03 0.01
0.0 0.0 0.0 0.0 0.0 0.0 0.0 0.0 0.0

3500. 0.0 0.0 0.0 0.0 0.0 0.0 0.0 0.0 0.0 0.01 0.02 0.04
0.08 0.16 0.31 0.44 0.54 0.60 0.61 0.60 0.54 0.45 0.32 0.16
0.08 0.04 0.02 0.02 0.02 0.02 0.02 0.04 0.08 0.16 0.32 0.45
0.55 0.61 0.62 0.61 0.55 0.46 0.32 0.16 0.08 0.04 0.02 0.01
0.0 0.0 0.0 0.0 0.0 0.0 0.0 0.0 0.0

3550. 0.0 0.0 0.0 0.0 0.0 0.0 0.0 0.0 0.0 0.0 0.01 0.02
0.04 0.09 0.16 0.23 0.29 0.33 0.34 0.33 0.29 0.23 0.16 0.09
0.04 0.02 0.01 0.01 0.01 0.01 0.01 0.02 0.04 0.09 0.16 0.23
0.29 0.33 0.34 0.33 0.29 0.23 0.16 0.09 0.04 0.02 0.01 0.0
0.0 0.0 0.0 0.0 0.0 0.0 0.0 0.0 0.0

3600. 0.0 0.0 0.0 0.0 0.0 0.0 0.0 0.0 0.0 0.0 0.01 0.01
0.02 0.04 0.08 0.11 0.15 0.17 0.18 0.17 0.15 0.11 0.08 0.04
0.02 0.01 0.01 0.01 0.01 0.01 0.01 0.01 0.02 0.04 0.08 0.12
0.15 0.17 0.18 0.17 0.15 0.12 0.08 0.04 0.02 0.01 0.01 0.0
0.0 0.0 0.0 0.0 0.0 0.0 0.0 0.0 0.0

3650. 0.0 0.0 0.0 0.0 0.0 0.0 0.0 0.0 0.0 0.0 0.0 0.01
0.01 0.02 0.04 0.06 0.08 0.09 0.09 0.09 0.08 0.06 0.04 0.02
0.01 0.01 0.0 0.0 0.0 0.0 0.0 0.01 0.01 0.02 0.04 0.06
0.08 0.09 0.09 0.09 0.08 0.06 0.04 0.02 0.01 0.01 0.0 0.0
0.0 0.0 0.0 0.0 0.0 0.0 0.0 0.0 0.0

3700. 0.0 0.0 0.0 0.0 0.0 0.0 0.0 0.0 0.0 0.0 0.0 0.0
0.01 0.01 0.02 0.03 0.04 0.04 0.04 0.04 0.04 0.03 0.02 0.01
0.01 0.0 0.0 0.0 0.0 0.0 0.0 0.0 0.01 0.01 0.02 0.03
0.03 0.04 0.04 0.04 0.03 0.03 0.02 0.01 0.01 0.0 0.0 0.0
0.0 0.0 0.0 0.0 0.0 0.0 0.0 0.0 0.0

3750. 0.0 0.0 0.0 0.0 0.0 0.0 0.0 0.0 0.0 0.0 0.0 0.0
0.0 0.0 0.01 0.01 0.01 0.02 0.02 0.02 0.01 0.01 0.01 0.0
0.0 0.0 0.0 0.0 0.0 0.0 0.0 0.0 0.0 0.0 0.01 0.01
0.01 0.02 0.02 0.02 0.01 0.01 0.01 0.0 0.0 0.0 0.0 0.0
0.0 0.0 0.0 0.0 0.0 0.0 0.0 0.0 0.0

3800. 0.0 0.0 0.0 0.0 0.0 0.0 0.0 0.0 0.0 0.0 0.0 0.0
0.0 0.0 0.0 0.0 0.0 0.01 0.01 0.01 0.0 0.0 0.0 0.0
0.0 0.0 0.0 0.0 0.0 0.0 0.0 0.0 0.0 0.0 0.0 0.0
0.0 0.01 0.01 0.01 0.0 0.0 0.0 0.0 0.0 0.0 0.0 0.0
0.0 0.0 0.0 0.0 0.0 0.0 0.0 0.0 0.0

3850. 0.0 0.0 0.0 0.0 0.0 0.0 0.0 0.0 0.0 0.0 0.0 0.0
0.0 0.0 0.0 0.0 0.0 0.0 0.0 0.0 0.0 0.0 0.0 0.0
0.0 0.0 0.0 0.0 0.0 0.0 0.0 0.0 0.0 0.0 0.0 0.0
0.0 0.0 0.0 0.0 0.0 0.0 0.0 0.0 0.0 0.0 0.0 0.0
0.0 0.0 0.0 0.0 0.0 0.0 0.0 0.0 0.0

4150. 0.0 0.0 0.0 0.0 0.0 0.0 0.0 0.0 0.0 0.0 0.0 0.0
0.0 0.0 0.0 0.0 0.0 0.0 0.0 0.0 0.0 0.0 0.0 0.0
0.0 0.0 0.0 0.0 0.0 0.0 0.0 0.0 0.0 0.0 0.0 0.0
0.0 0.0 0.0 0.0 0.0 0.0 0.0 0.0 0.0 0.0 0.0 0.0
0.0 0.0 0.0 0.0 0.0 0.0 0.0 0.0 0.0

4200. 0.0 0.0 0.0 0.0 0.0 0.0 0.0 0.0 0.0 0.0 0.0 0.0
0.0 0.0 0.0 0.0 0.0 0.0 0.0 0.0 0.0 0.0 0.0 0.0
0.0 0.0 0.0 0.0 0.0 0.0 0.0 0.0 0.0 0.0 0.0 0.0
0.0 0.0 0.0 0.0 0.0 0.0 0.0 0.0 0.0 0.0 0.0 0.0
0.0 0.0 0.0 0.0 0.0 0.0 0.0 0.0 0.0

CONTOURING CONDUCTED USING ABSOLUTE SURFACE DISPLACEMENTS

THERE IS (ARE) 0 CROSS-SECTION(S) REQUESTED

APPENDIX D

PUBLICATIONS BASED ON THIS RESEARCH

A. GRADUATE THESES

1. Goodman, G. (1980), "Computer Modeling of Mining Subsidence Using the Zone Area Method," M.S. Thesis.
2. Webb, B. (1982), "A Study of Longwall Subsidence in the Appalachian Coalfield," M.S. Thesis.
3. Triplett, T. (1983), "Ground Movements and Deformation above Mined Panels in Appalachia," M.S. Thesis.

B. PUBLICATIONS

1. Karmis, M., G. Goodman, C. Haycocks, I. Eitani (1981), "Computer Modeling of Mining Subsidence Using the Zone Area Method," Proceedings, 22nd Symposium on Rock Mechanics, Cambridge, Massachusetts, June 29 - July 2, pp. 272-277.
2. Karmis, M., C. Haycocks, I. Eitani and B. Webb (1981), "A Study of Longwall Subsidence in the Appalachian Coal Region Using Field Measurements and Computer Modeling Techniques," Proceedings, 1st Conference on Ground Control in Mining, West Virginia University, July 27-29, pp. 220-229.
3. Karmis, M., C. Haycocks, B. Webb and T. Triplett (1981), "The Potential of the Zone Area Methods for Mining Subsidence Prediction in the Appalachian Coalfield," Proceedings, Workshop on Surface Subsidence due to Underground Mining, Morgantown, West Virginia, November 30 - December 2, pp. 48-62.
4. Karmis, M., G. Goodman, C. Haycocks and T. Triplett (1982), "The Development and Testing of a Regionalized Subsidence Prediction Model," Proceedings, 17th International Symposium on Computer Applications in the Mining Industry, Denver, Colorado, April 19-23, pp. 240-252.

